Online Material

The following figures display for each of our program stars the observed spectrum (blue) with a model (red). The upper panel, corresponding to Fig. 3, shows the spectral energy distribution (IUE low-resolution spectrum if available, visual and 2MASS photometry). The model SED was geometrically diluted according to the distance modulus *DM* and reddened with E_{b-v} as given in the figure. Keywords CARDELLI or FITZPATRICK indicate the applied reddening law (default: Seaton's law), the given parameter being R_V (see Sect. 4.2).

Most models were taken from our PoWR model grids (see Hamann & Gräfener 2004). The grid parameters are $\log T_*$ and $\log R_t$. Note that the grids were calculated for a fixed luminosity of $\log L/L_\odot$ = 5.3, and only scaled for the individual star; the scaling factor is indicated as the logarithmic "shift" in the plots. The so-called WNE grid is calculated for zero hydrogen and a terminal wind velocity of 1600 km/s, while the models in the WNL grid have 20% hydrogen (by mass) and v_∞ = 1000 km/s.

As the plotted models are mostly taken from the prepared grids (if not otherwise stated), their hydrogen abundance X_H and terminal velocity v_∞ do generally not agree precisely with the final parameters of our analysis as given in Table 2.

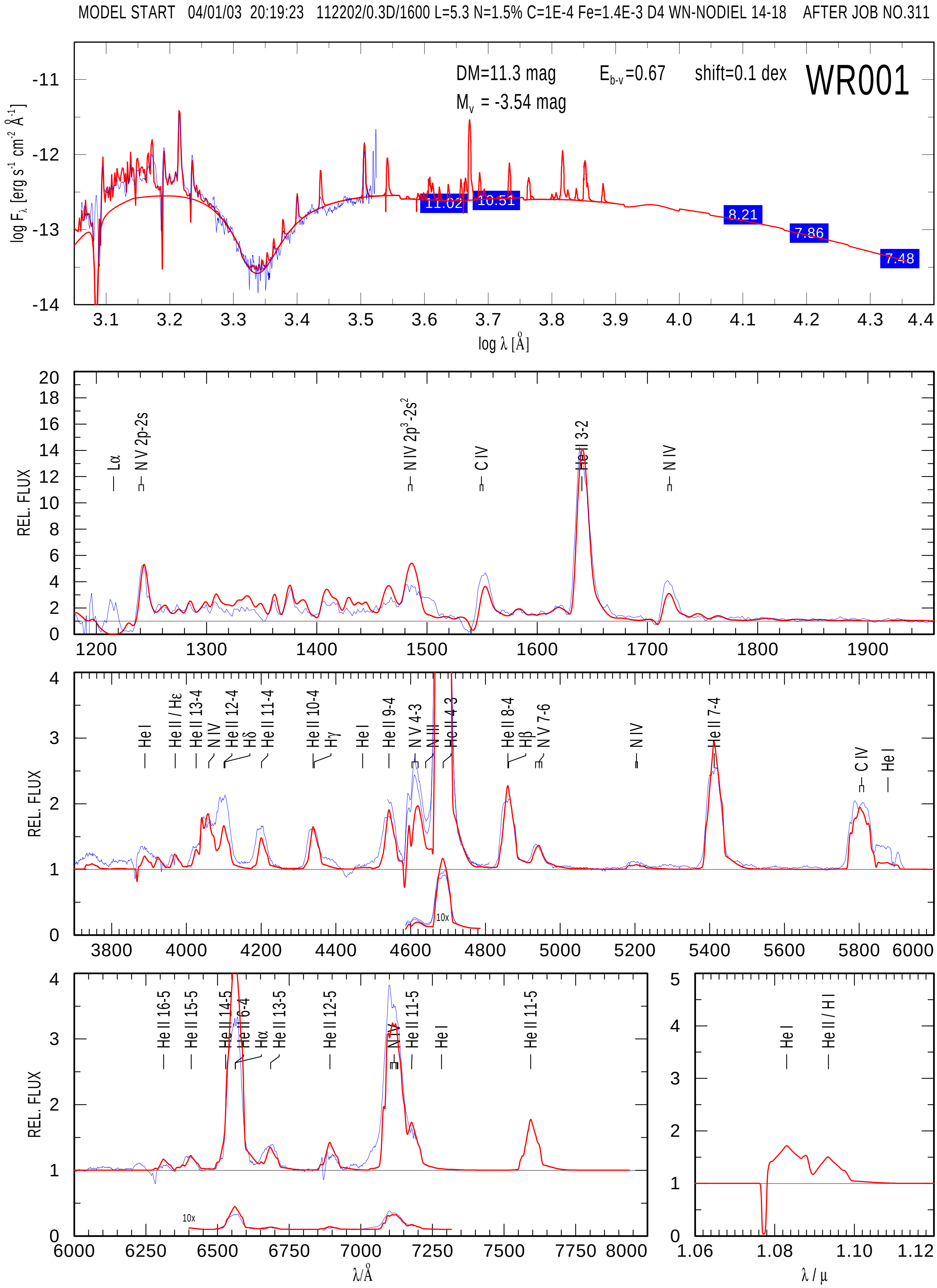

Fig. 12. Model: WNE 14-18, $T_* = 112$ kK, $\log(R_t/R_\odot) = 0.3$

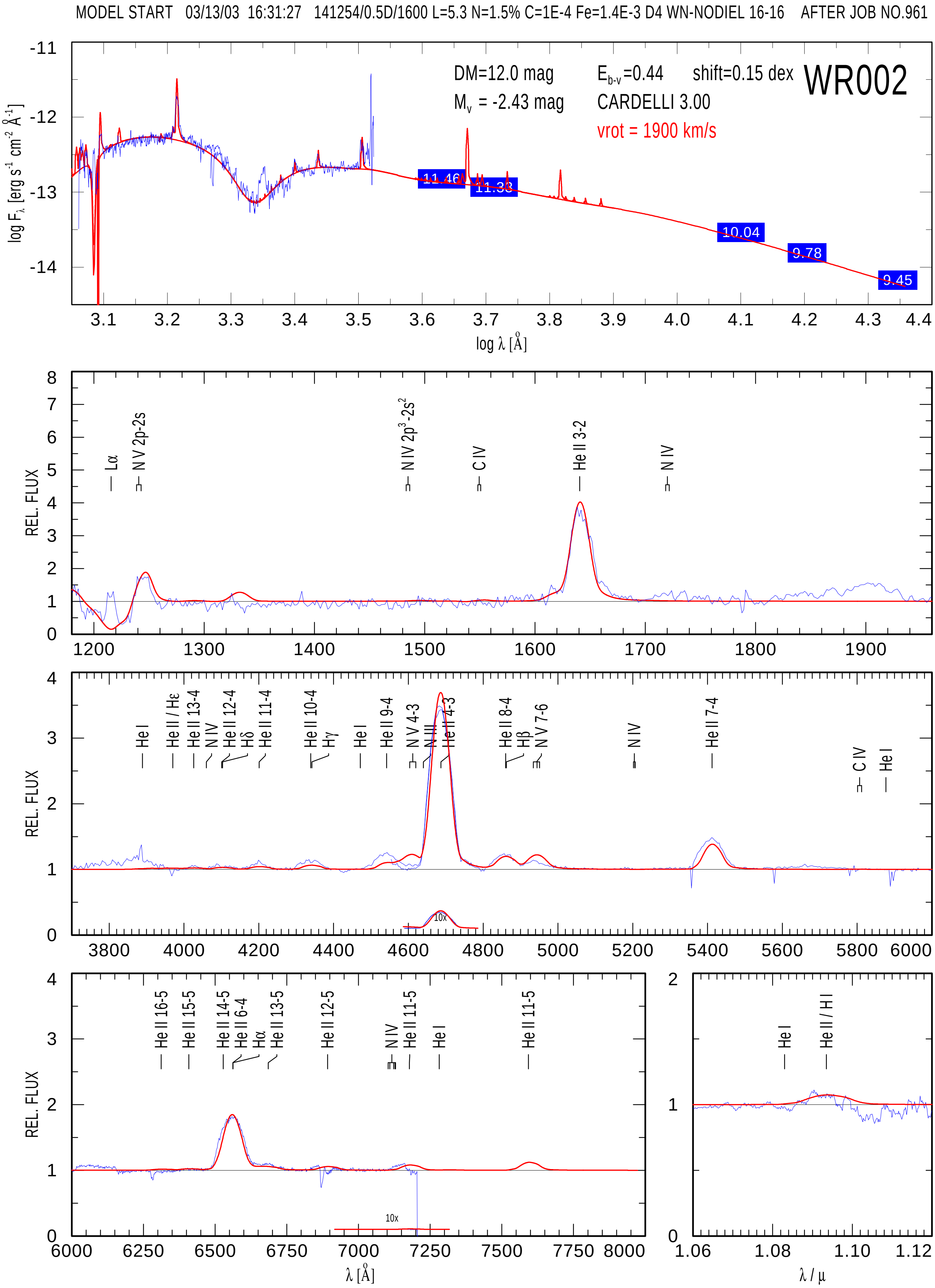

Fig. 13. Model: WNE 16-16, T_{*} = 141 kK, $\log(R_{\rm t}/R_{\odot})$ = 0.5

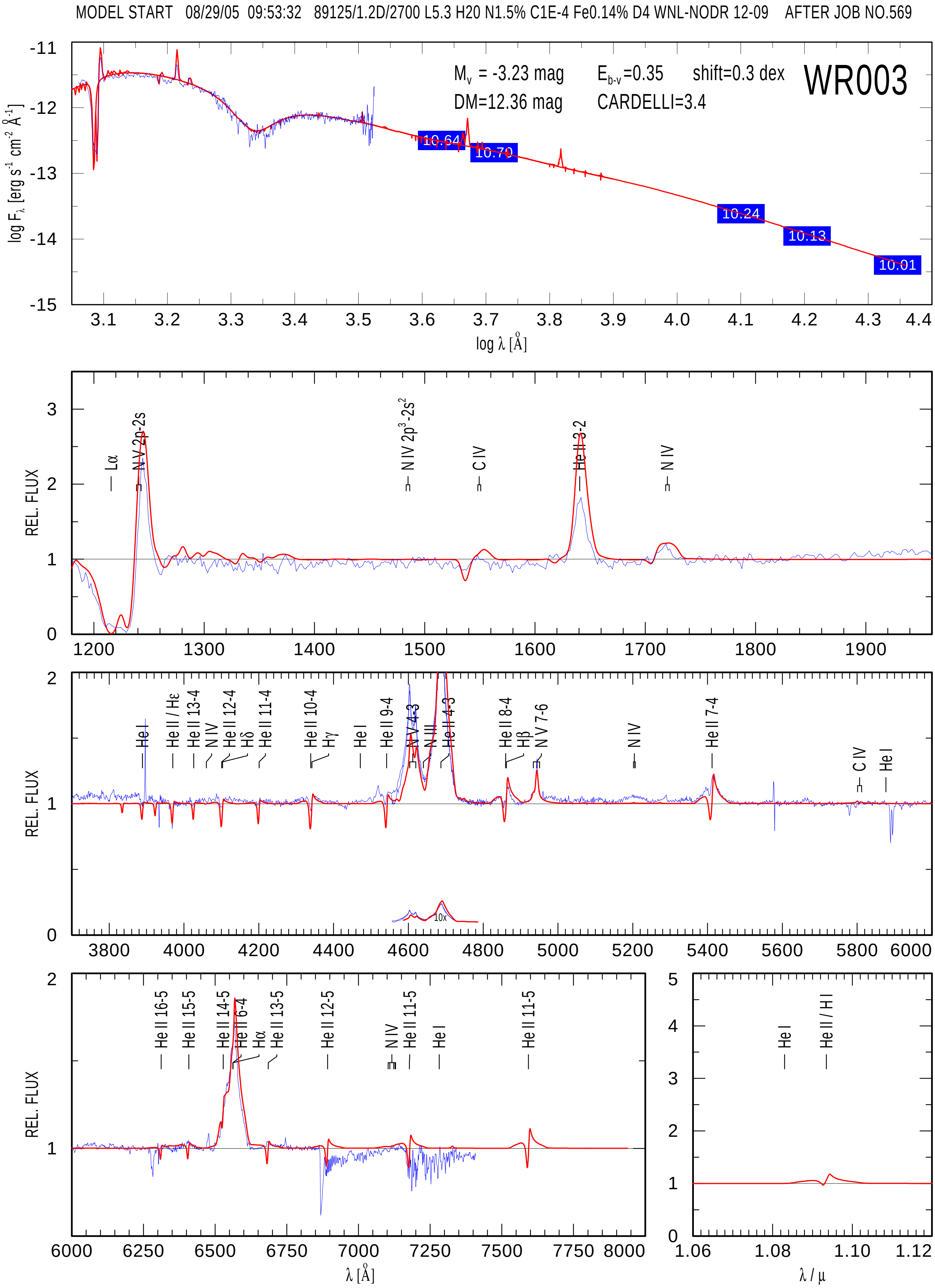

Fig. 14. Individual Model: WNL 12-09, $T_* = 89$ kK, $\log(R_t/R_\odot) = 1.2$ but $v_\infty = 2700$ km/s

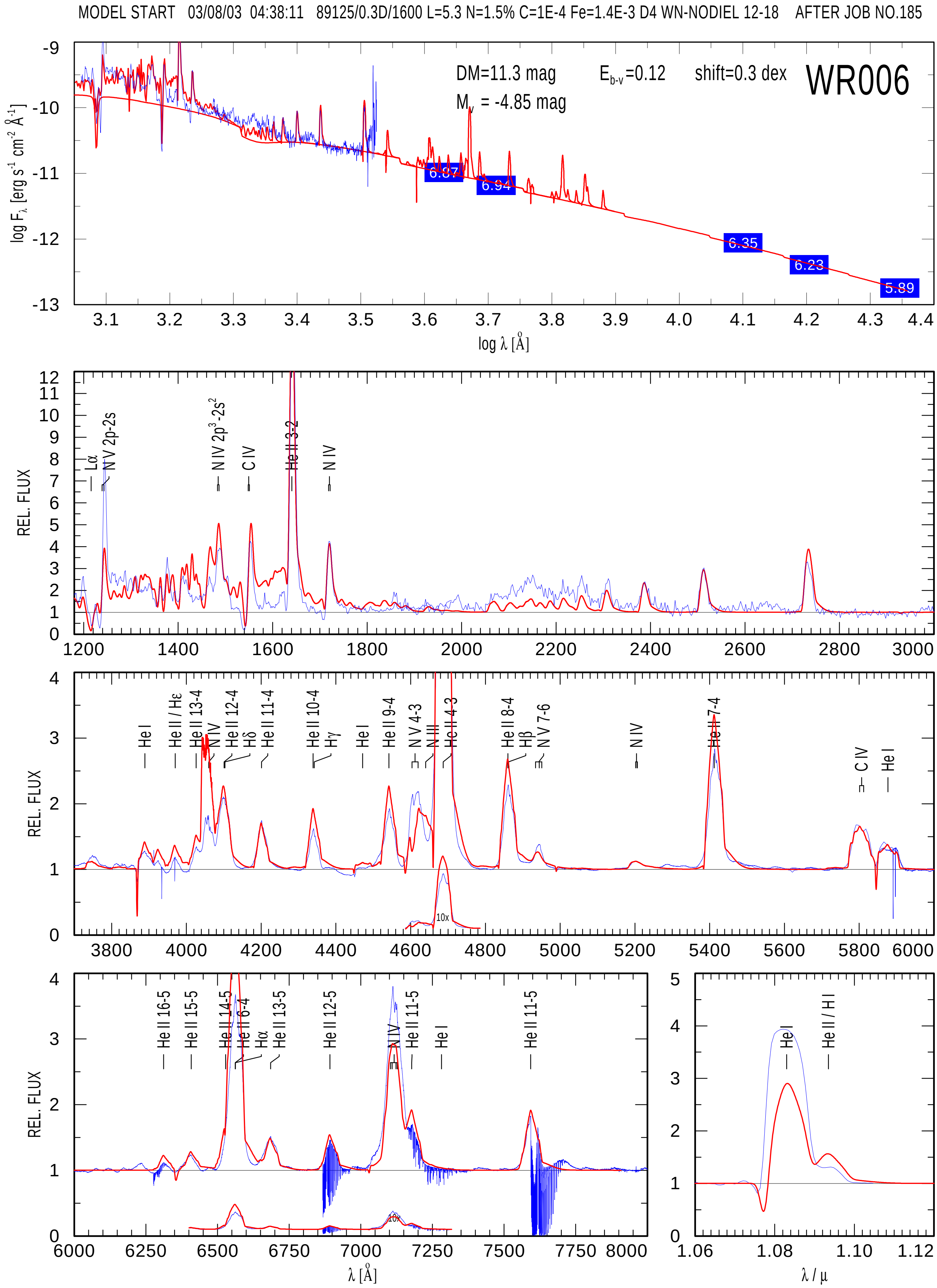

Fig. 15. Model: WNE 12-18, $T_* = 89\,\mathrm{kK}$, $\log(R_t/R_\odot) = 0.3$

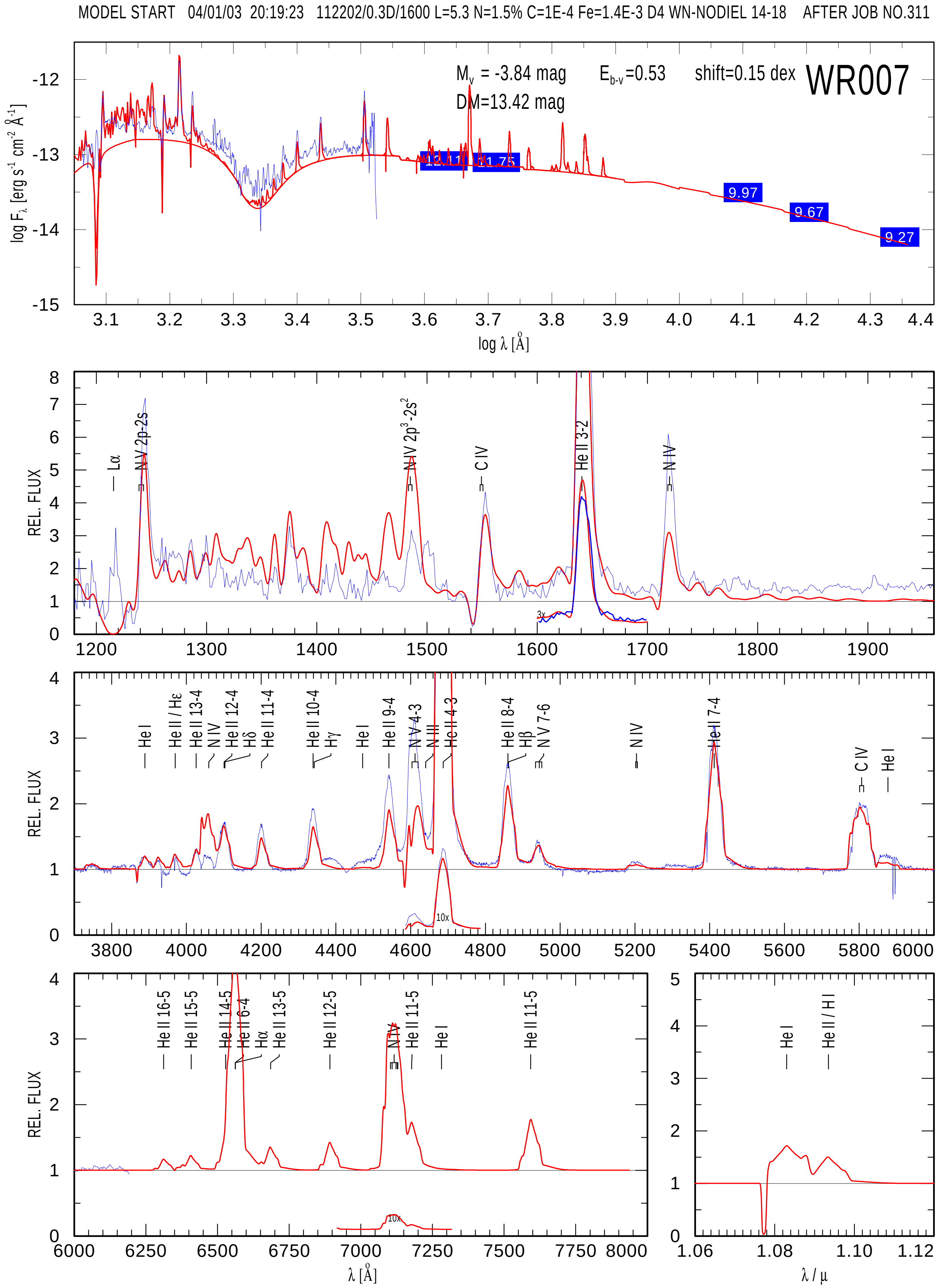

Fig. 16. Model: WNE 14-18, T_{*} = 112 kK, $\log(R_{t}/R_{\odot}) = 0.3$

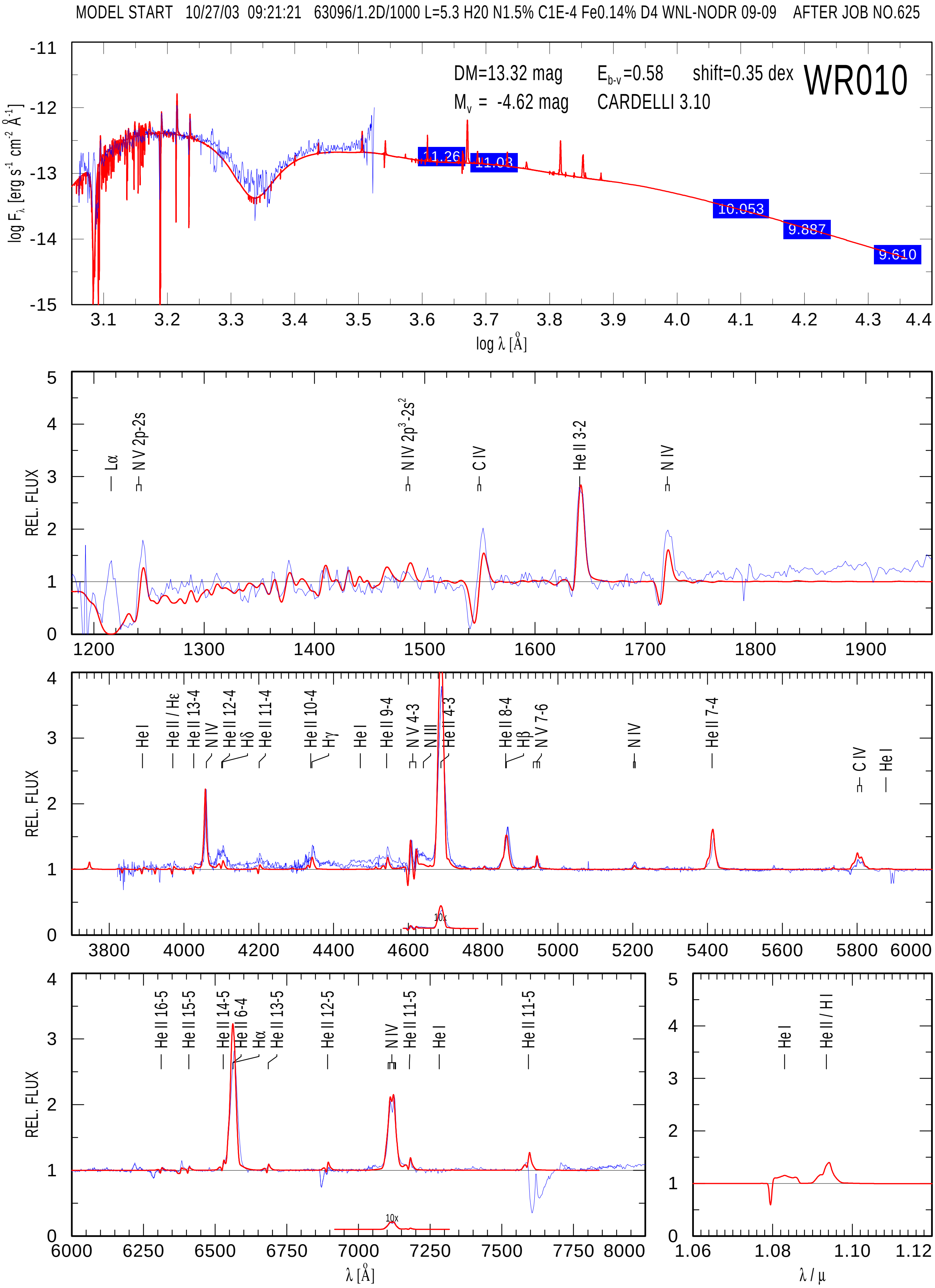

Fig. 17. Model: WNL 09-09, T_* = 63 kK, $\log(R_t/R_\odot)$ = 1.2

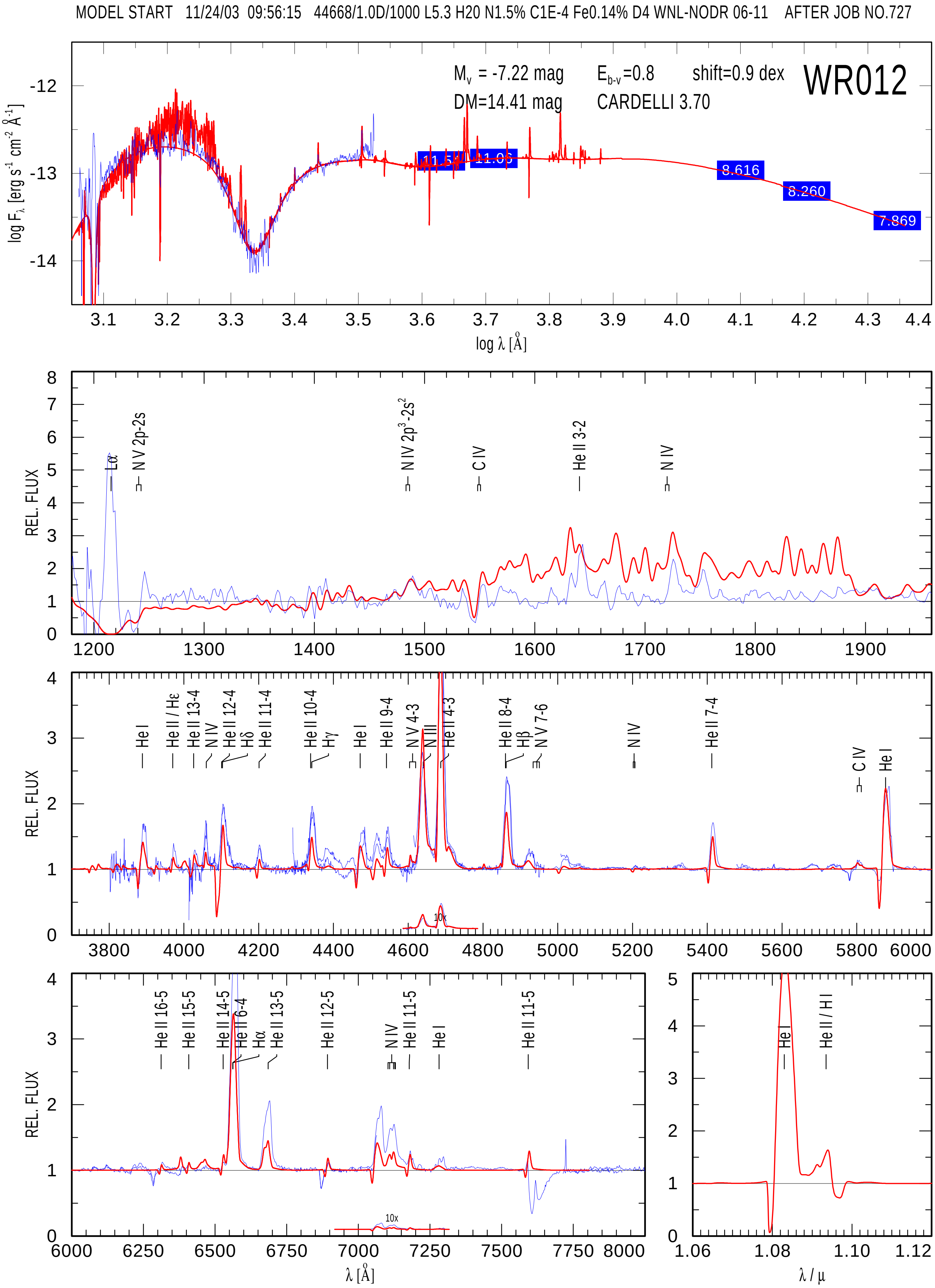

Fig. 18. Model: WNL 06-11, $T_* = 45\,\mathrm{kK}$, $\log(R_t/R_\odot) = 1.0$

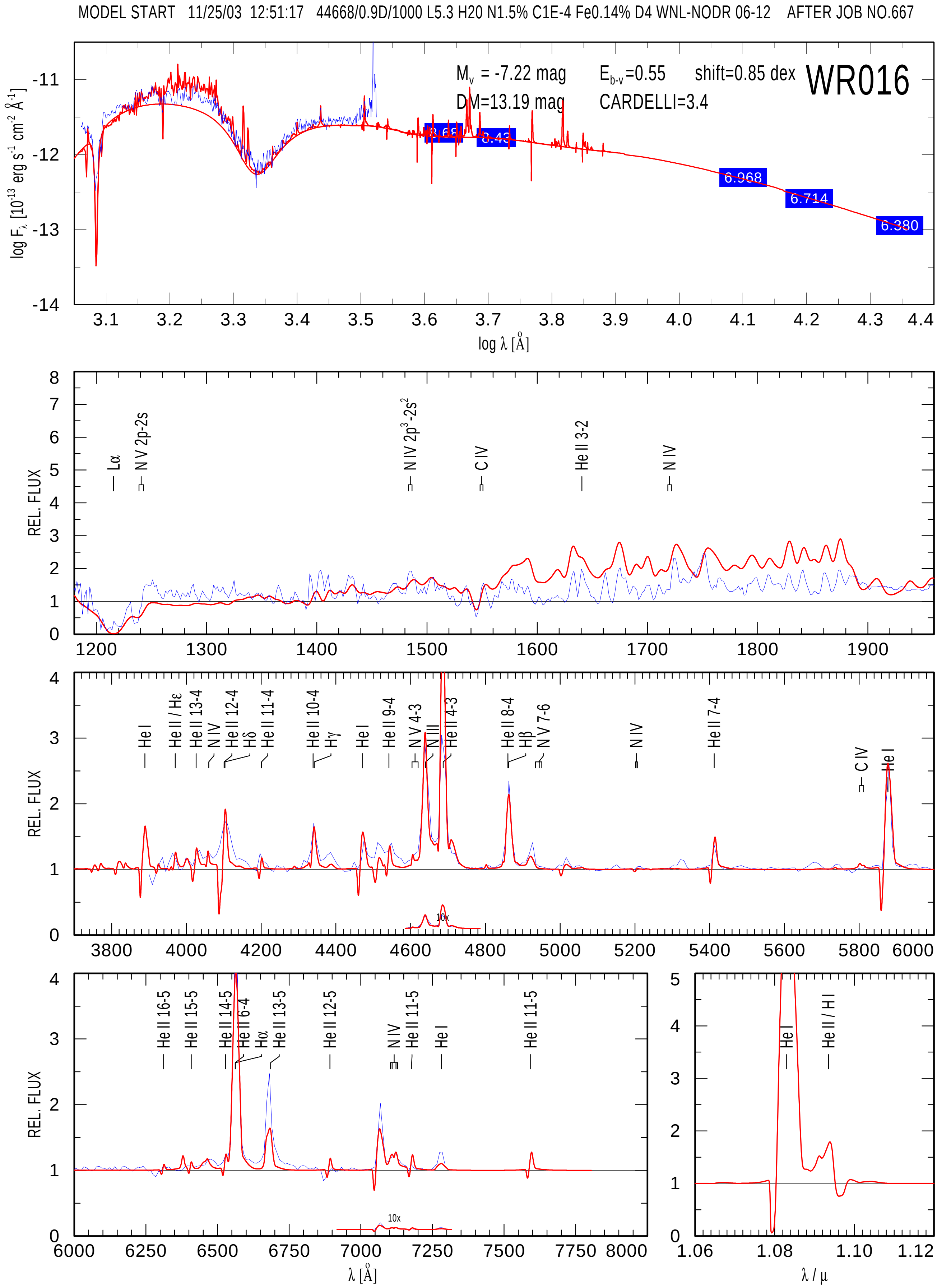

Fig. 19. Model: WNL 06-12, $T_* = 45$ kK, $\log(R_t/R_\odot) = 0.9$

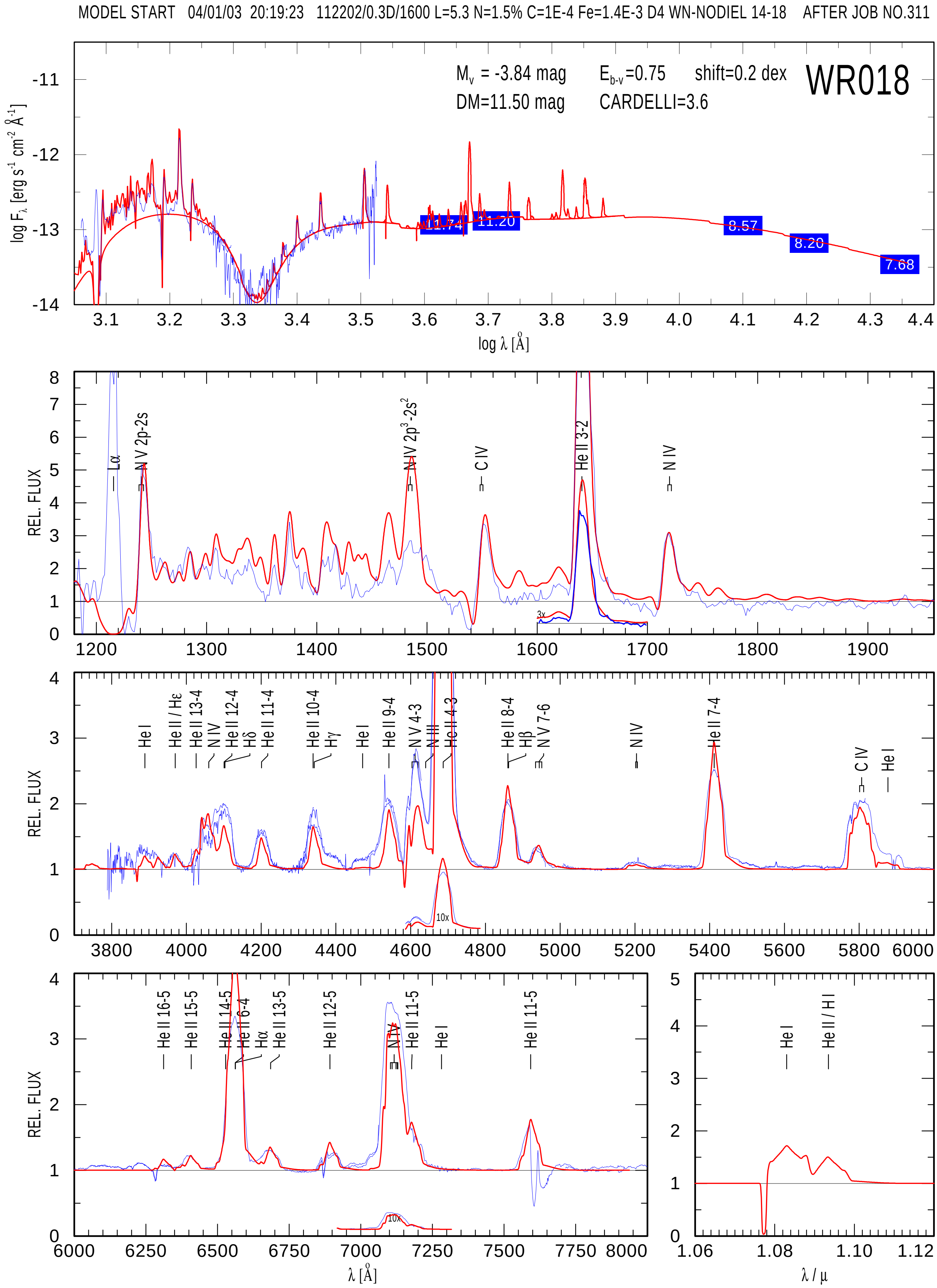

Fig. 20. Model: WNE 14-18, $T_* = 112$ kK, $\log(R_t/R_\odot) = 0.3$

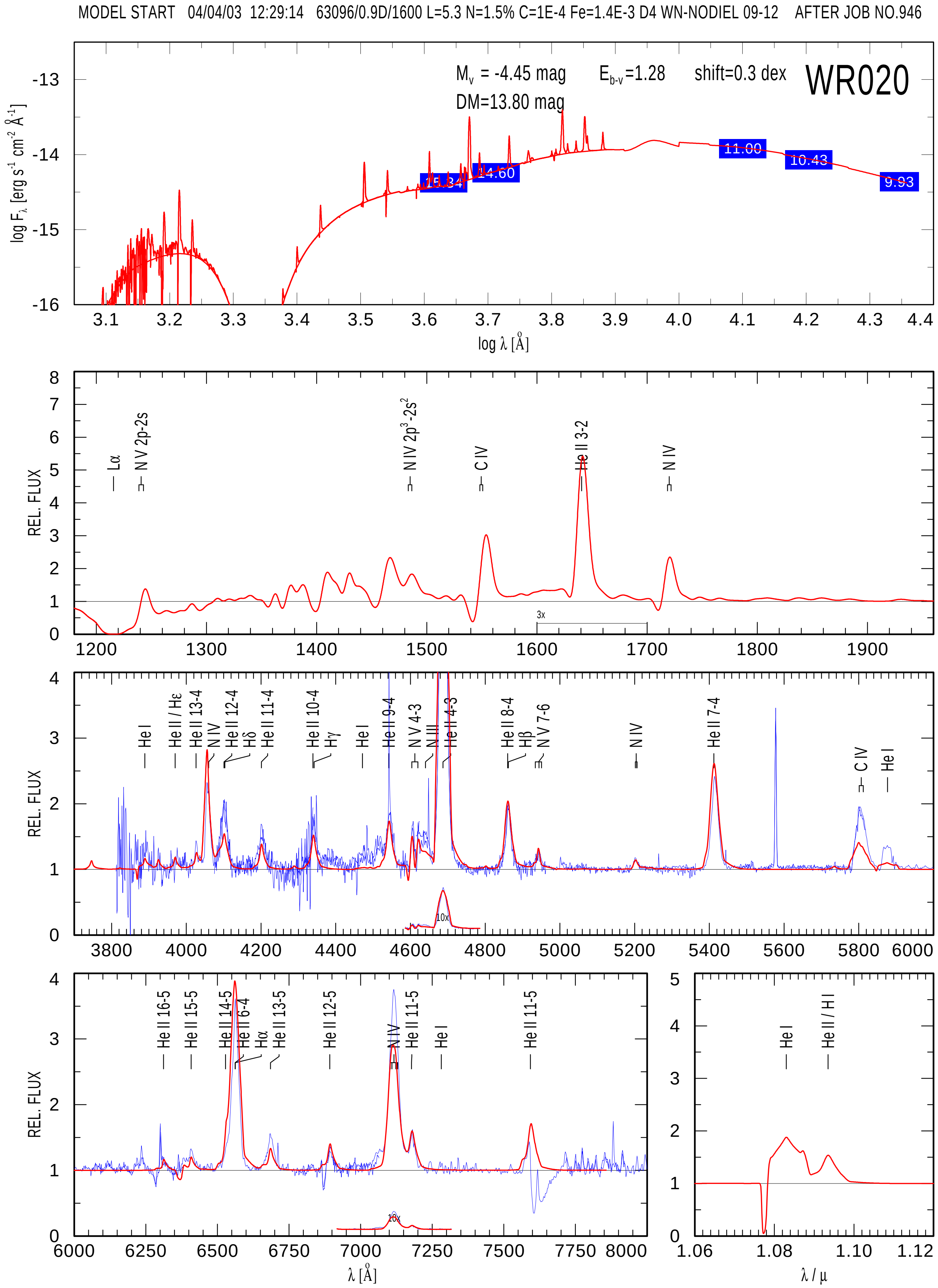

Fig. 21. Model: WNE 09-12, $T_* = 63\,\mathrm{kK}$, $\log(R_t/R_\odot) = 0.9$

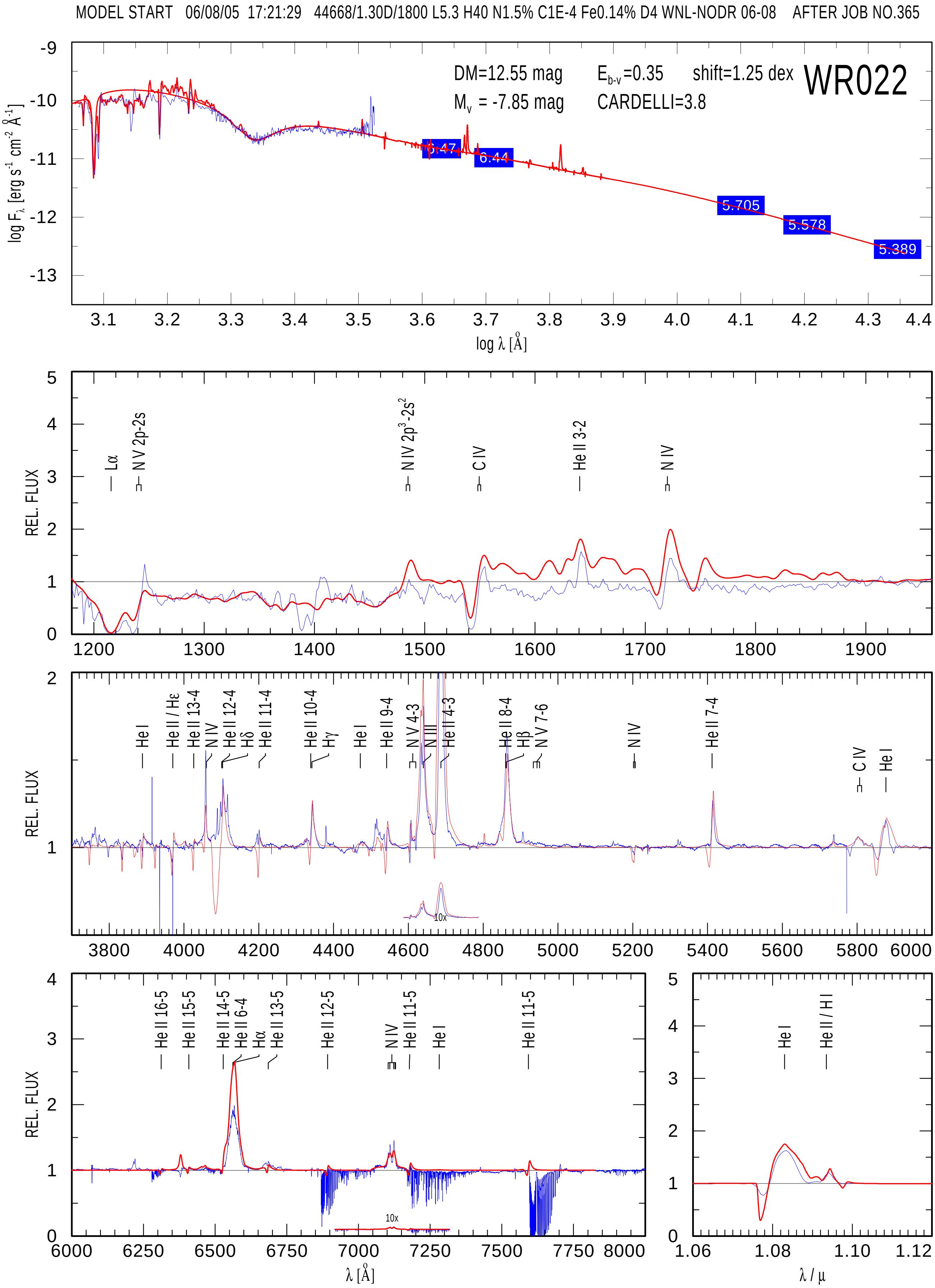

Fig. 22. Individual Model: 06-08, $T_* = 45$ kK, $\log(R_t/R_\odot) = 1.3$ with $v_\infty = 1800$ km/s and $X_H = 0.40$

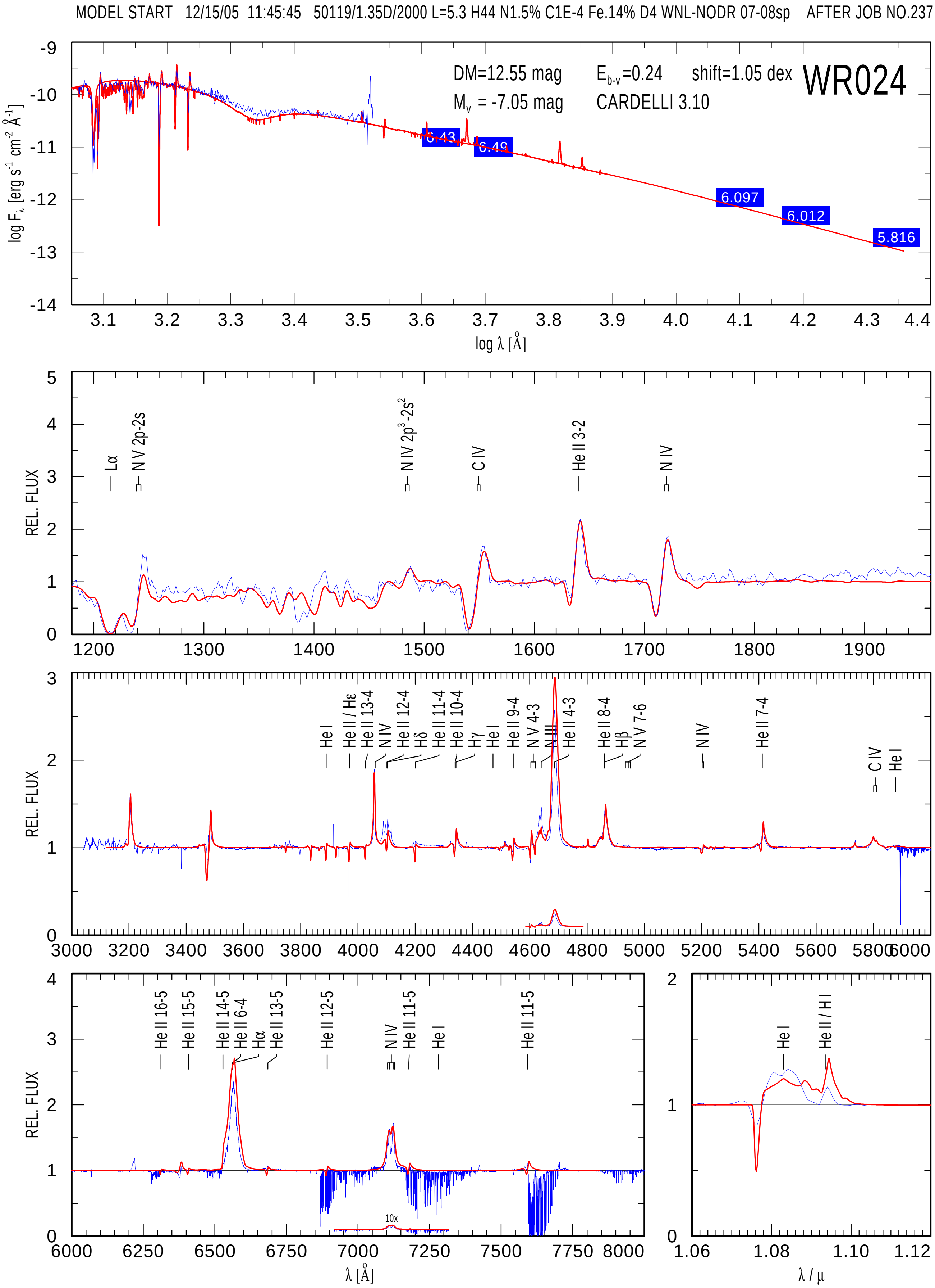

Fig. 23. Individual Model: 07-08, $T_* = 50\,\mathrm{kK}$, $\log(R_t/R_\odot) = 1.35$ with $\upsilon_\infty = 2000$ km/s and $X_H = 0.44$

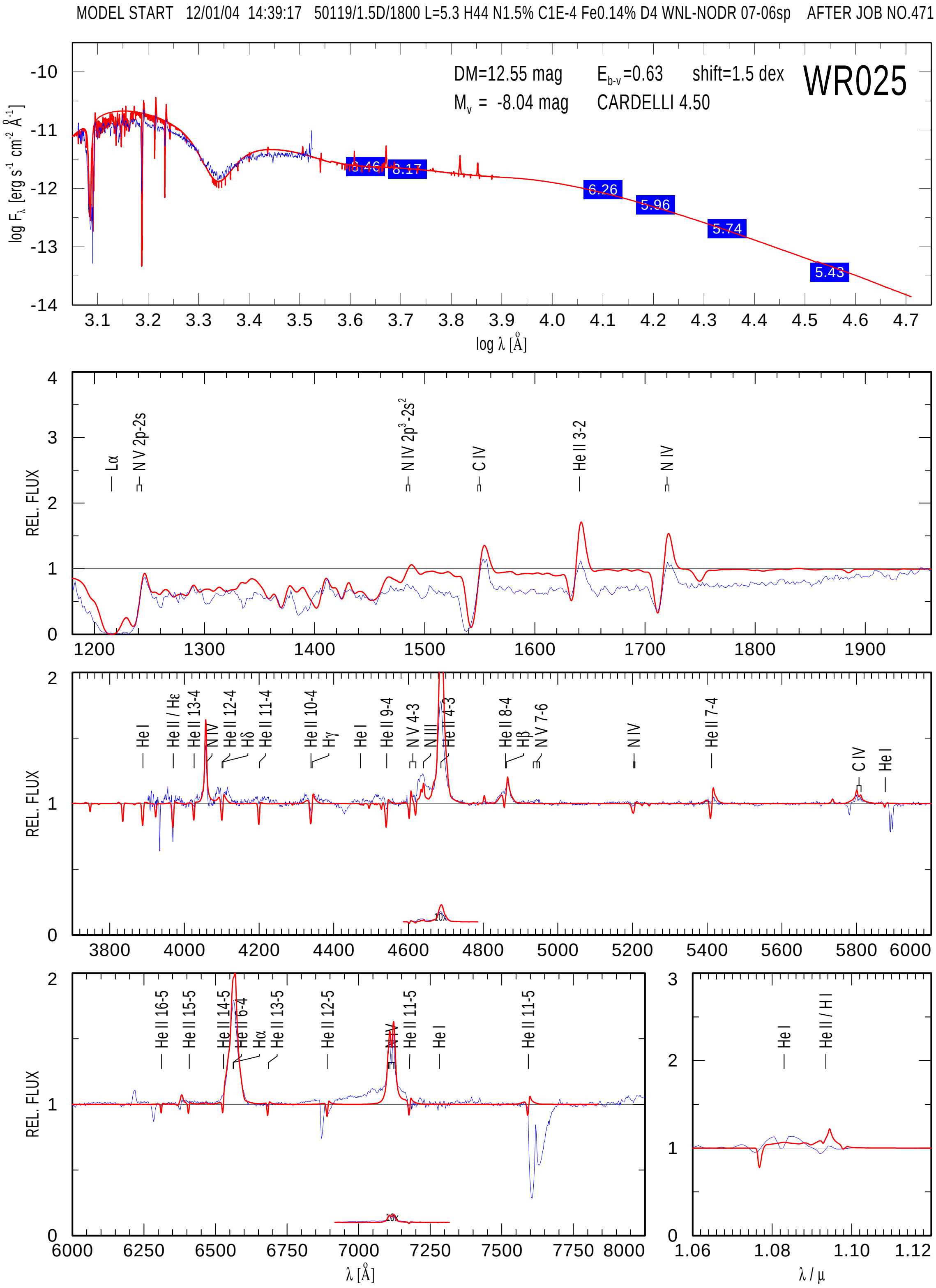

Fig. 24. Individual Model: 07-06, $T_* = 50\,\mathrm{kK}$, $\log(R_\mathrm{t}/R_\odot) = 1.5$ with $\upsilon_\infty = 1800$ km/s and $X_\mathrm{H} = 0.44$

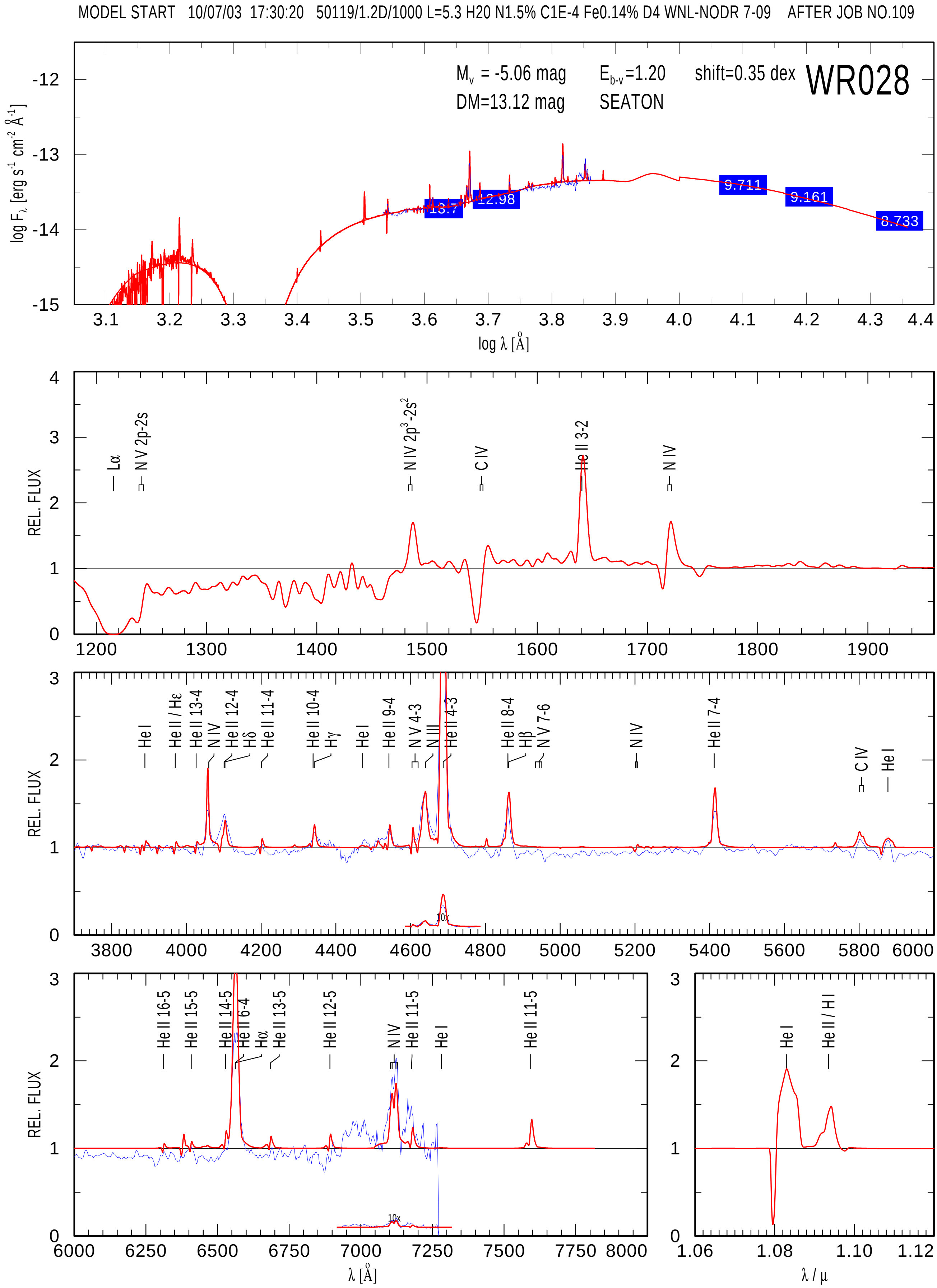

Fig. 25. Model: WNL 07-09, T_{*} = 50 kK, $\log(R_t/R_\odot)$ = 1.2

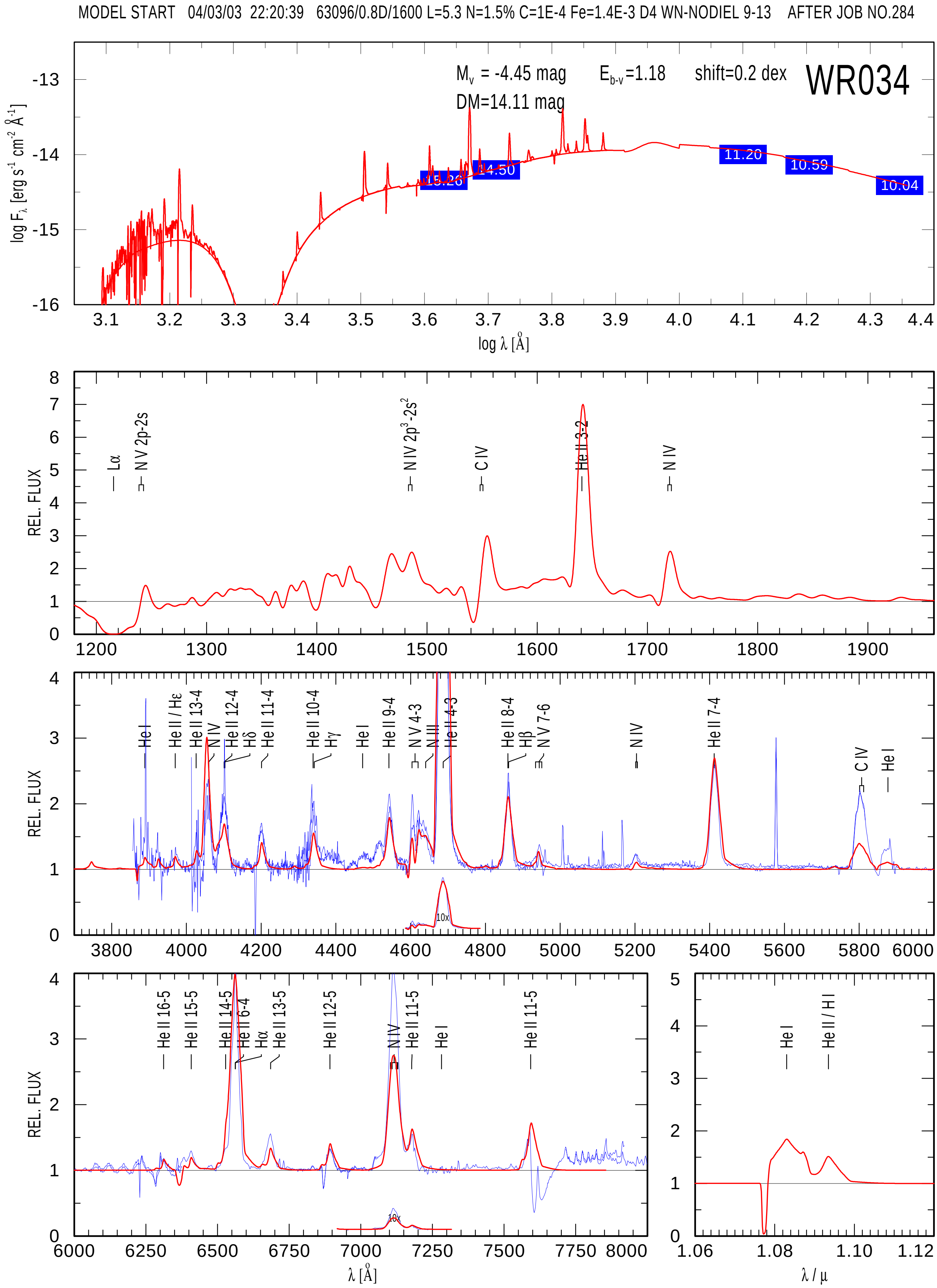

Fig. 26. Model: WNE 09-13, T_{*} = 63 kK, $\log(R_{t}/R_{\odot})$ = 0.8

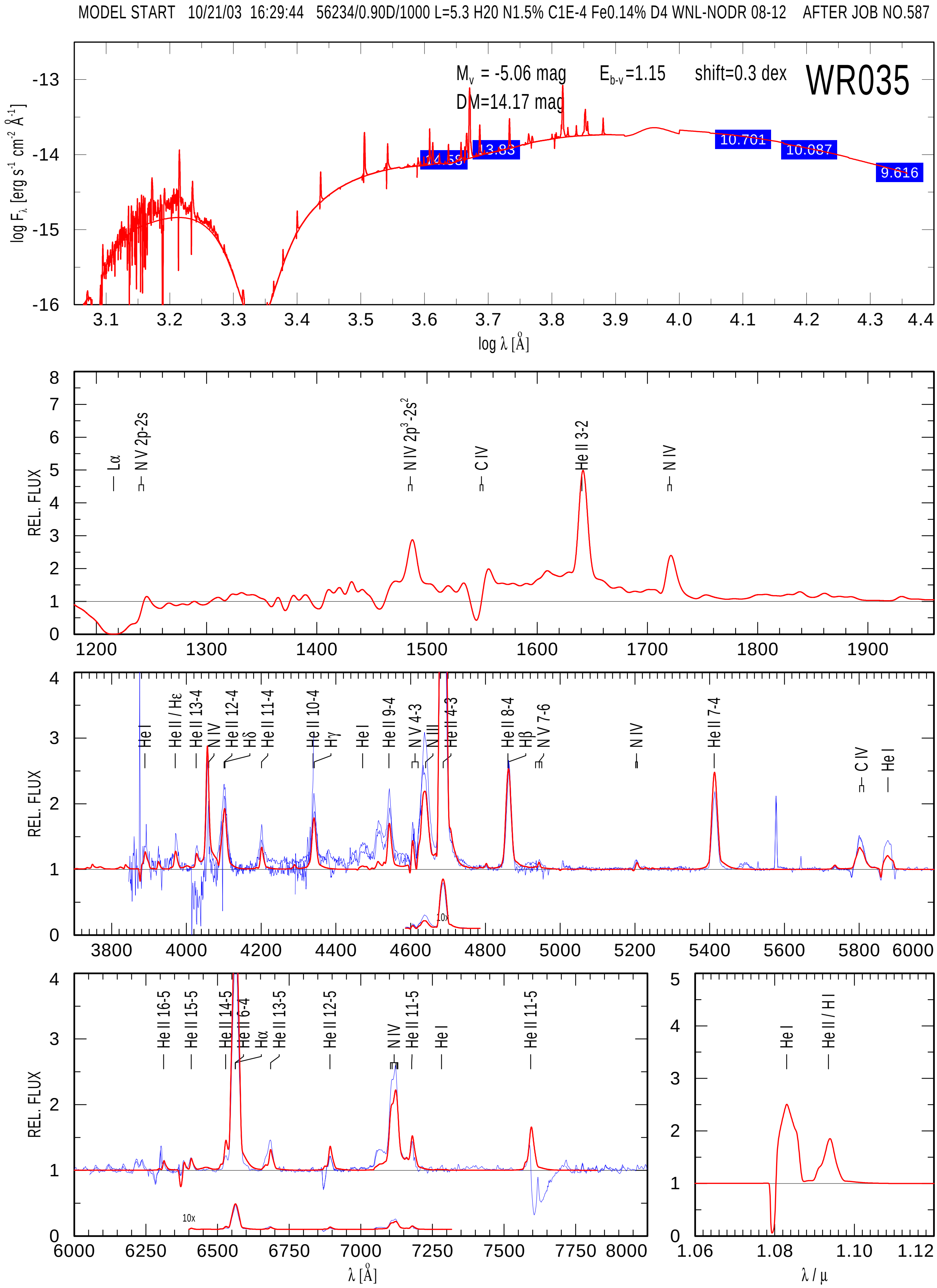

Fig. 27. Model: WNL 08-12, $T_* = 56\,\mathrm{kK}$, $\log(R_t/R_\odot) = 0.9$

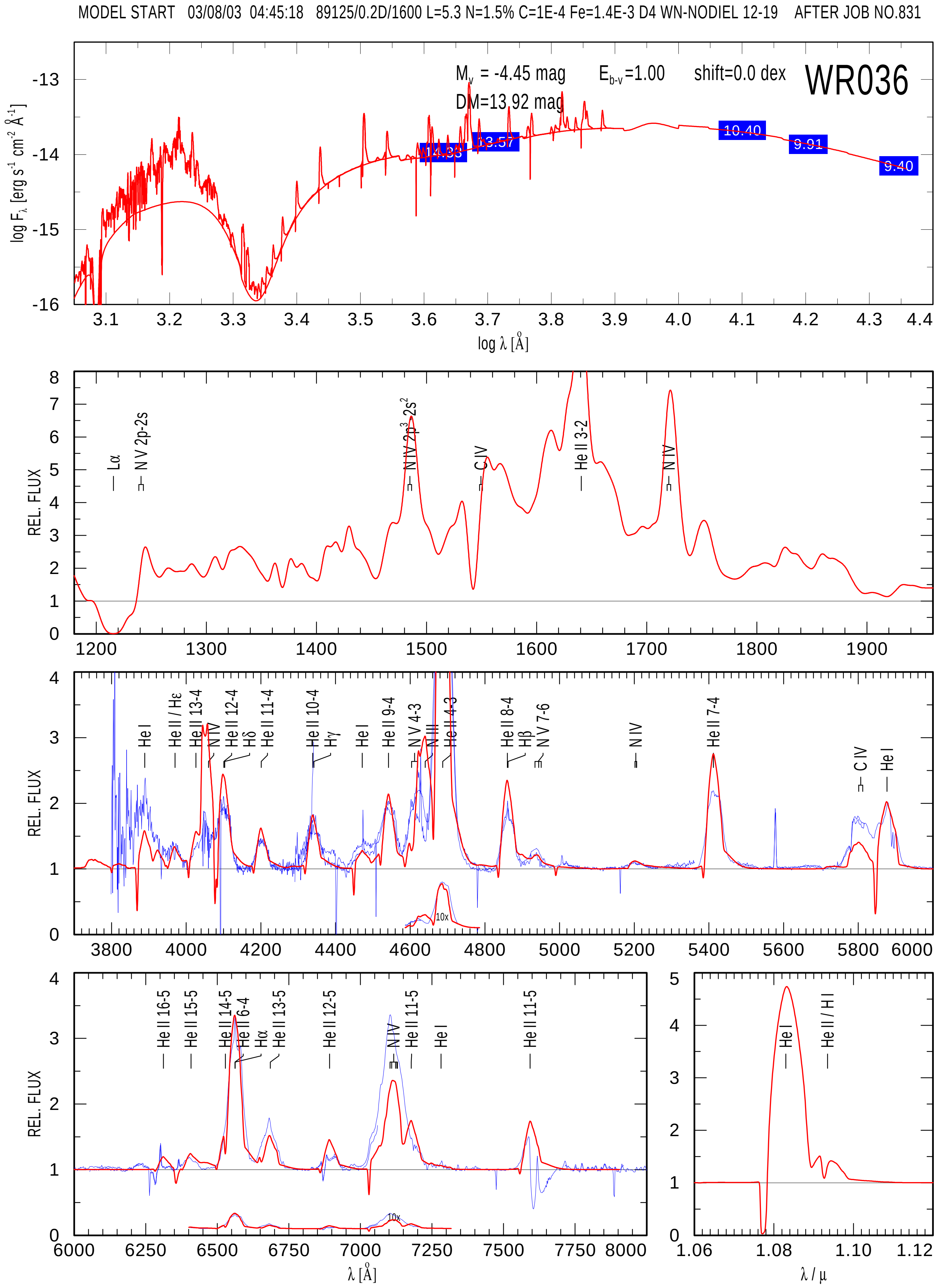

Fig. 28. Model: WNE 12-19, $T_* = 89$ kK, $\log(R_t/R_\odot) = 0.2$

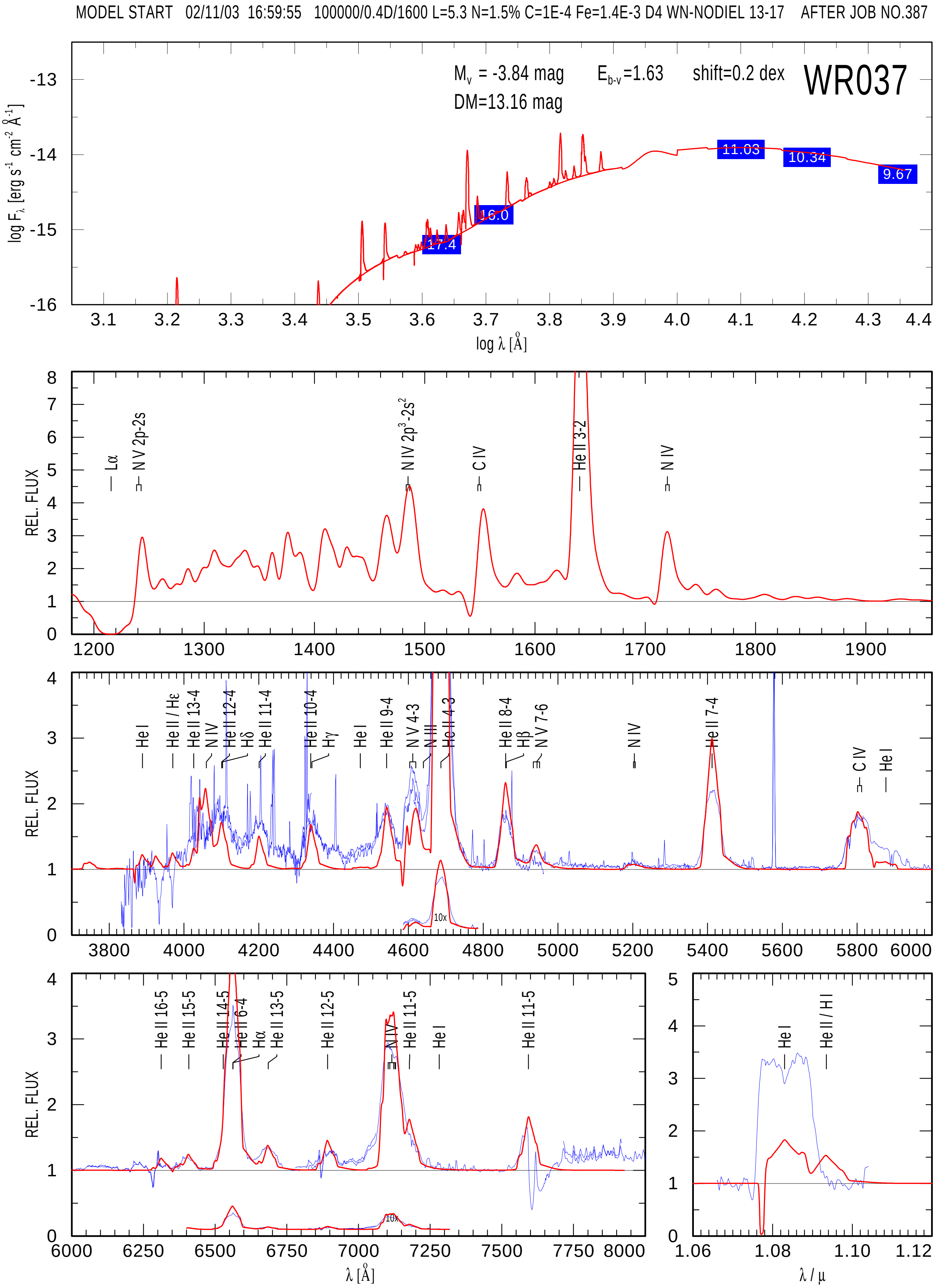

Fig. 29. Model: WNE 13-17, T_{*} = 100 kK, $\log(R_{\rm t}/R_{\odot})$ = 0.4

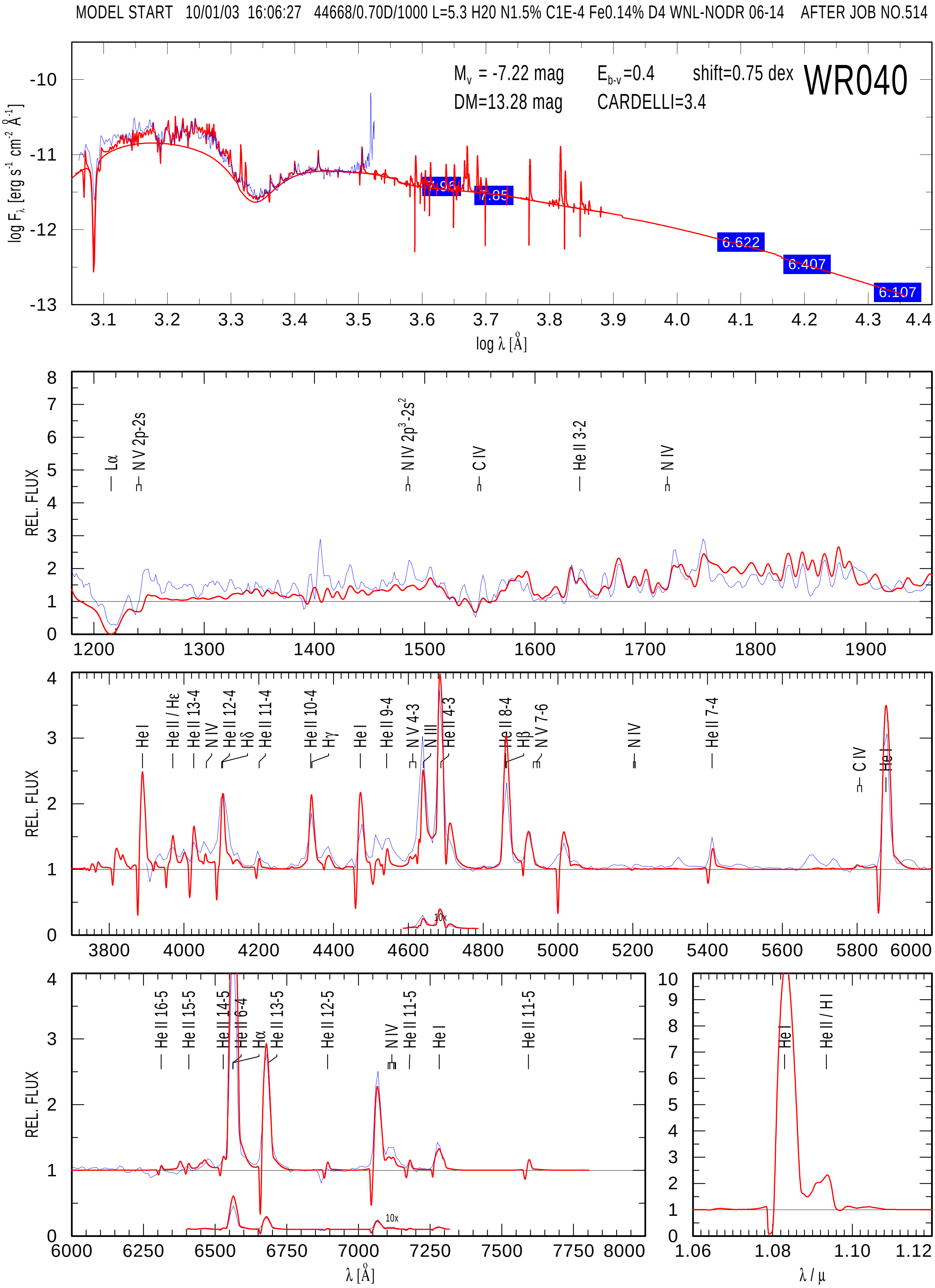

Fig. 30. Model: WNL 06-14, T_{*} = 45 kK, $\log(R_{\rm t}/R_{\odot})$ = 0.7

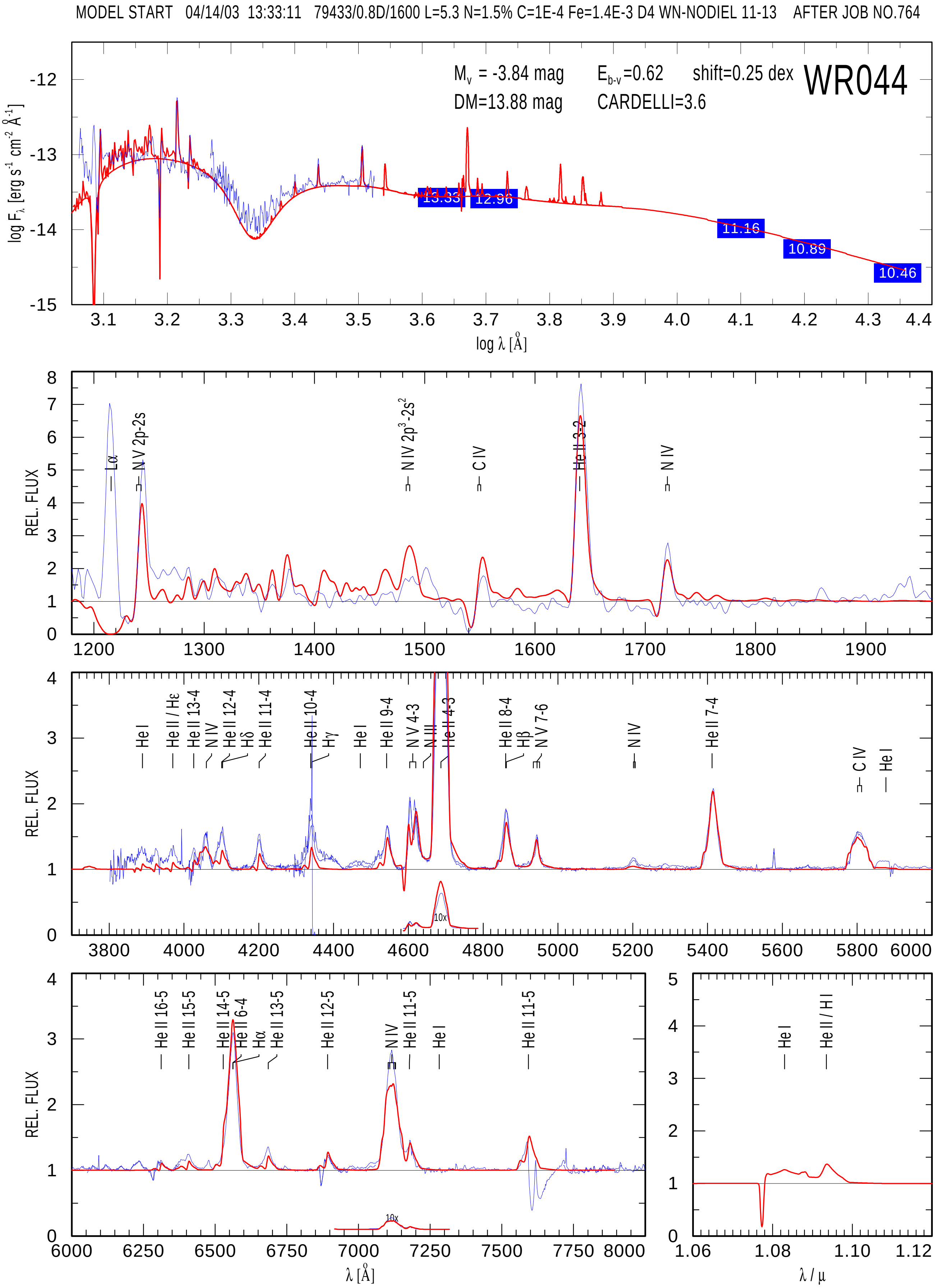

Fig. 31. Model: WNE 11-13, T_{*} = 79 kK, $\log(R_t/R_\odot)$ = 0.8

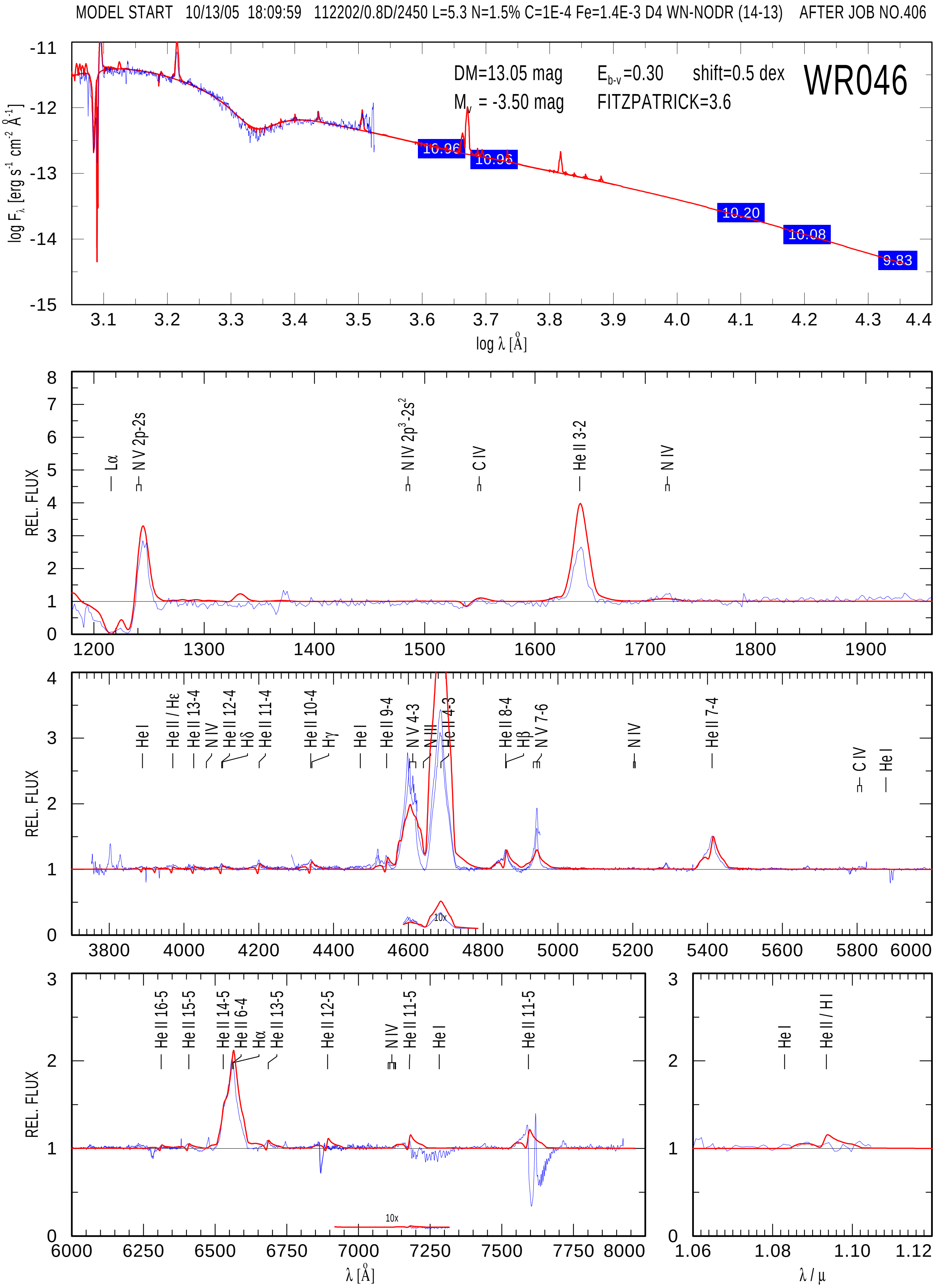

Fig. 32. Individual Model: WNE 14-13 $T_* = 112$ kK, $\log(R_t/R_\odot) = 0.8$ but $v_\infty = 2450$ km/s

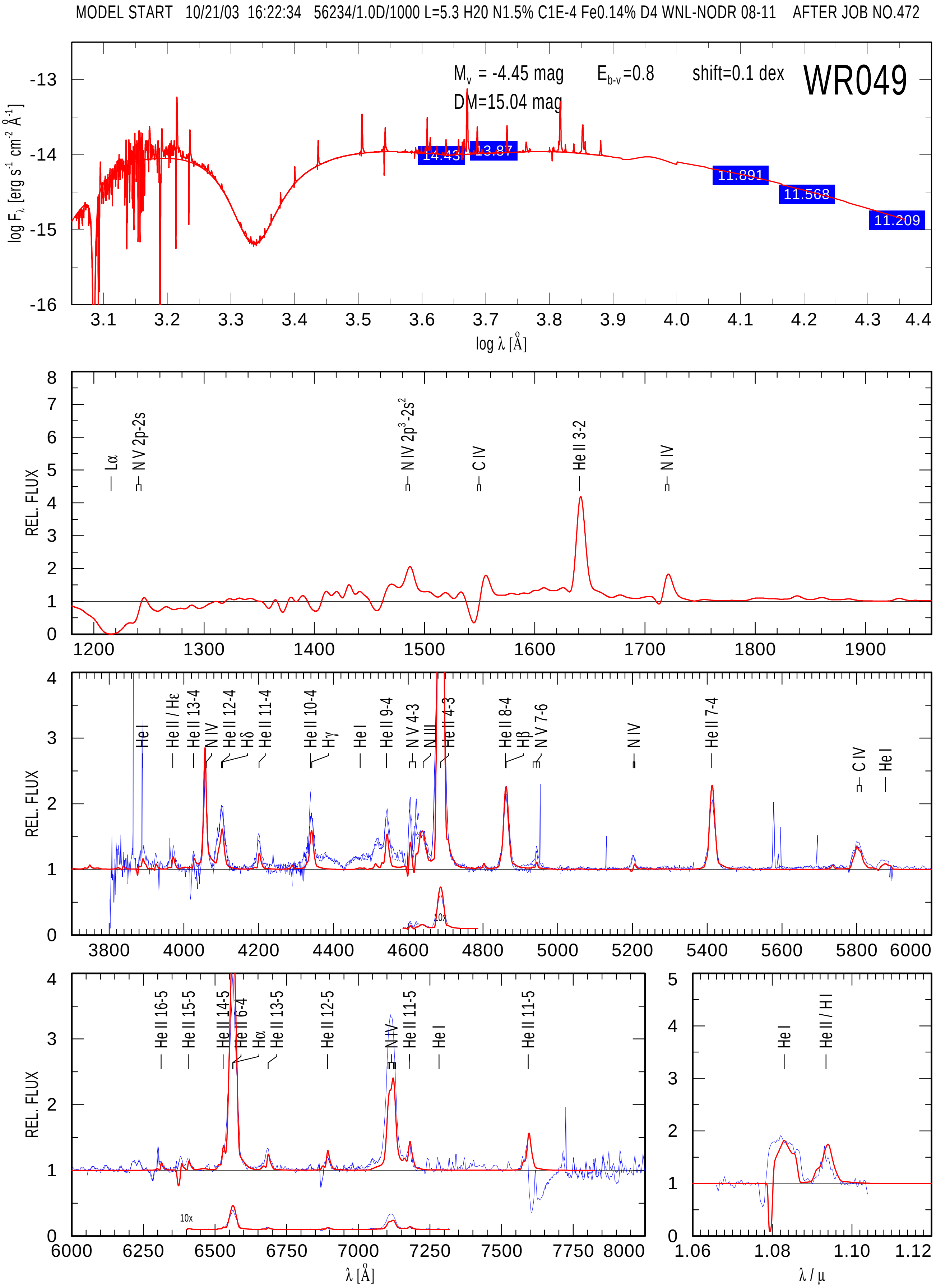

Fig. 33. Model: WNL 08-11, $T_* = 56\,\mathrm{kK}$, $\log(R_t/R_\odot) = 1.0$

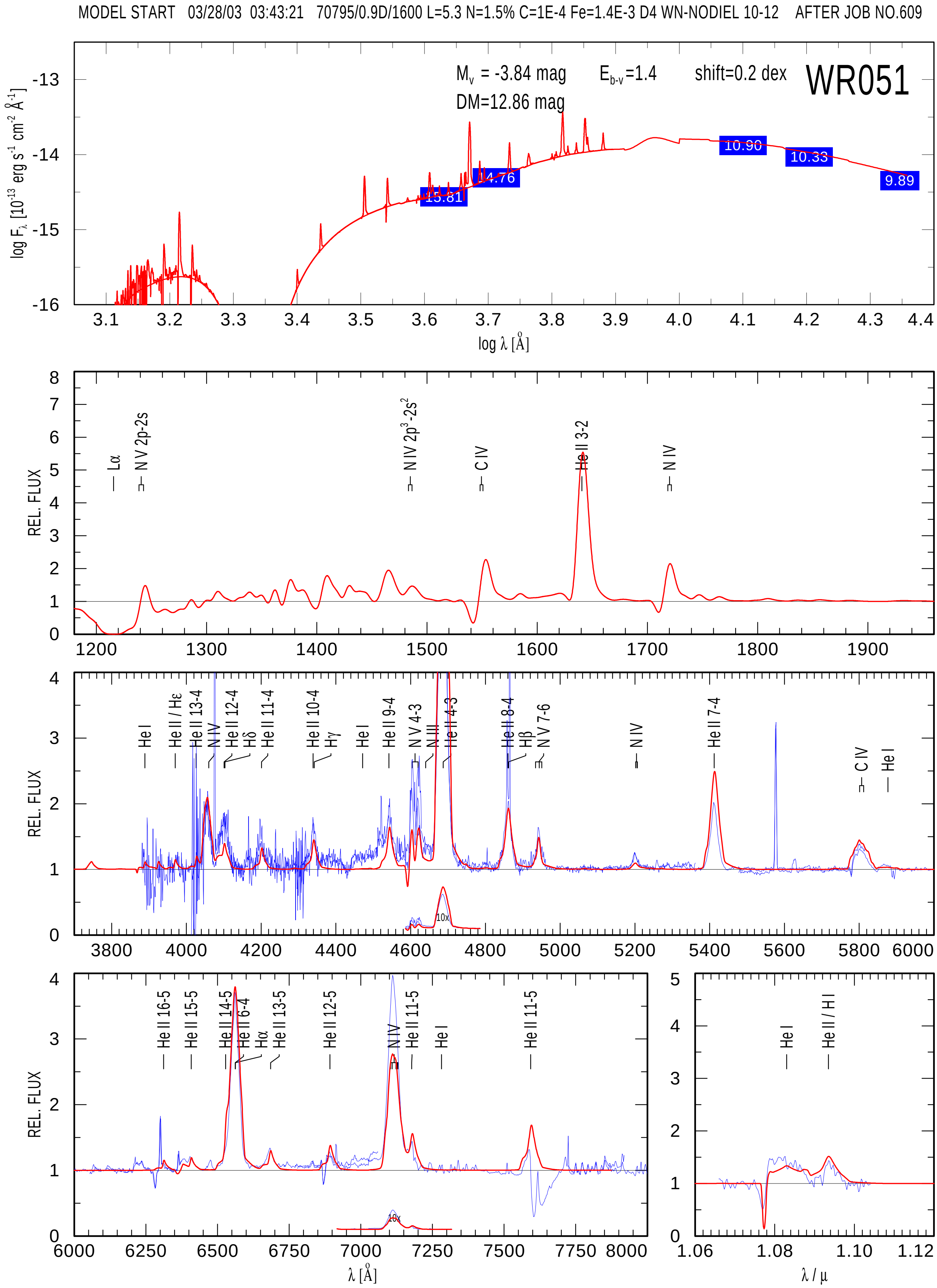

Fig. 34. Model: WNE 10-12, $T_* = 71$ kK, $\log(R_t/R_\odot) = 0.9$

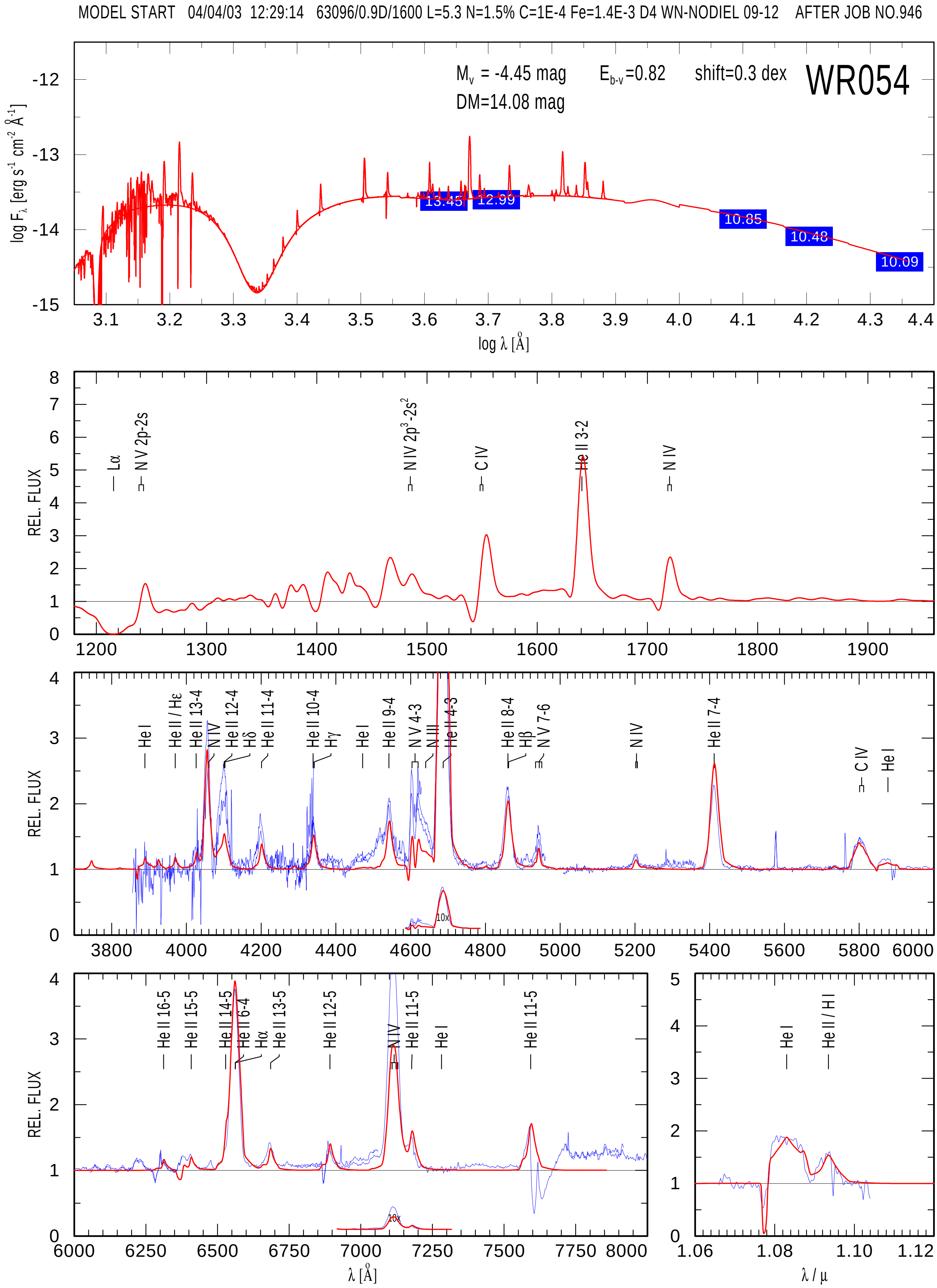

Fig. 35. Model: WNE 09-12, $T_* = 63$ kK, $\log(R_t/R_\odot) = 0.9$

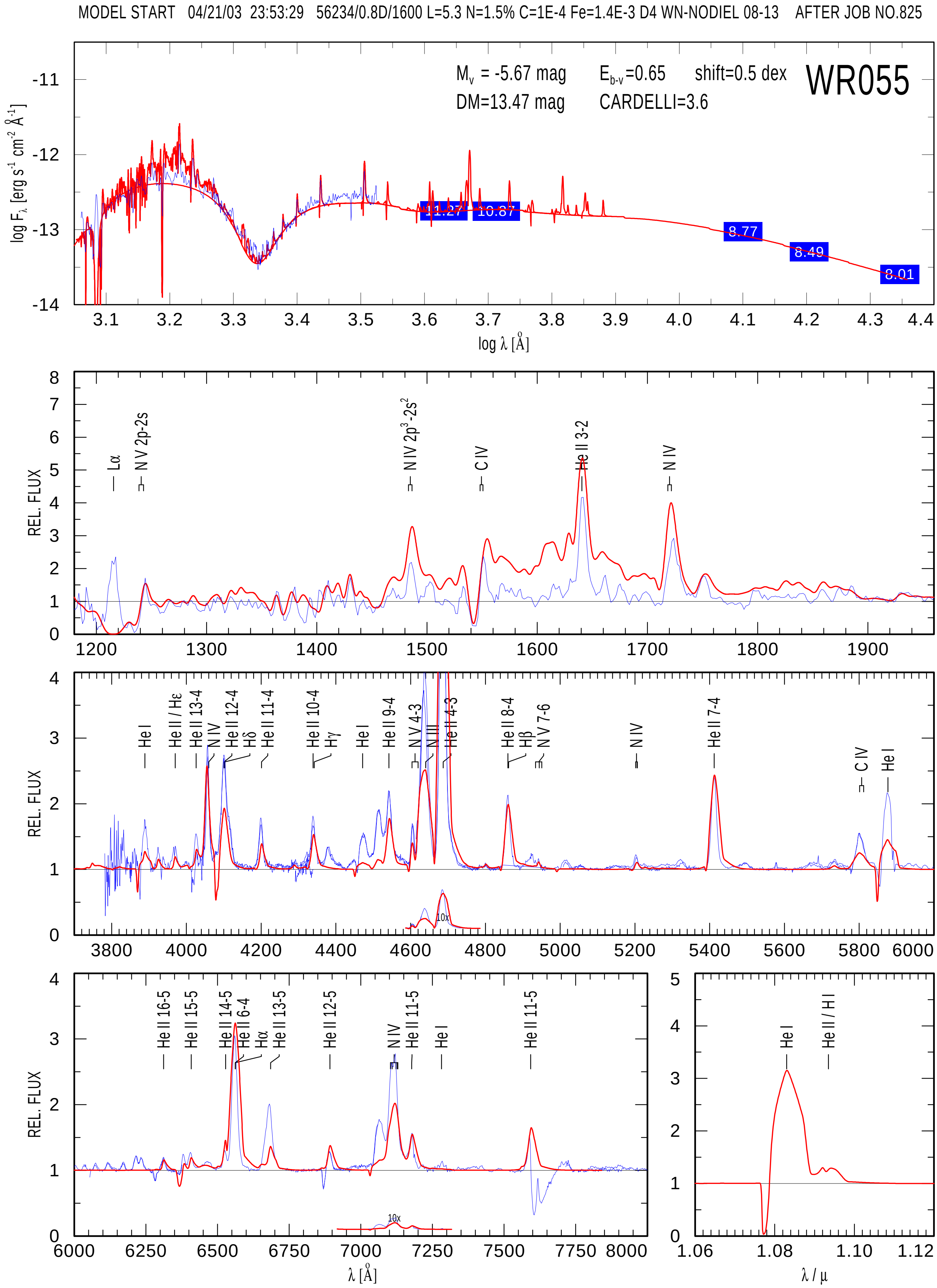

Fig. 36. Model: WNE 08-13, T_{*} = 56 kK, $\log(R_{t}/R_{\odot})$ = 0.8

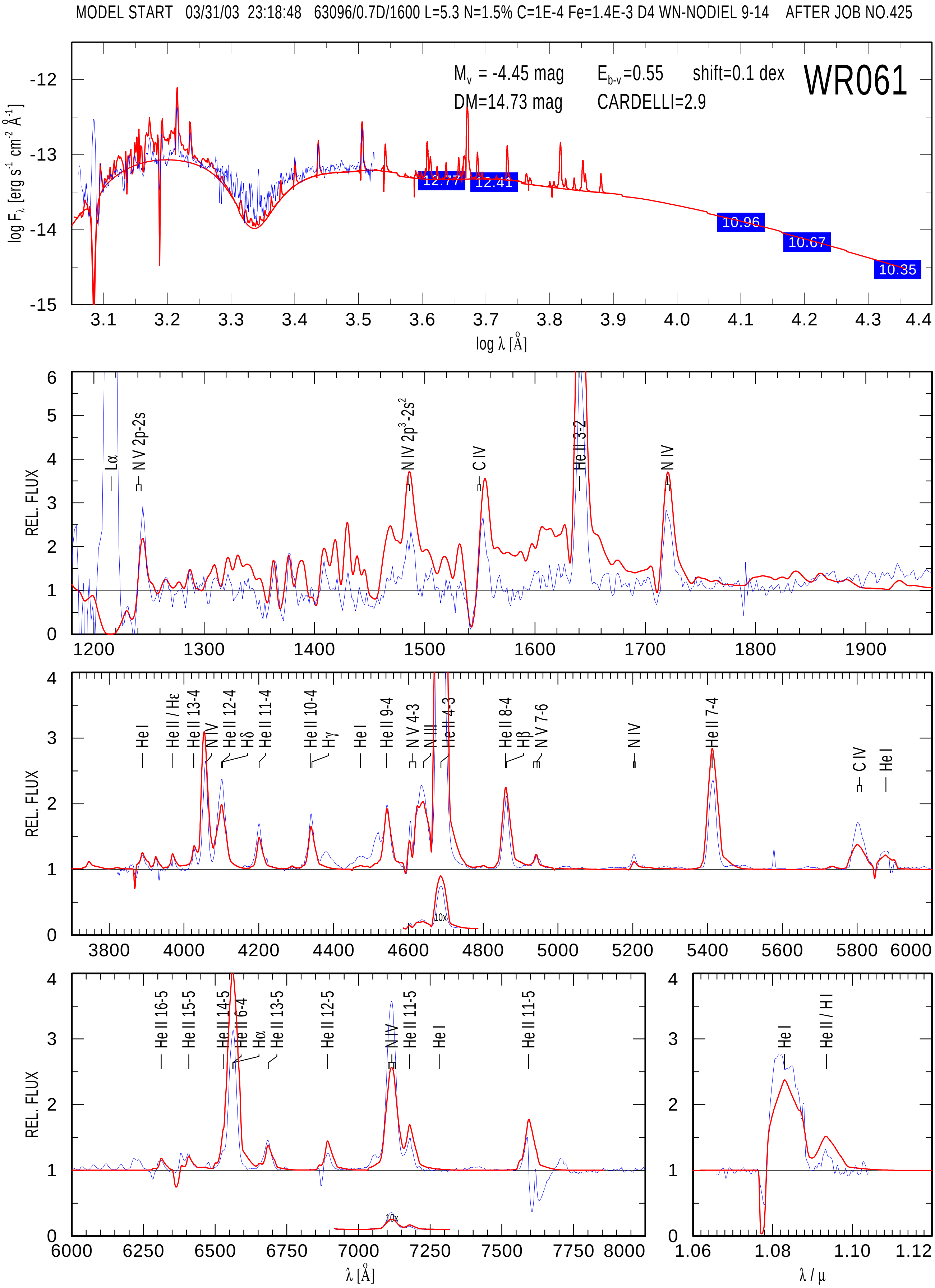

Fig. 37. Model: WNE 09-14, $T_* = 63\,\mathrm{kK}$, $\log(R_t/R_\odot) = 0.7$

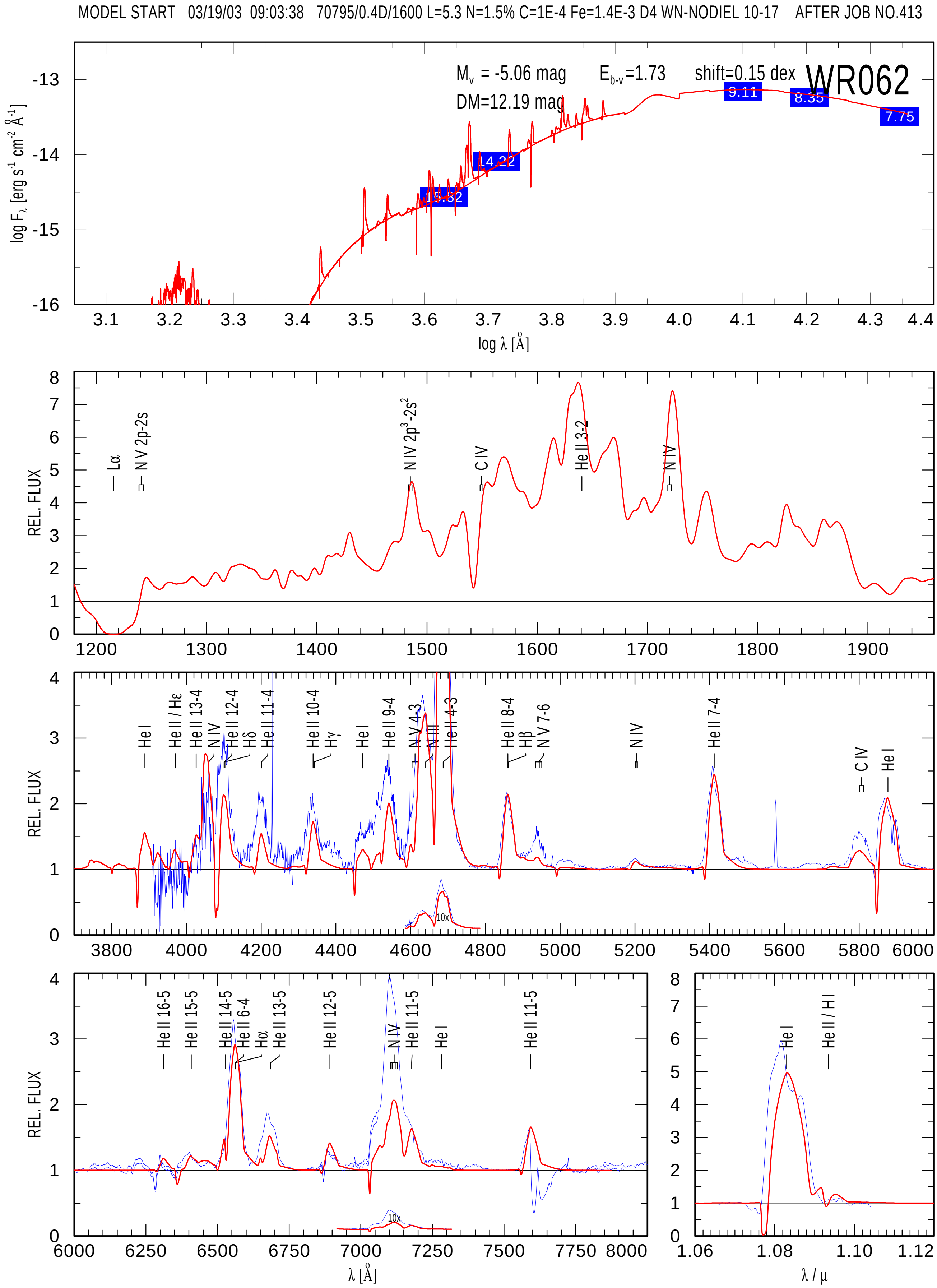

Fig. 38. Model: WNE 10-17, $T_* = 71$ kK, $\log(R_t/R_\odot) = 0.4$

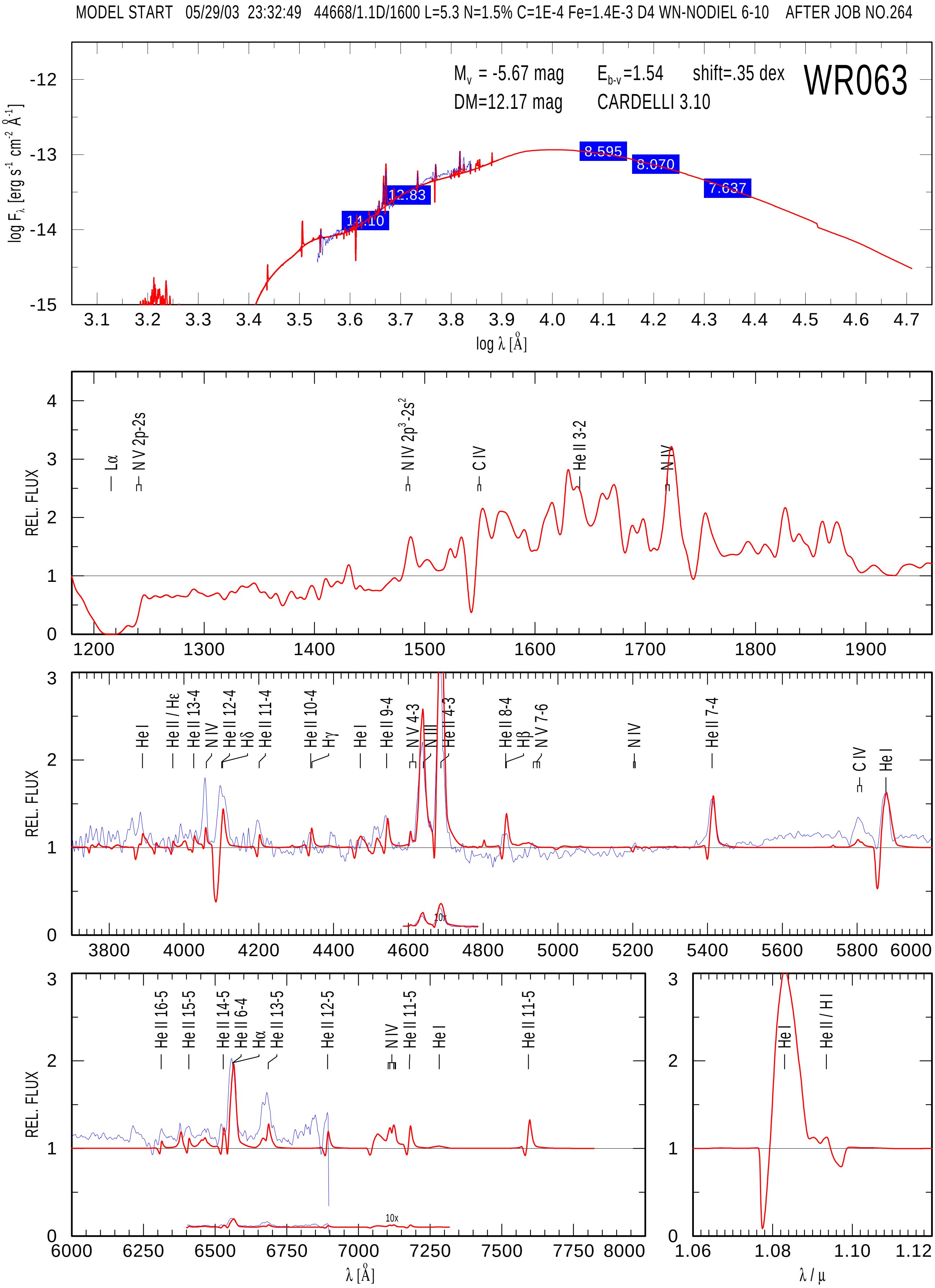

Fig. 39. Model: WNE 06-10, T_* = 45 kK, $\log(R_t/R_\odot)$ = 1.1

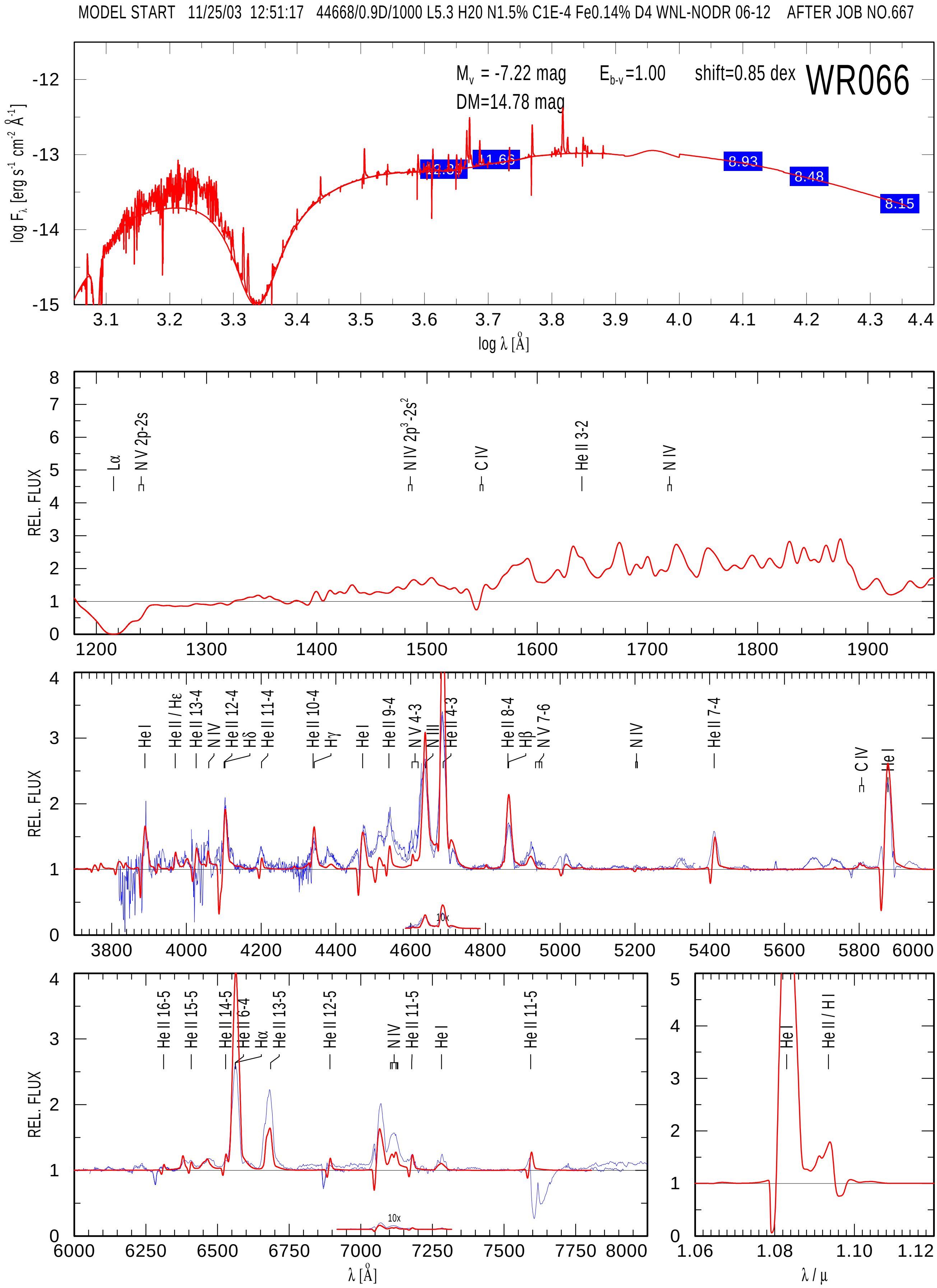

Fig. 40. Model: WNL 06-12, $T_* = 45$ kK, $\log(R_t/R_\odot) = 0.9$

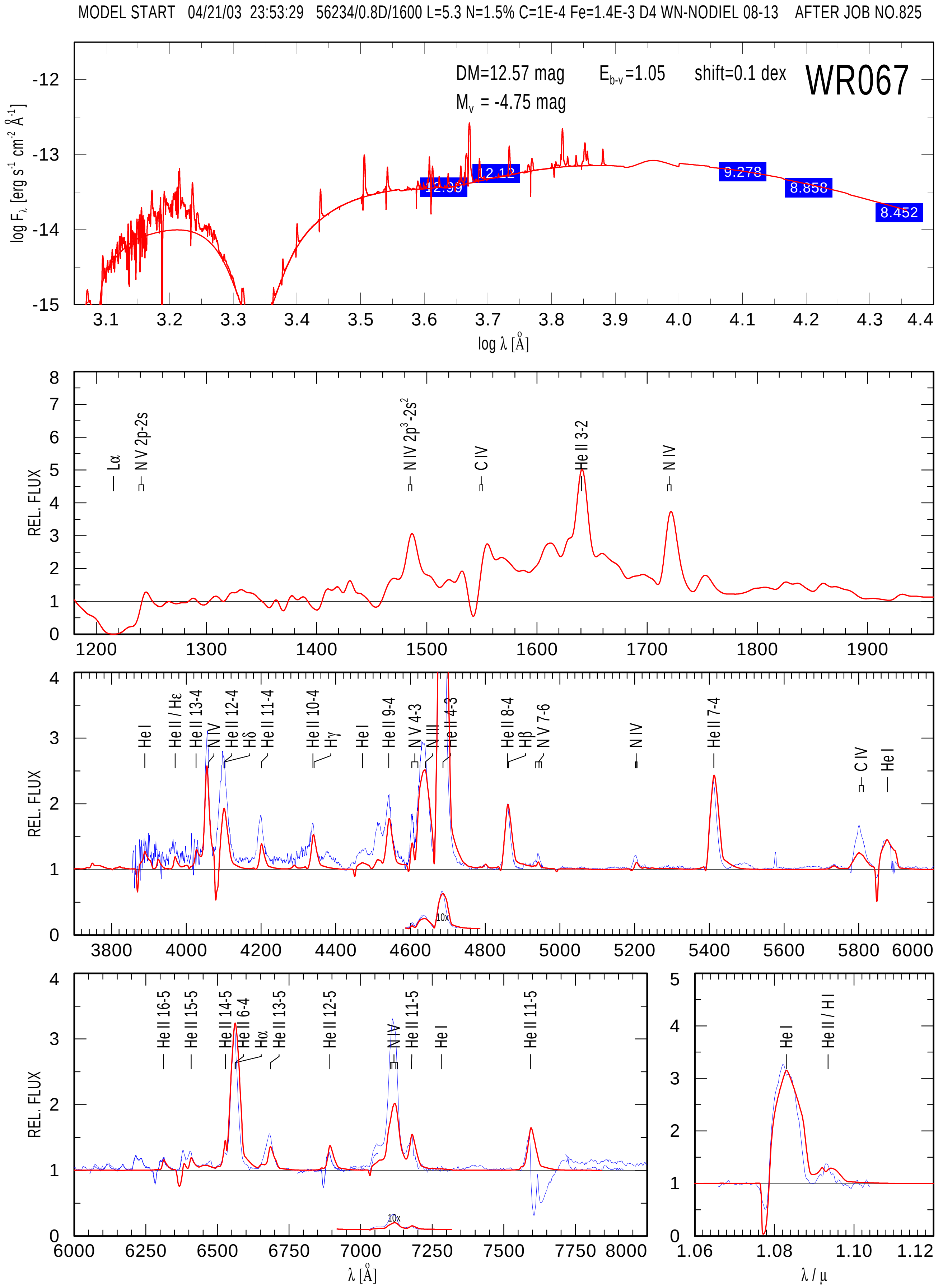

Fig. 41. Model: WNE 08-13, $T_* = 56\,\mathrm{kK}$, $\log(R_t/R_\odot) = 0.8$

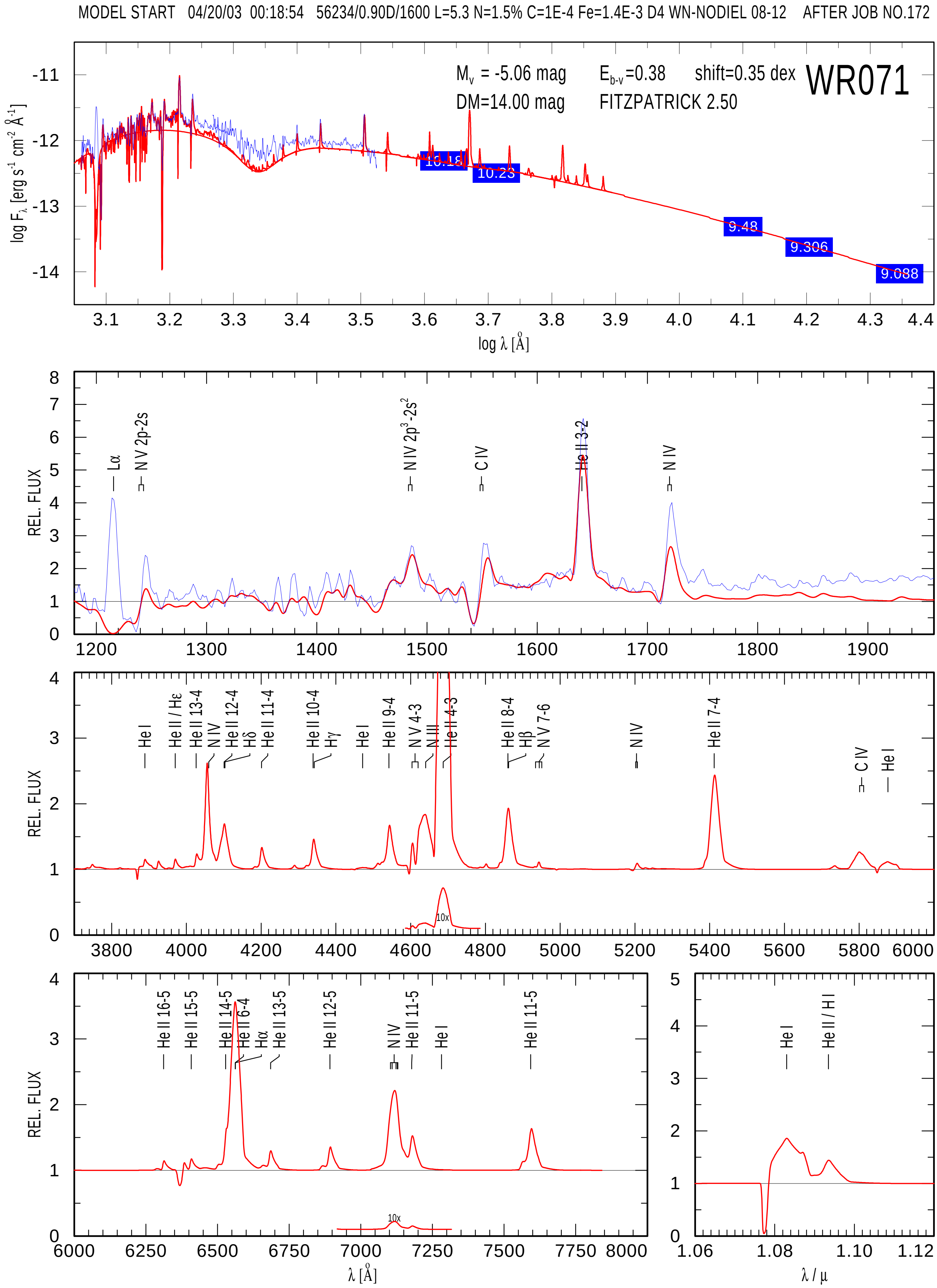

Fig. 42. Model: WNE 08-12, $T_* = 56$ kK, $\log(R_t/R_\odot) = 0.9$

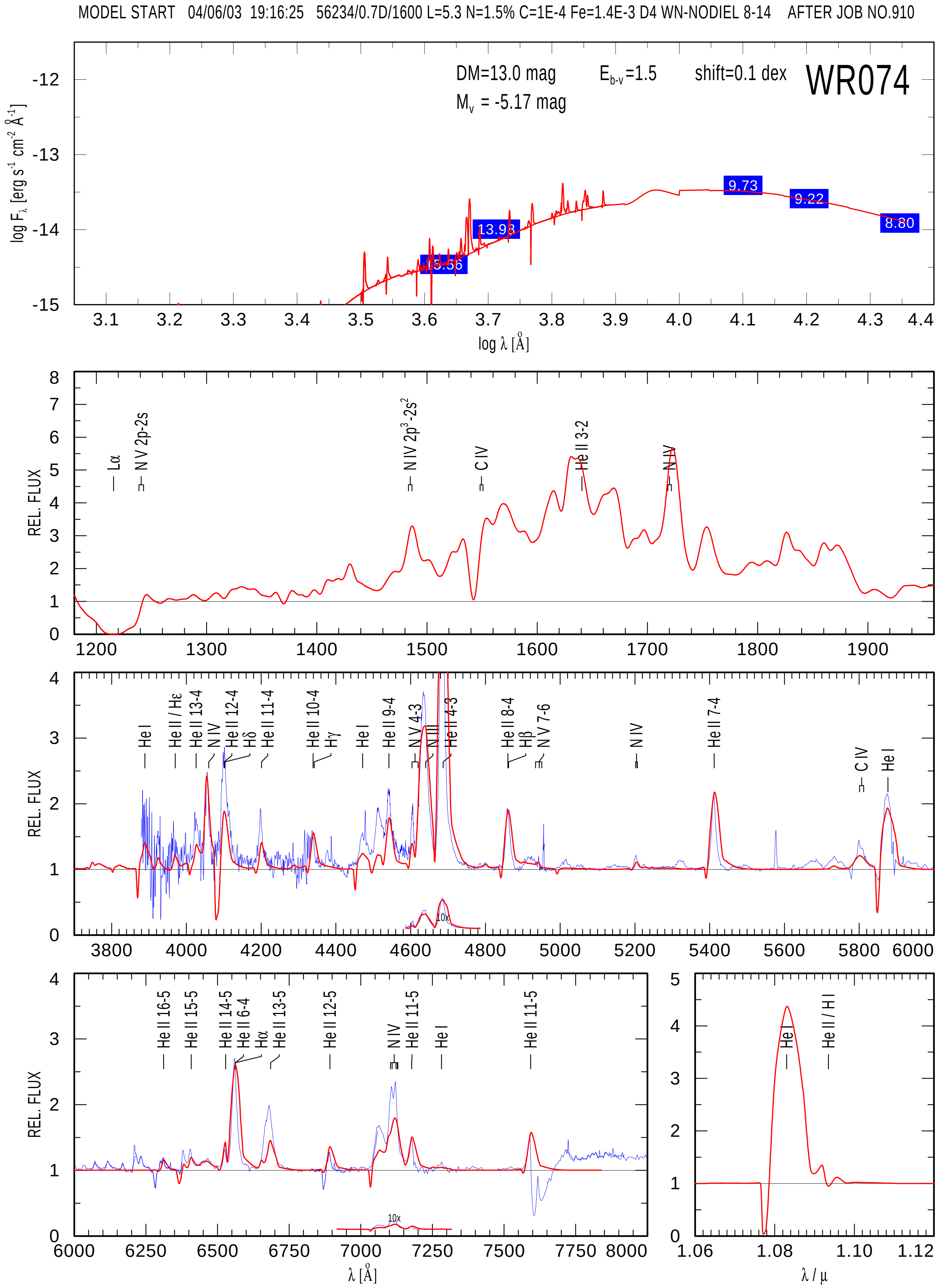

Fig. 43. Model: WNE 08-14, T_{*} = 56 kK, $\log(R_{t}/R_{\odot})$ = 0.7

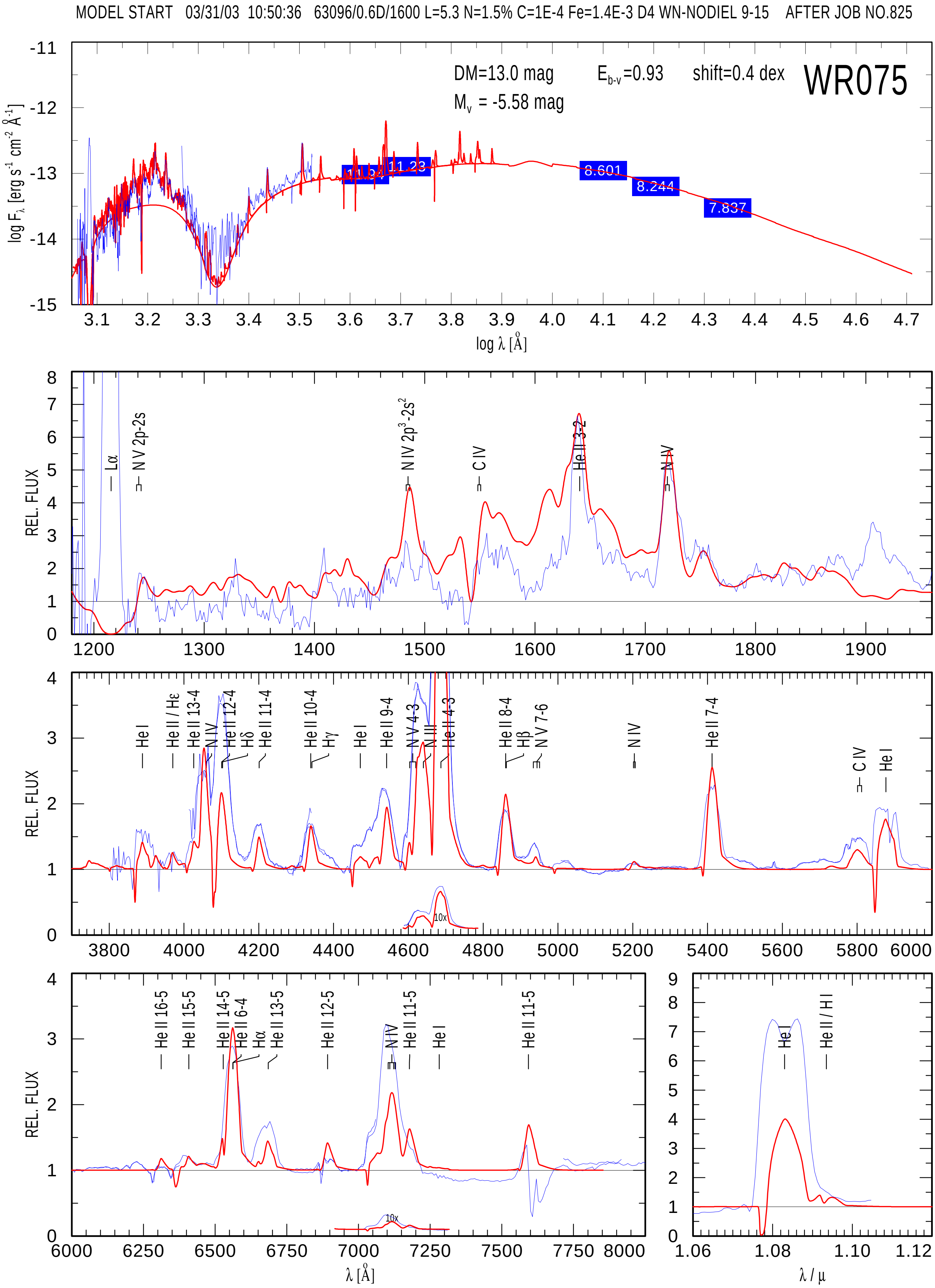

Fig. 44. Model: WNE 09-15, T_{*} = 63 kK, $\log(R_{\mathrm{t}}/R_{\odot})$ = 0.6

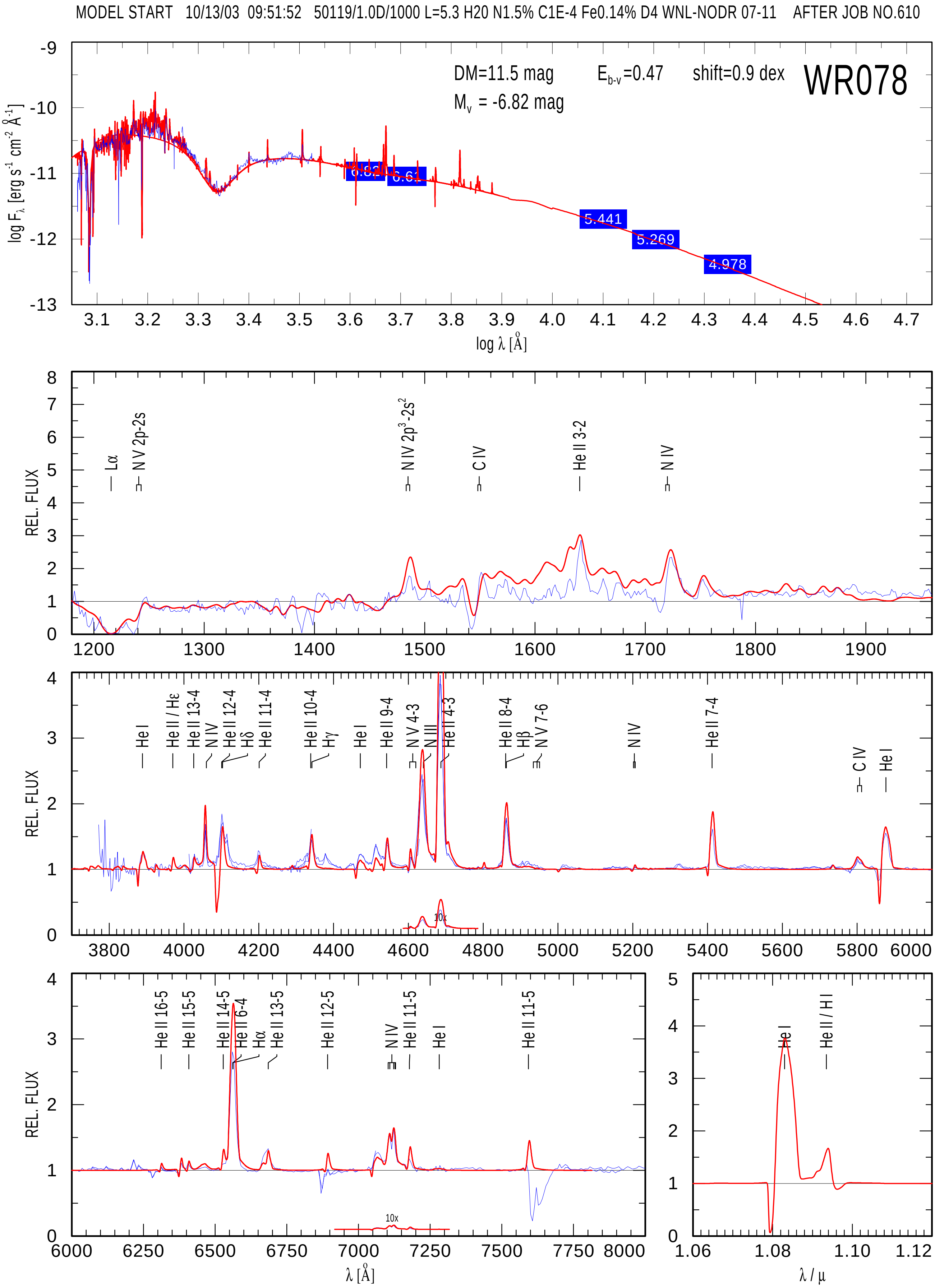

Fig. 45. Model: WNL 07-11, T_{*} = 50 kK, $\log(R_t/R_\odot)$ = 1.0

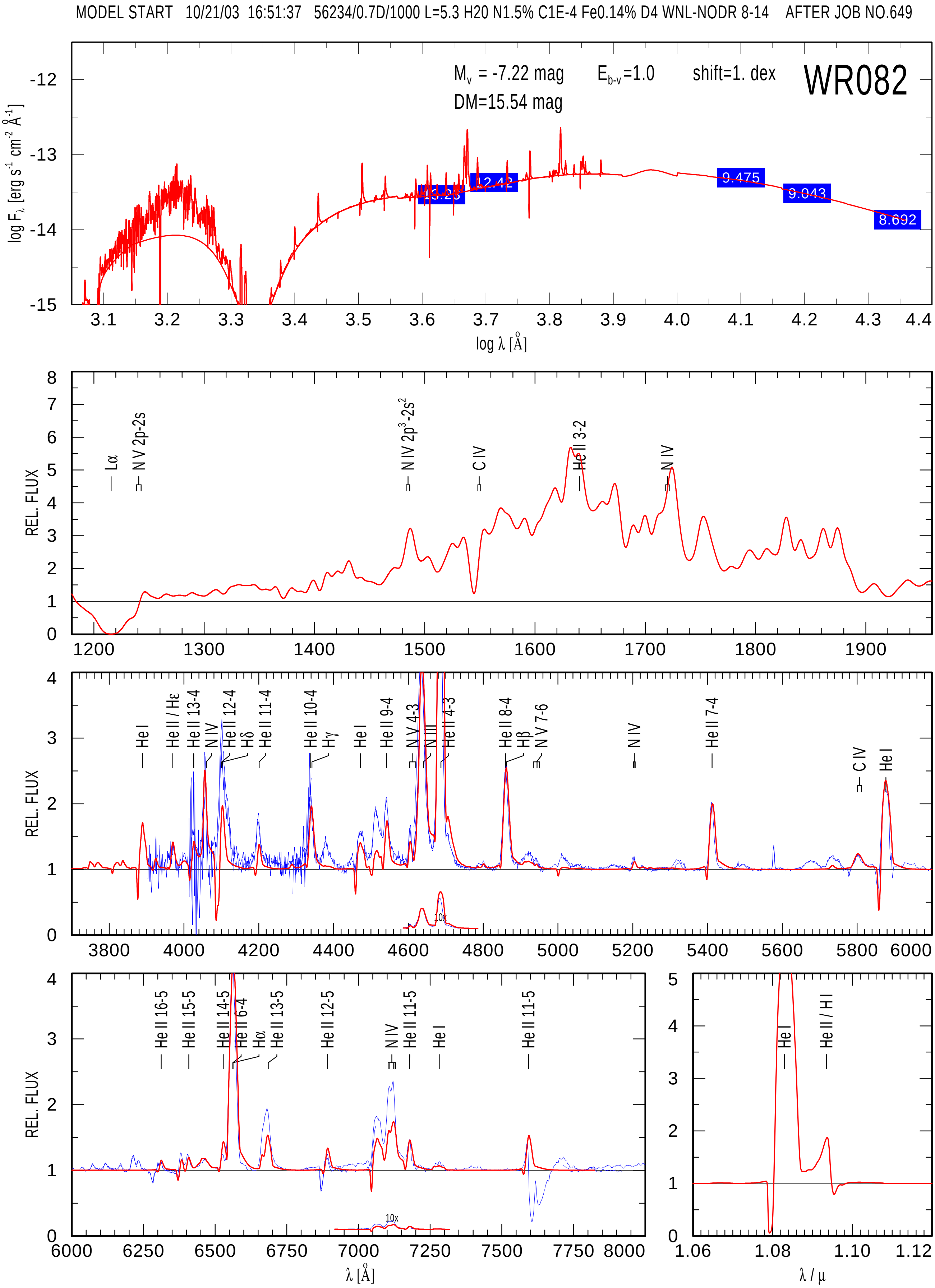

Fig. 46. Model: WNL 08-14, $T_* = 56\,\mathrm{kK}$, $\log(R_t/R_\odot) = 0.7$

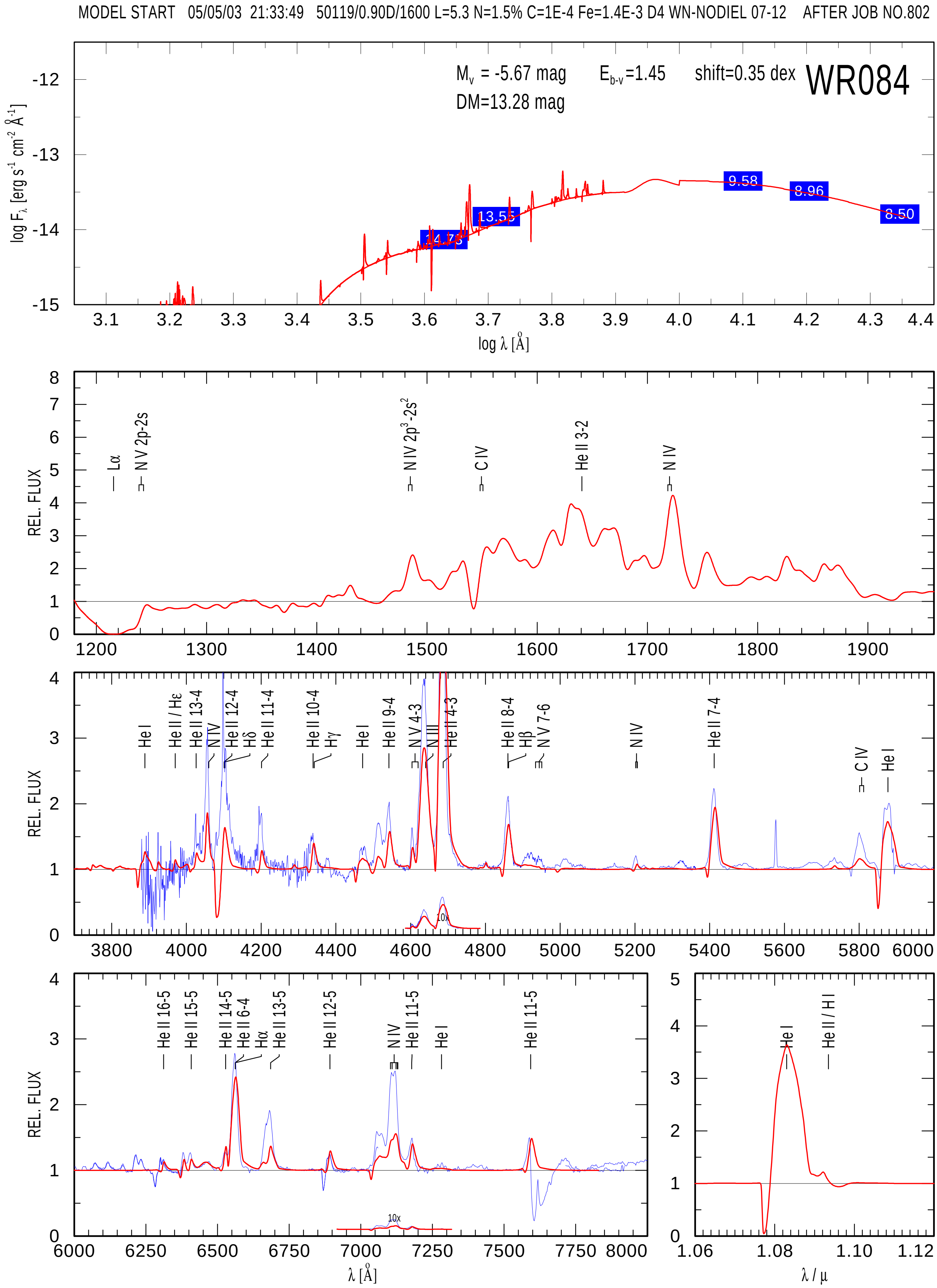

Fig. 47. Model: WNE 07-12, T_{*} = 50 kK, $\log(R_{t}/R_{\odot})$ = 0.9

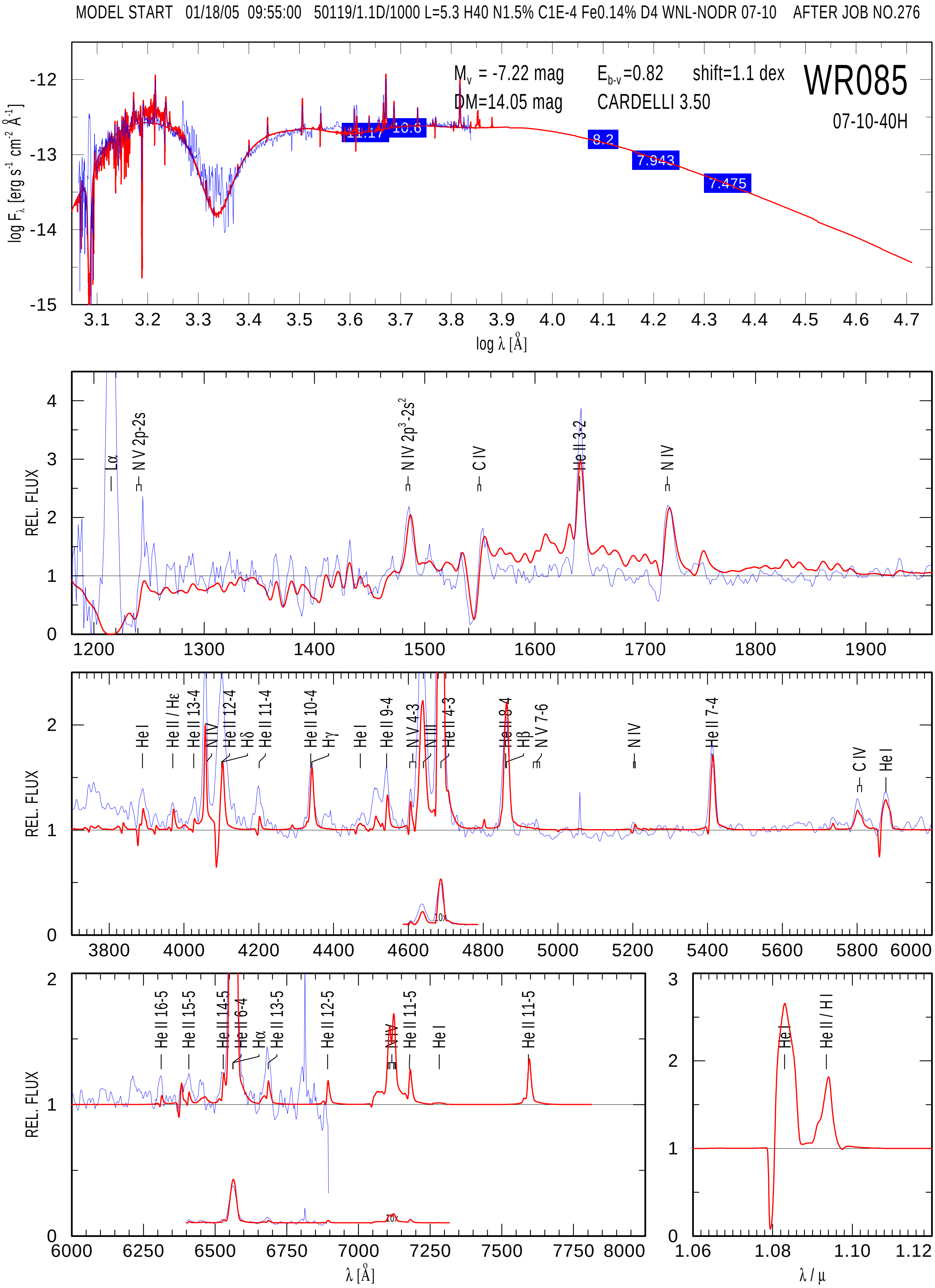

Fig. 48. Individual Model: 07-10, T_* = 50 kK, $\log(R_t/R_\odot)$ = 1.1 with v_∞ = 1000 km/s and X_H = 0.40

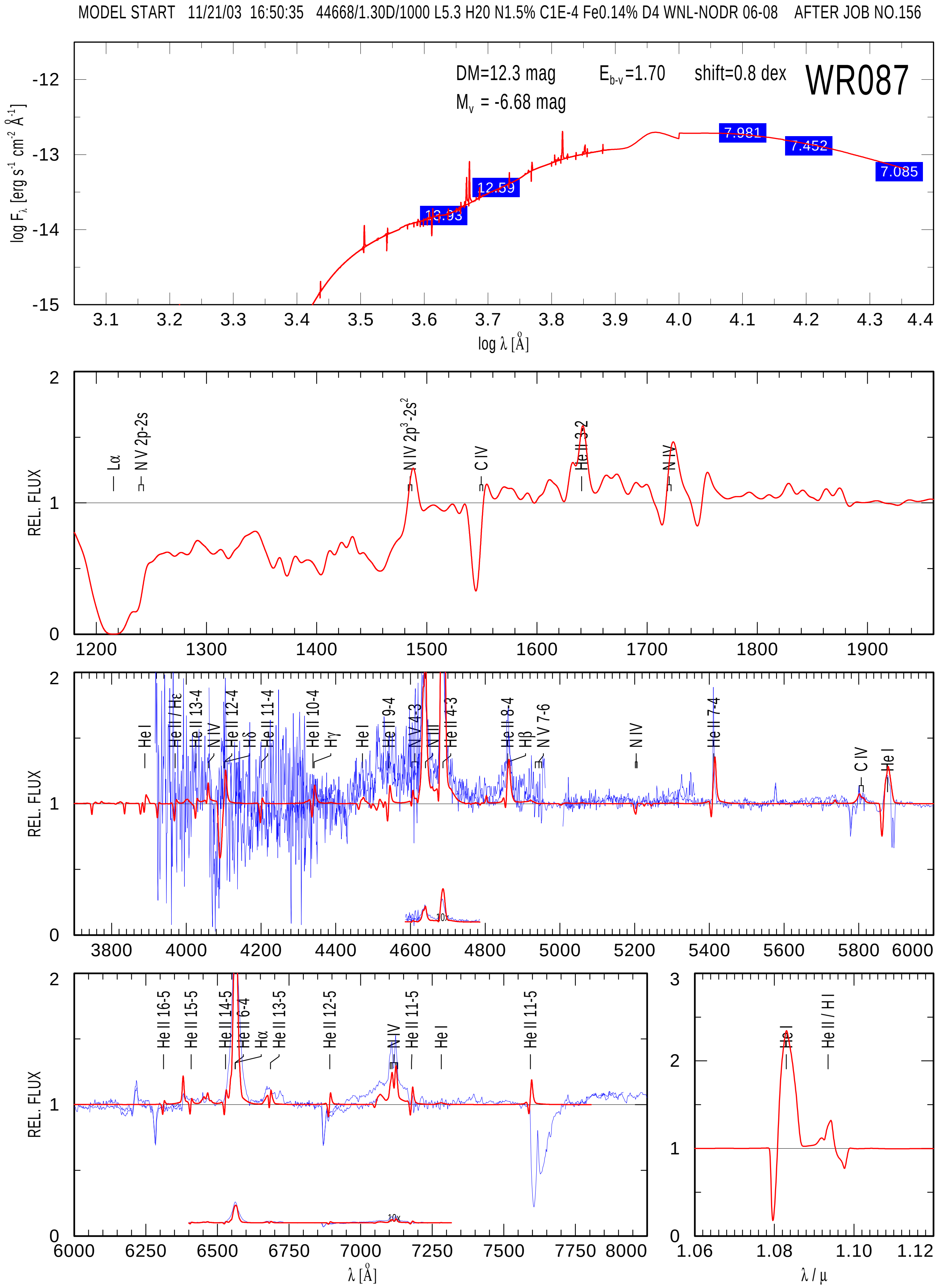

Fig. 49. Model: WNL 06-08, $T_{*} = 45\,\mathrm{kK}$, $\log(R_{\mathrm{t}}/R_{\odot}) = 1.3$

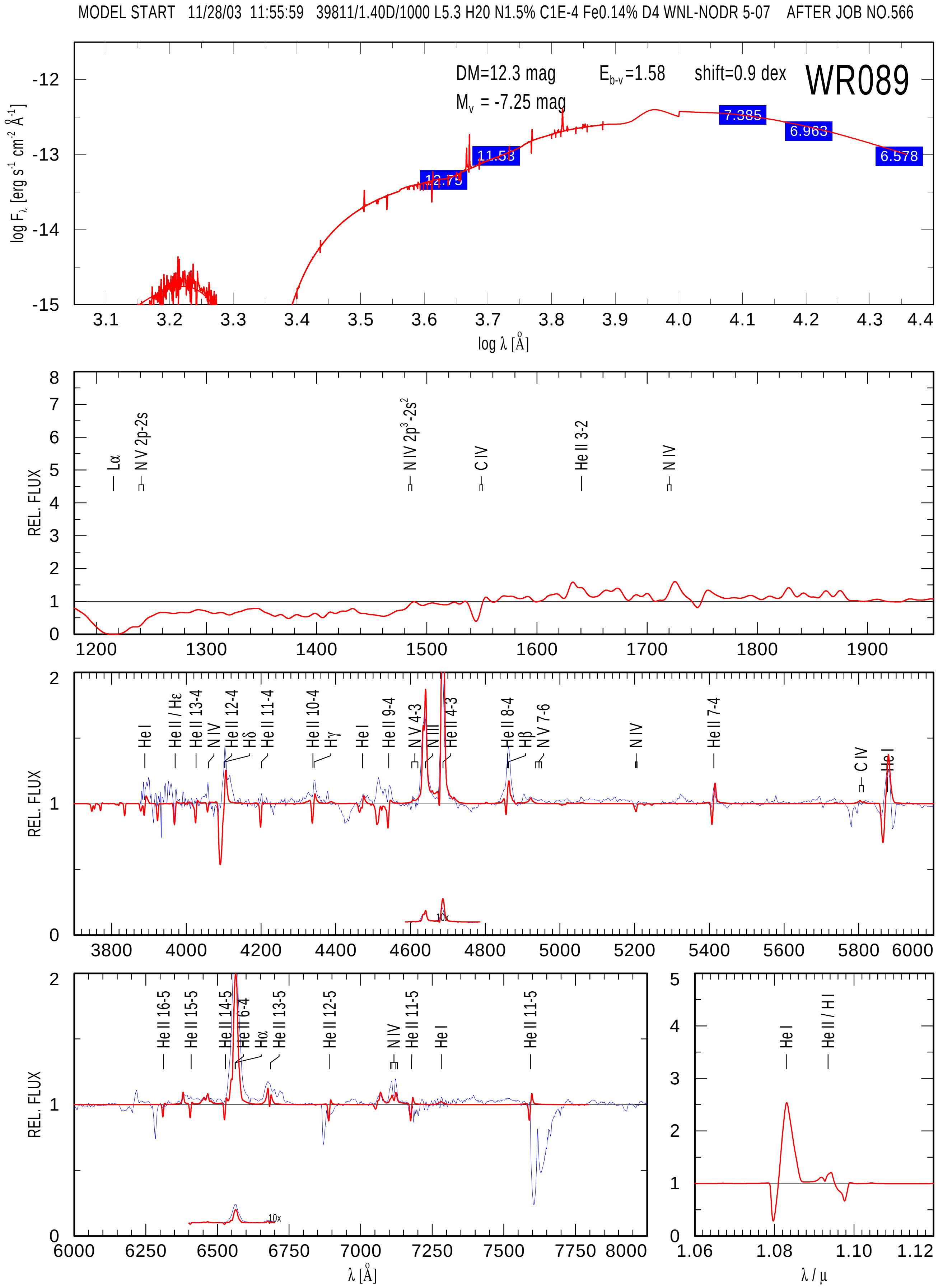

Fig. 50. Model: WNL 05-07, $T_* = 40$ kK, $\log(R_t/R_\odot) = 1.4$

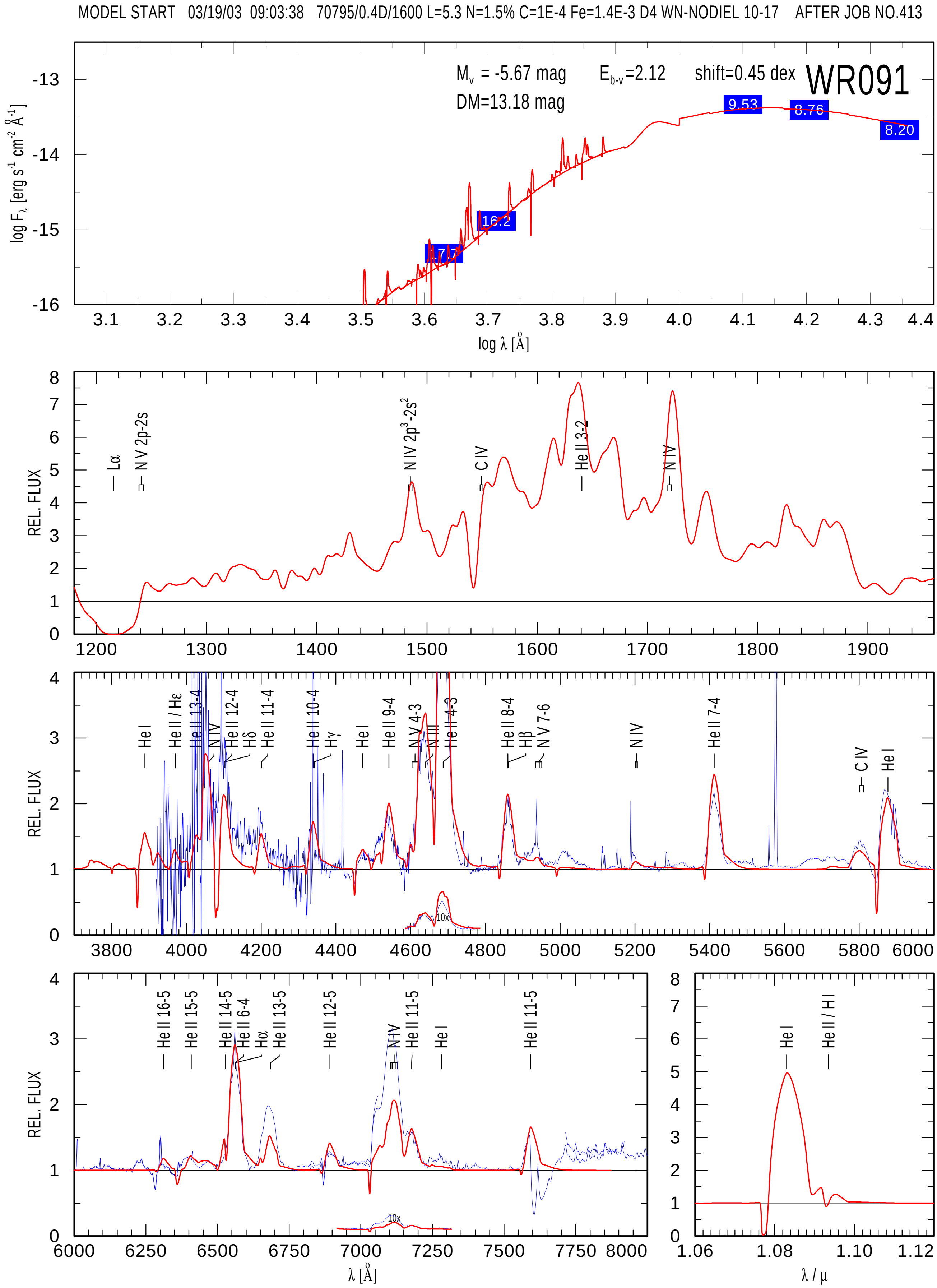

Fig. 51. Model: WNE 10-17, T_{*} = 71 kK, $\log(R_{t}/R_{\odot})$ = 0.4

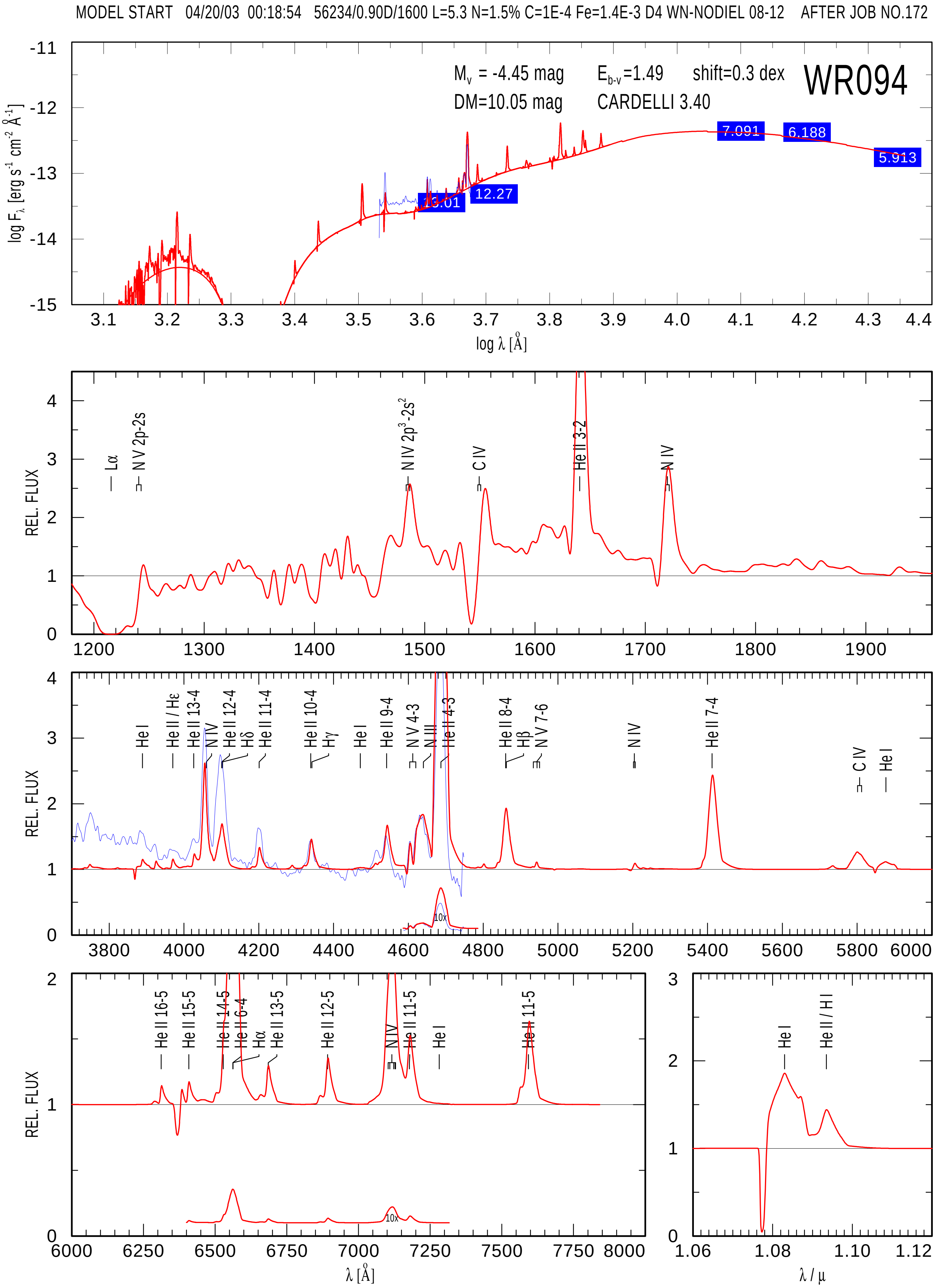

Fig. 52. Model: WNE 08-12, $T_* = 56$ kK, $\log(R_t/R_\odot) = 0.9$

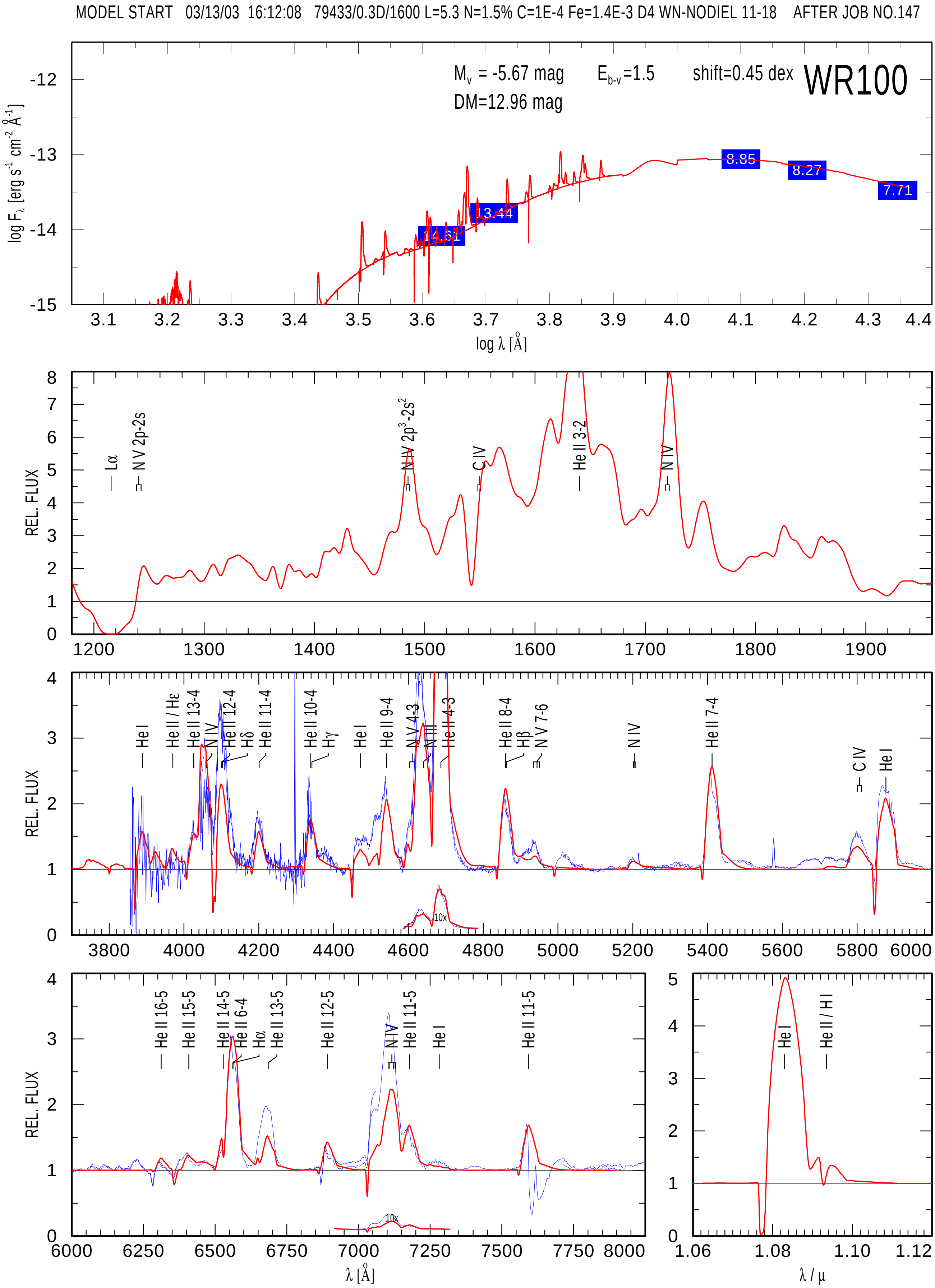

Fig. 53. Model: WNE 11-18, $T_* = 79$ kK, $\log(R_t/R_\odot) = 0.3$

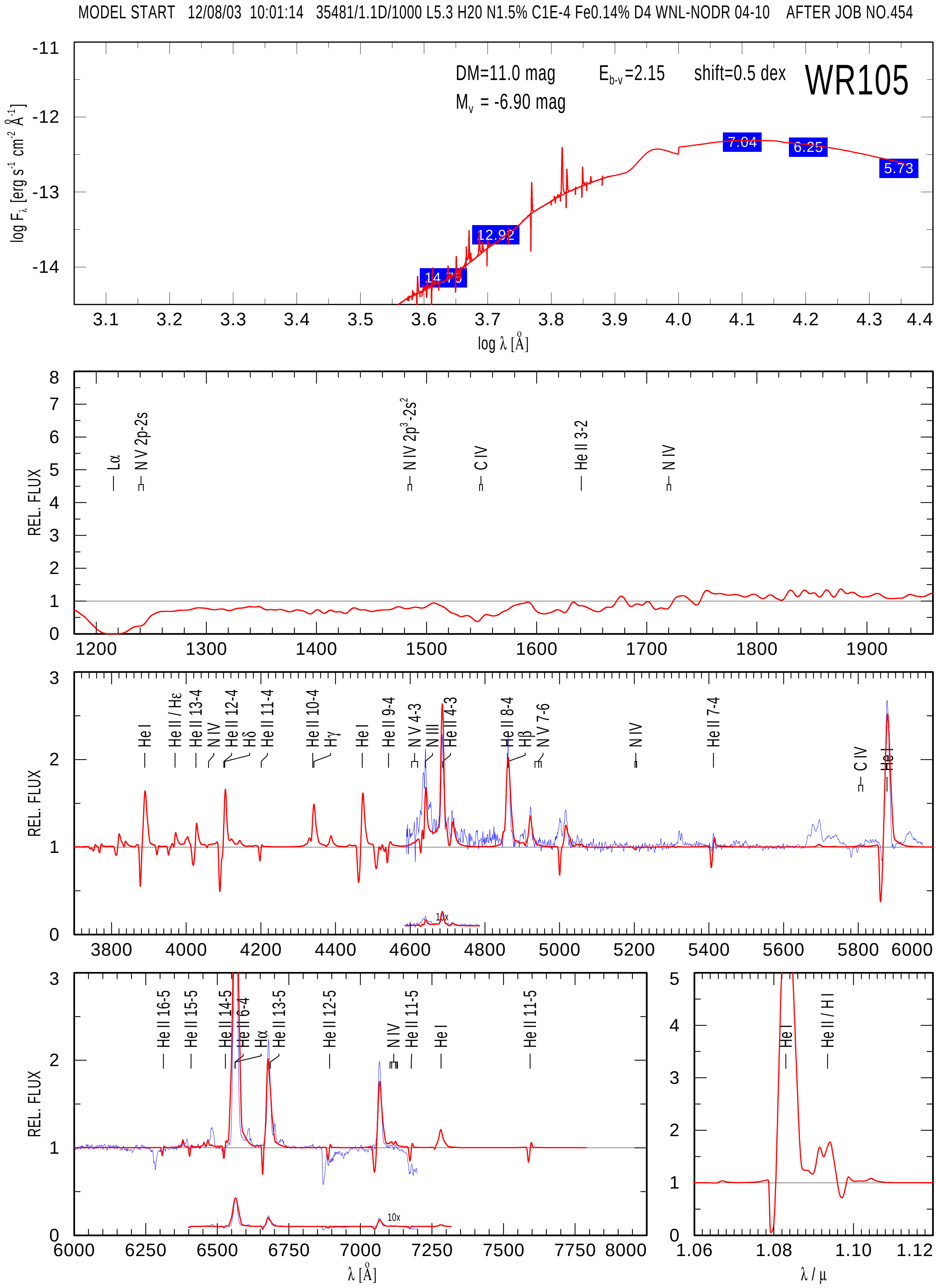

Fig. 54. Model: WNL 04-10, $T_* = 35$ kK, $\log(R_t/R_\odot) = 1.1$

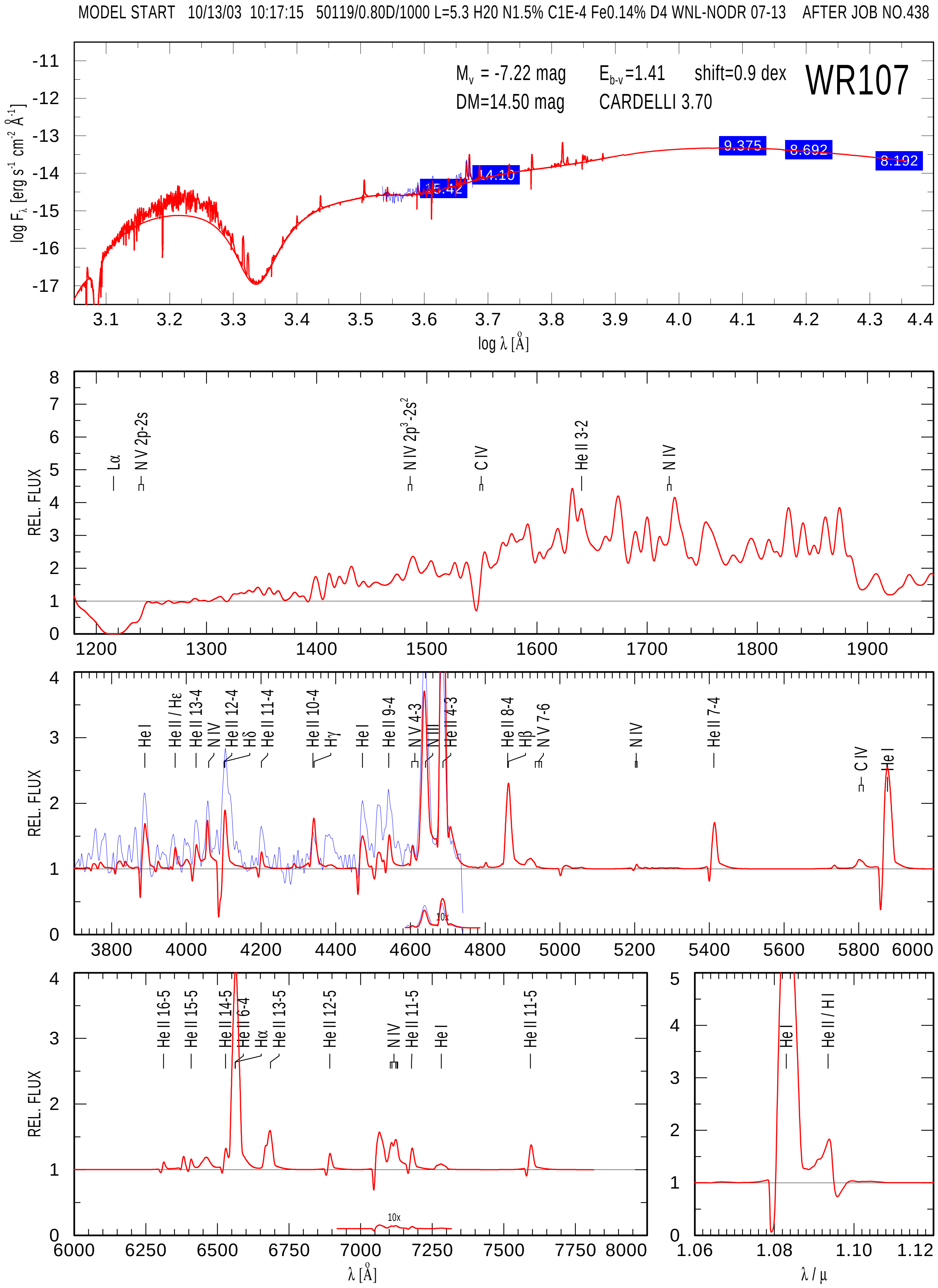

Fig. 55. Model: WNL 07-13, $T_* = 50\,\mathrm{kK}$, $\log(R_t/R_\odot) = 0.8$

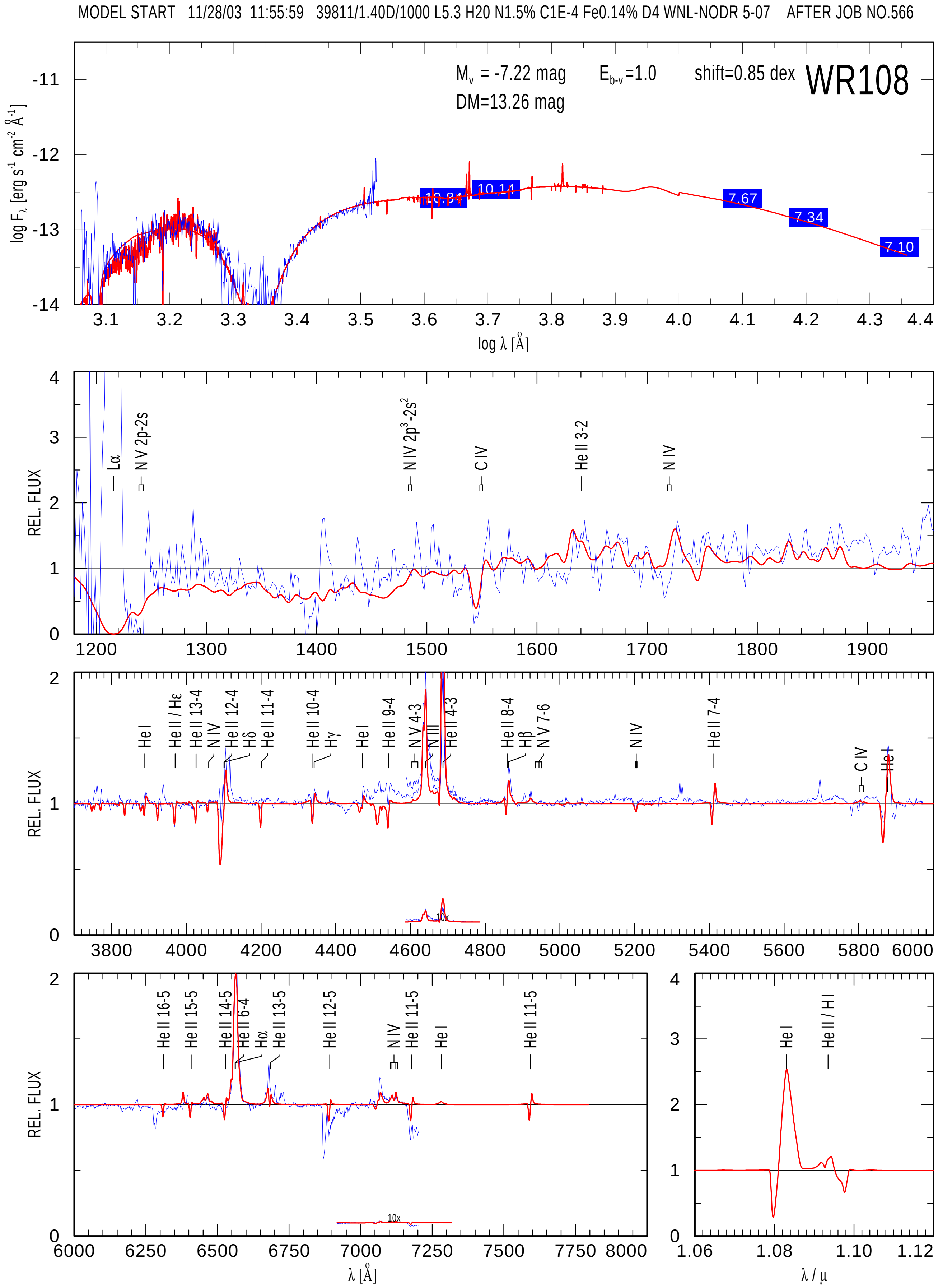

Fig. 56. Model: WNL 05-07, $T_* = 40\,\mathrm{kK}$, $\log(R_t/R_\odot) = 1.4$

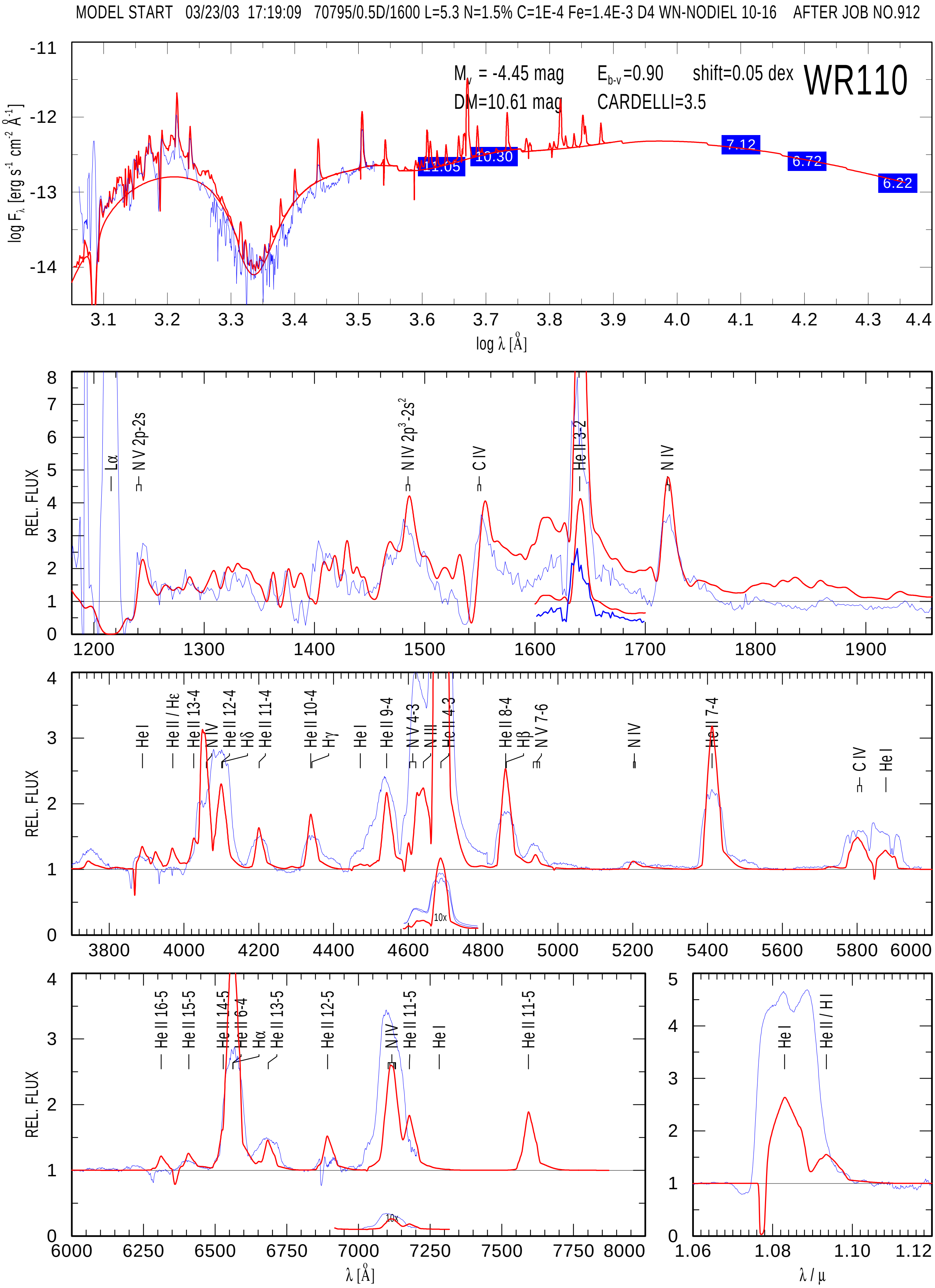

Fig. 57. Model: WNE 10-16, $T_* = 71$ kK, $\log(R_t/R_\odot) = 0.5$

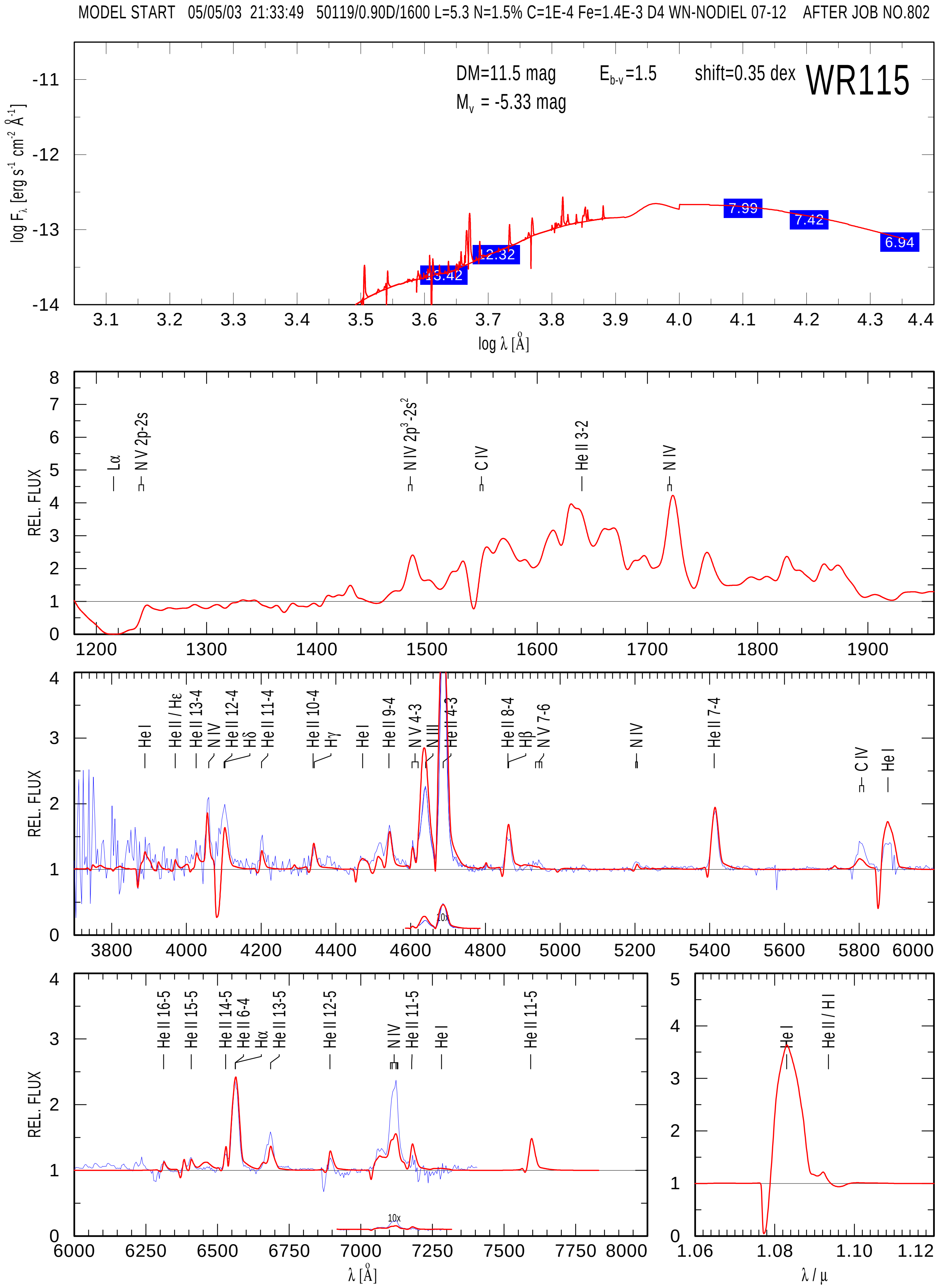

Fig. 58. Model: WNE 07-12, $T_* = 50$ kK, $\log(R_t/R_\odot) = 0.9$

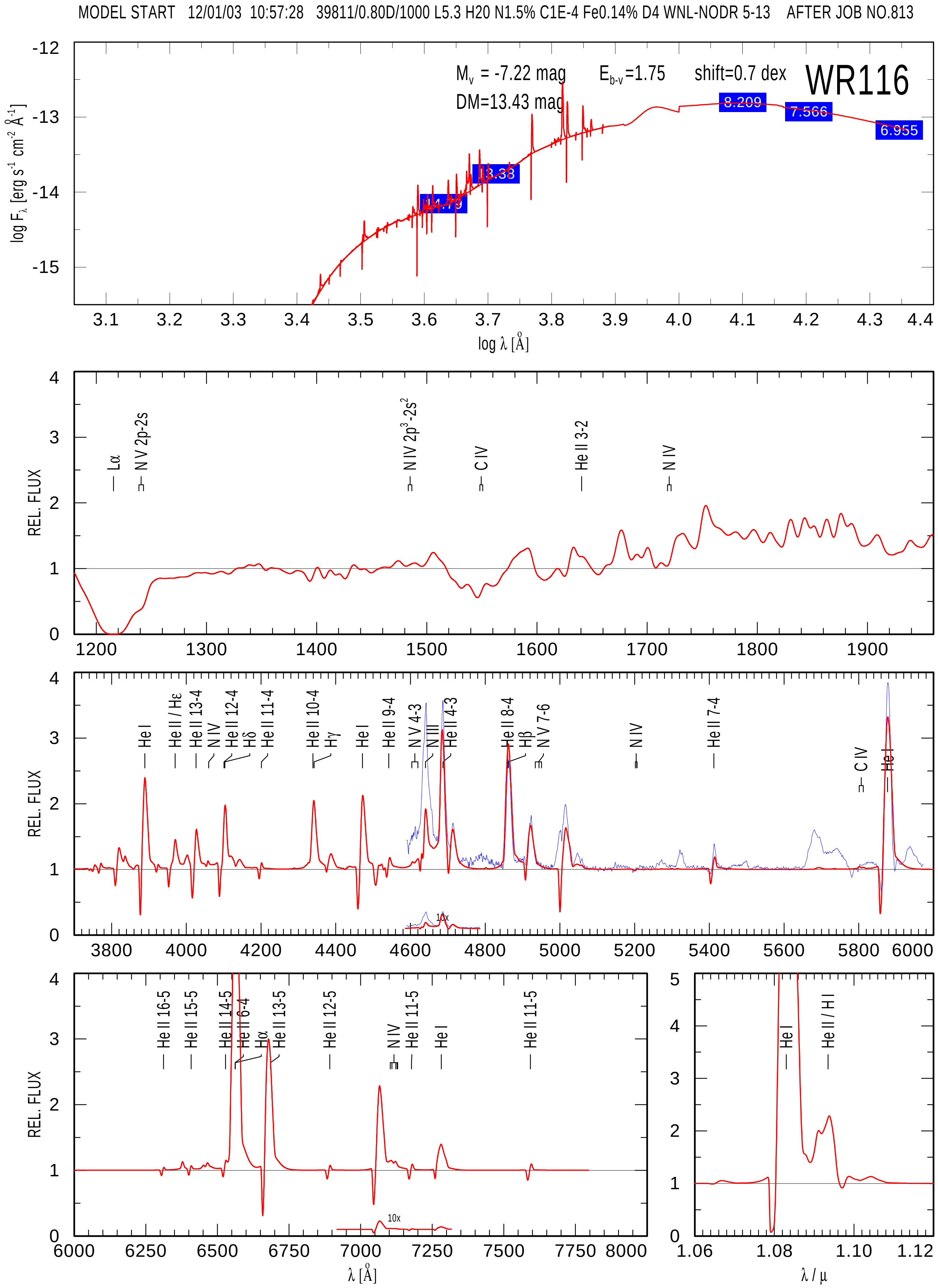

Fig. 59. Model: WNL 05-13, T_* = 40 kK, $\log(R_t/R_\odot)$ = 0.8

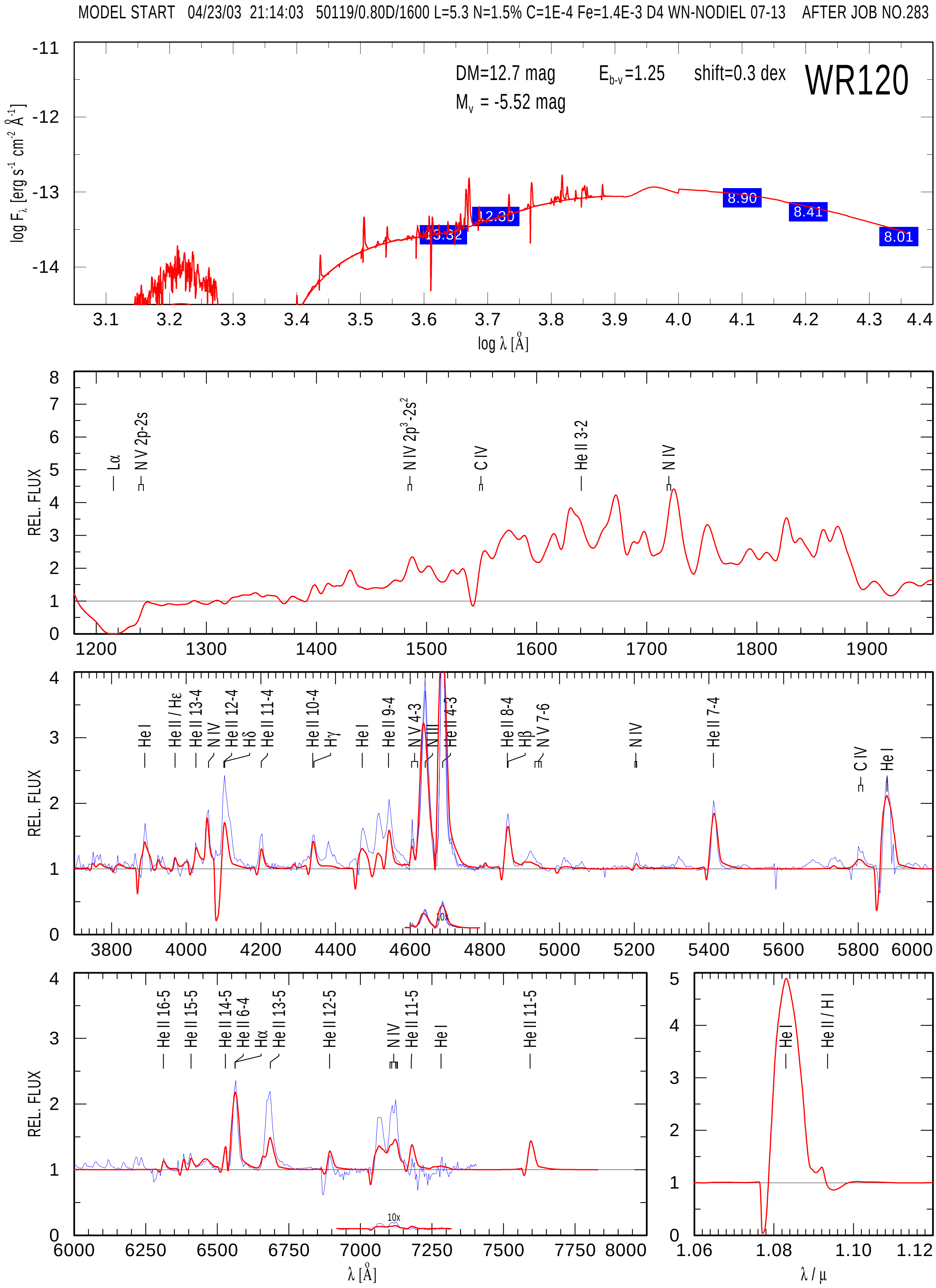

Fig. 60. Model: WNE 07-13, T_{*} = 50 kK, $\log(R_{t}/R_{\odot})$ = 0.8

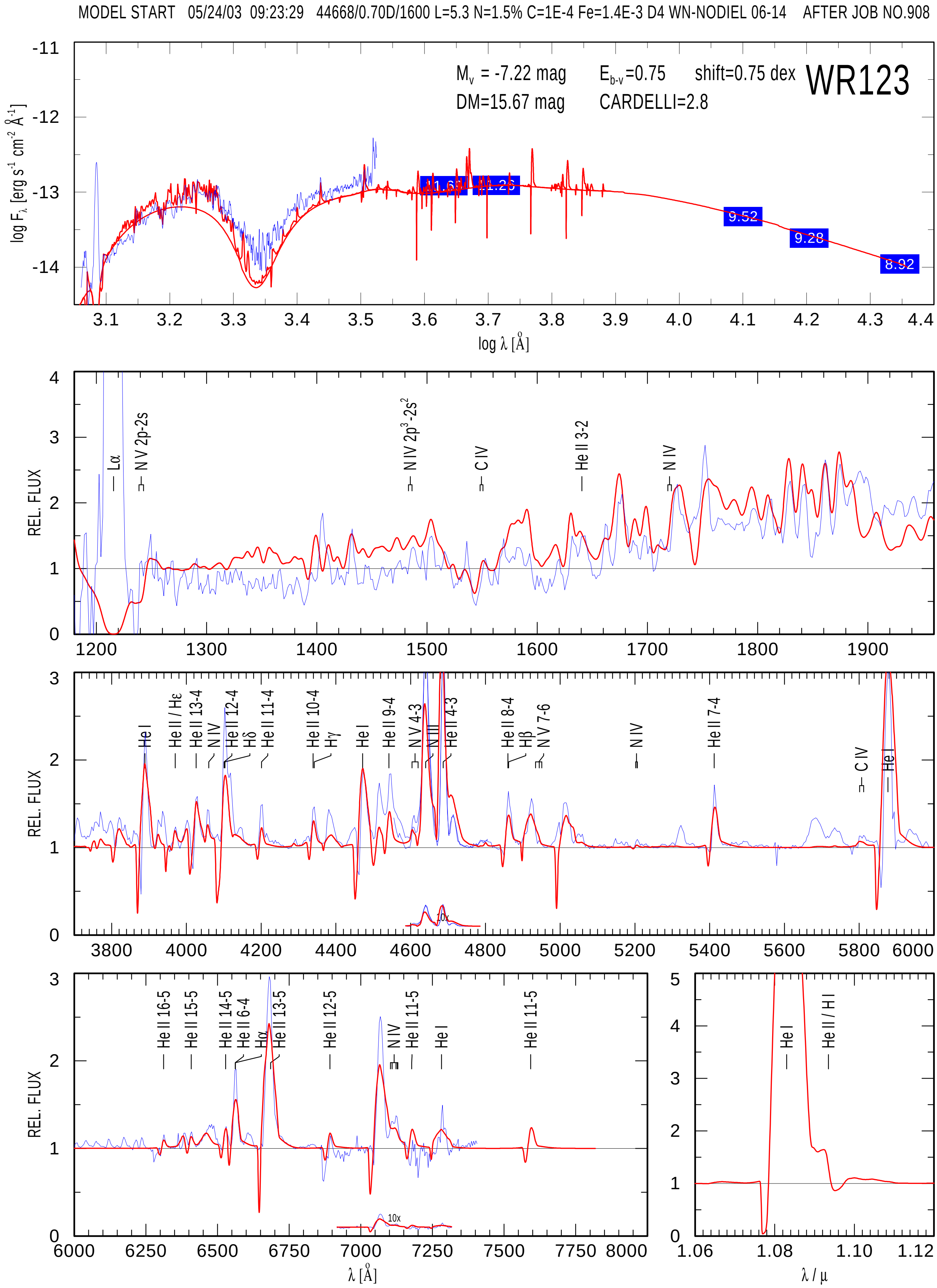

Fig. 61. Model: WNE 06-14, $T_{*} = 45\,\mathrm{kK}$, $\log(R_{t}/R_{\odot}) = 0.7$

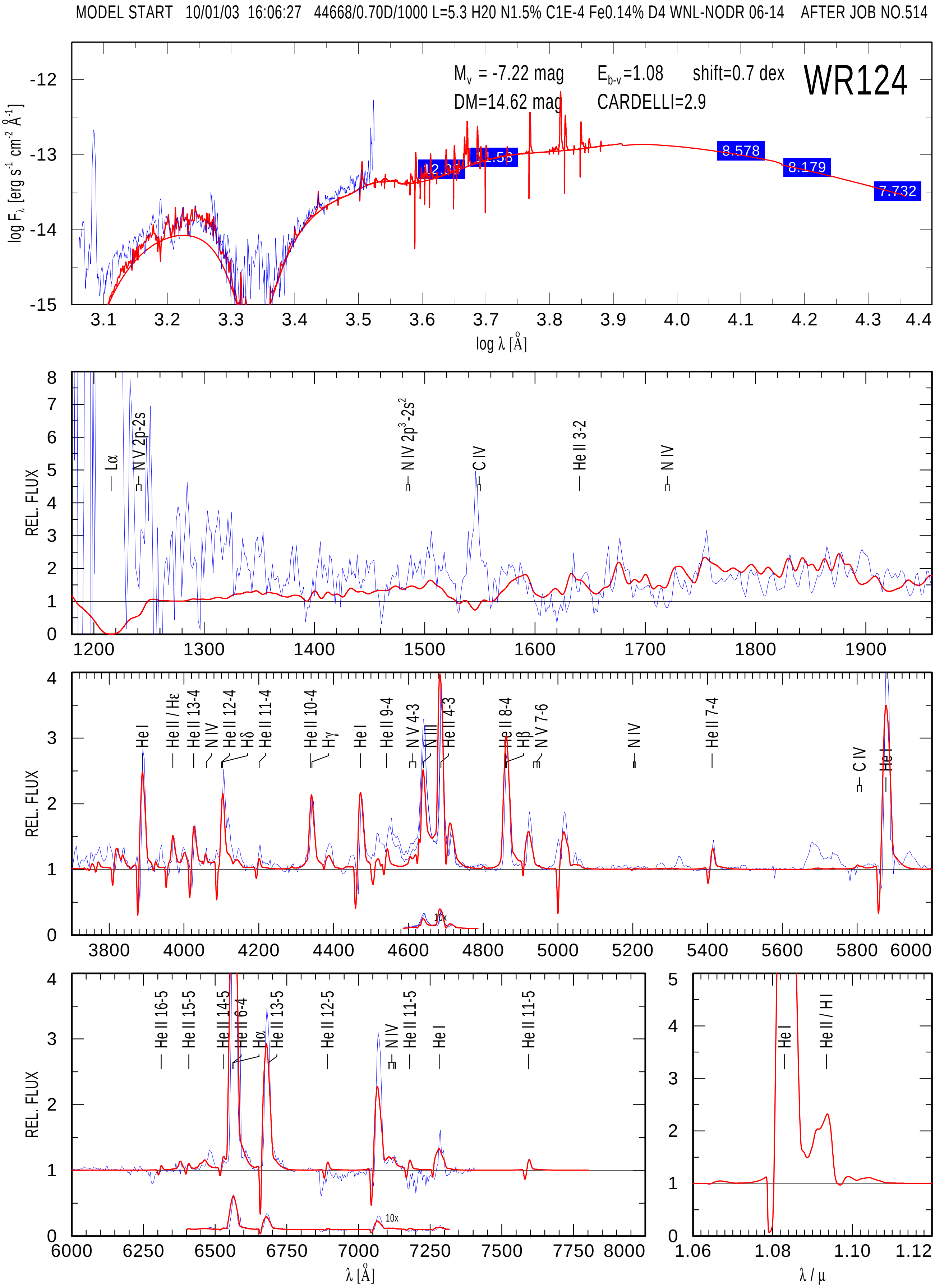

Fig. 62. Model: WNL 06-14, $T_{*} = 45\,\mathrm{kK}$, $\log(R_{\mathrm{t}}/R_{\odot}) = 0.7$

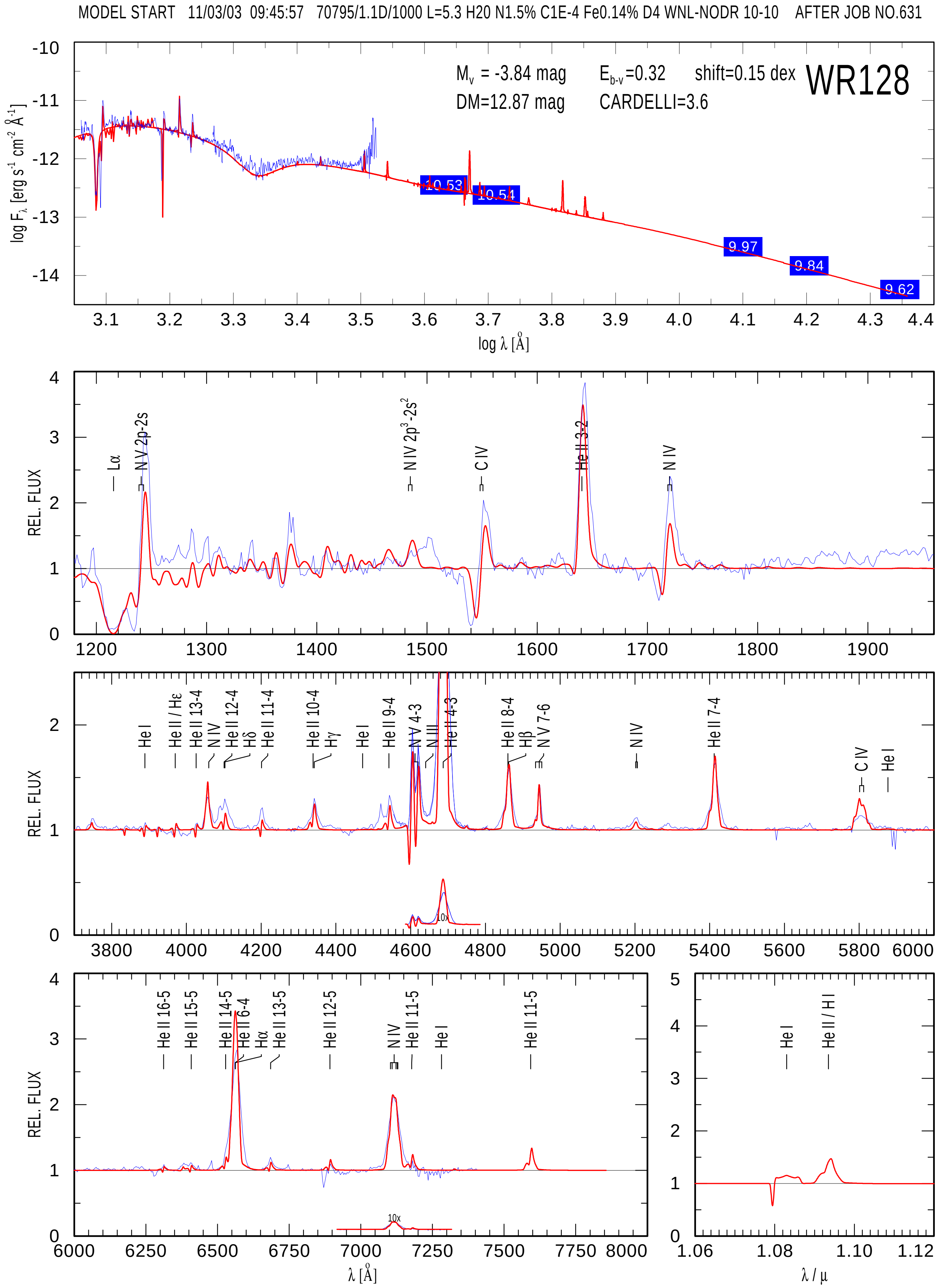

Fig. 63. Model: WNL 10-10, T_{*} = 71 kK, $\log(R_t/R_{\odot})$ = 1.1

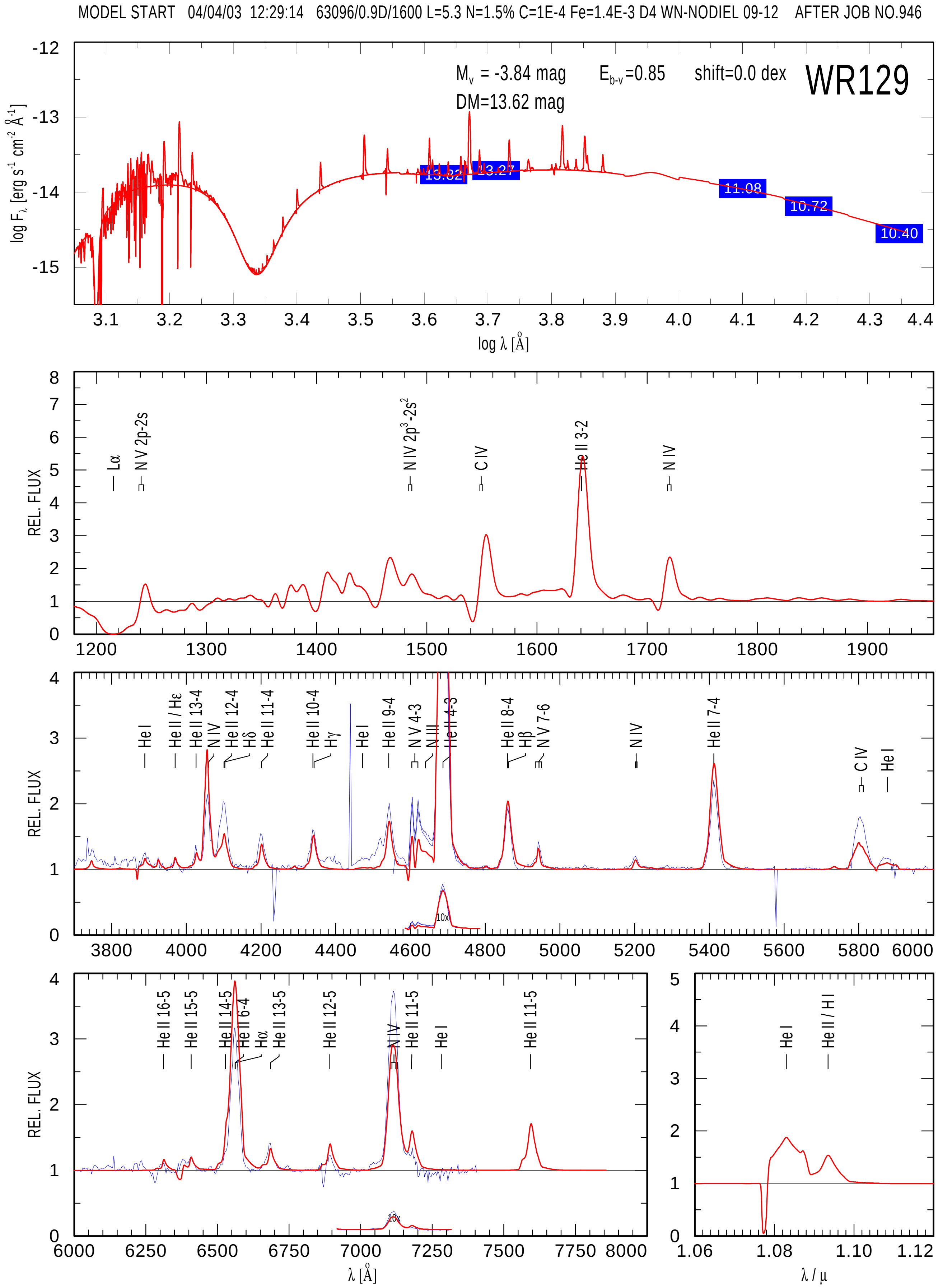

Fig. 64. Model: WNE 09-12, $T_{*} = 63\,\mathrm{kK}$, $\log(R_{t}/R_{\odot}) = 0.9$

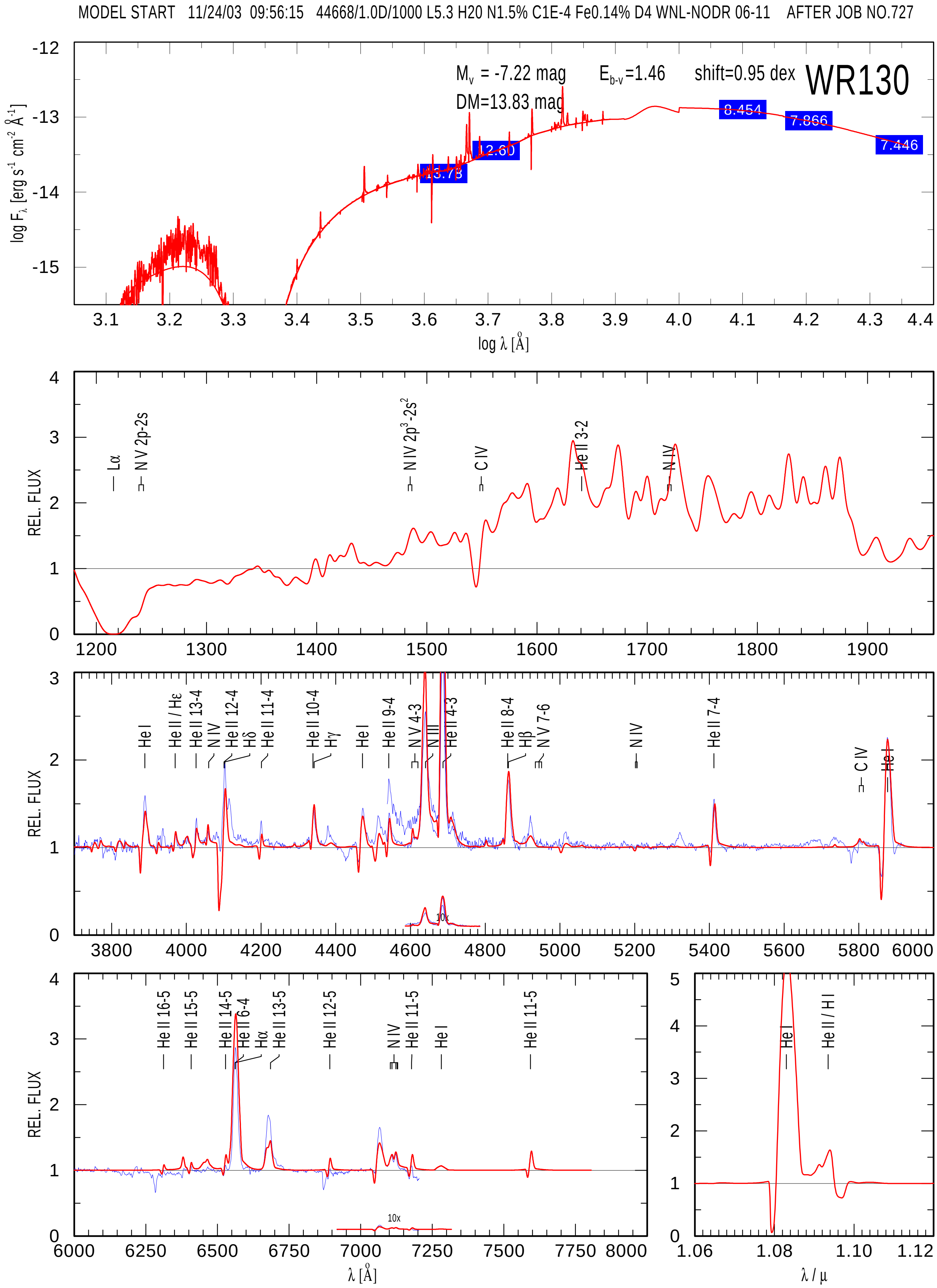

Fig. 65. Model: WNL 06-11, $T_* = 45$ kK, $\log(R_t/R_\odot) = 1.0$

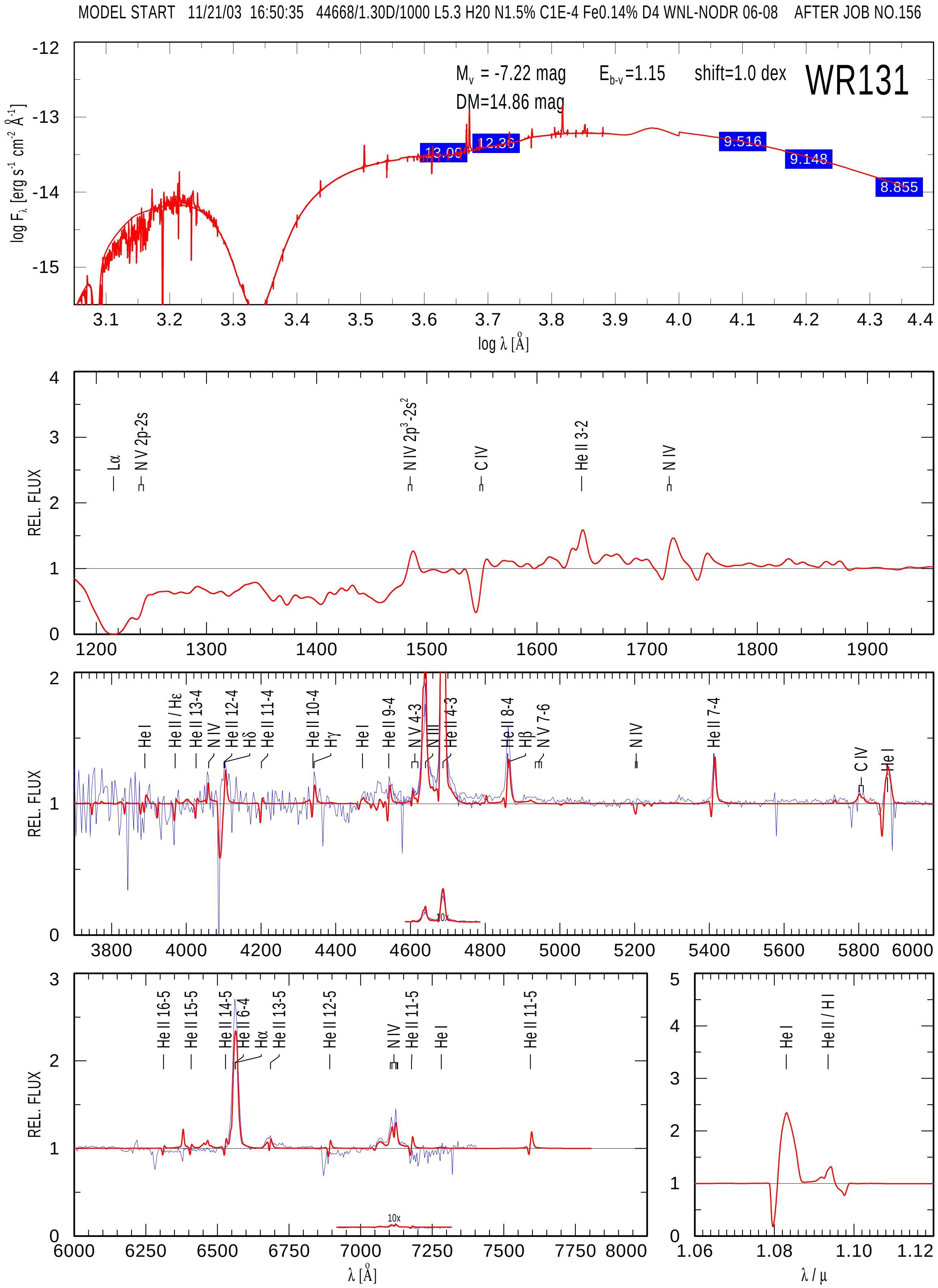

Fig. 66. Model: WNL 06-08, $T_* = 45$ kK, $\log(R_t/R_\odot) = 1.3$

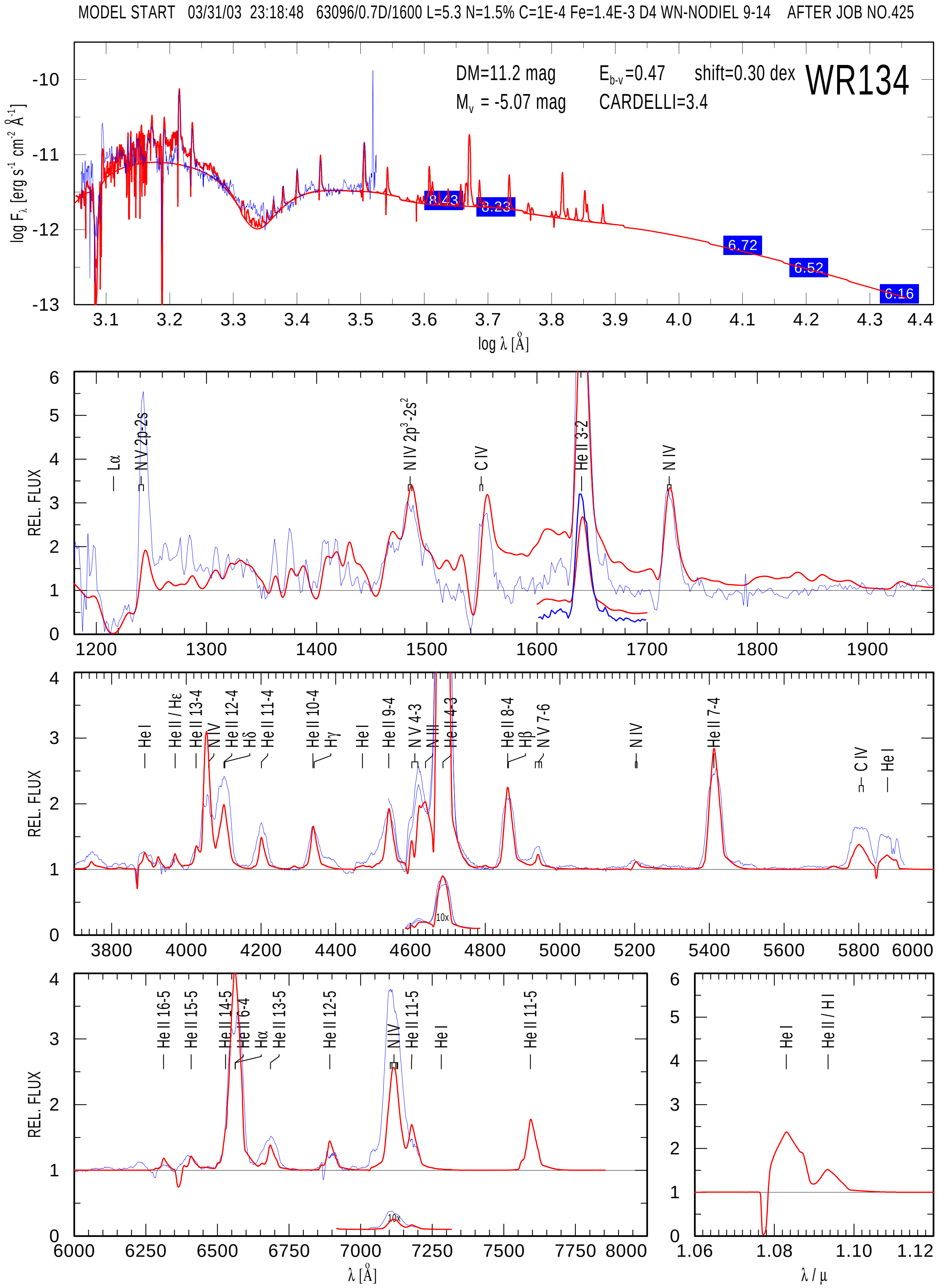

Fig. 67. Model: WNE 09-14, $T_* = 63$ kK, $\log(R_t/R_\odot) = 0.7$

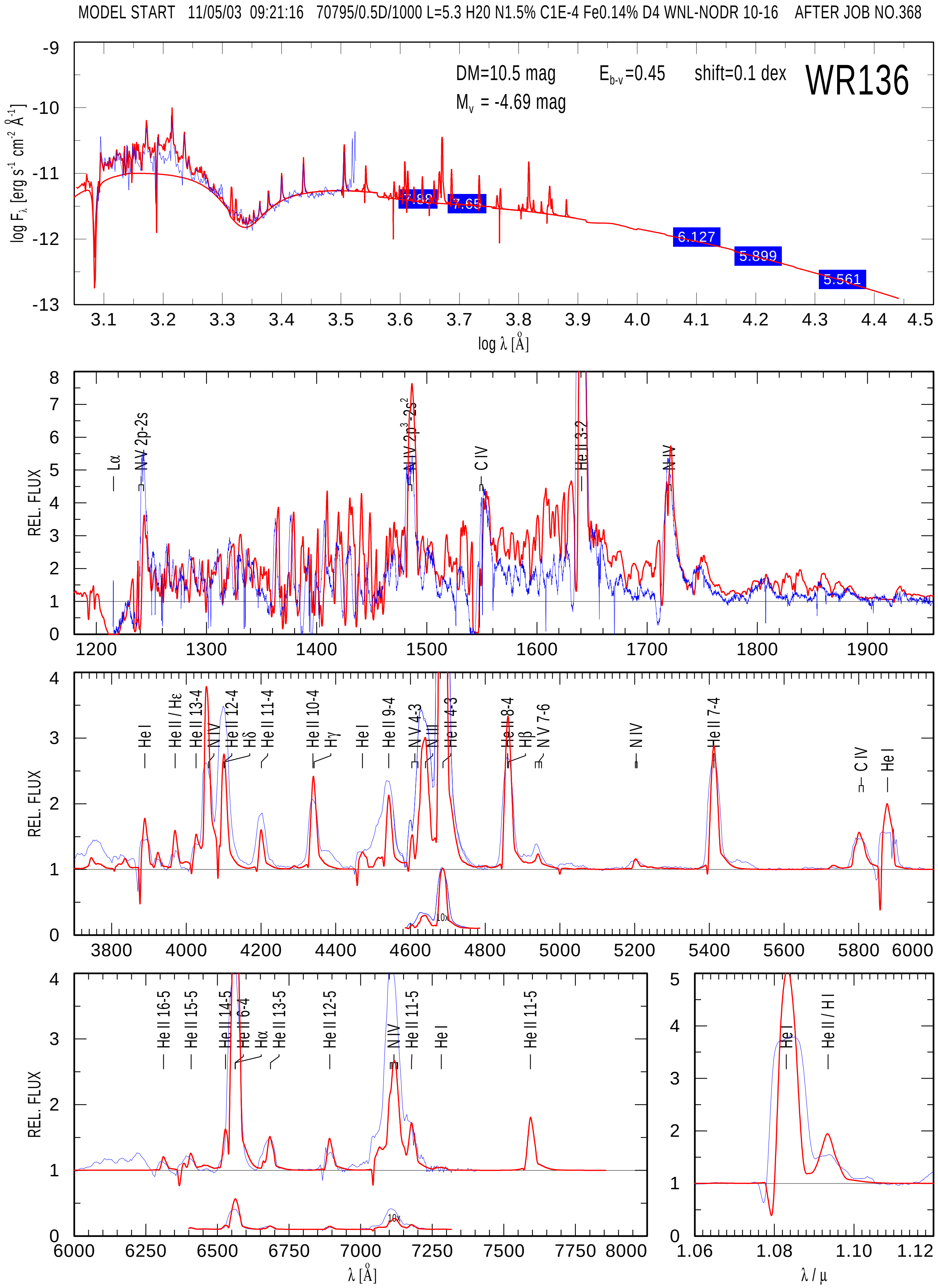

Fig. 68. Model: WNL 10-16, T_{*} = 71 kK, $\log(R_{t}/R_{\odot})$ = 0.5

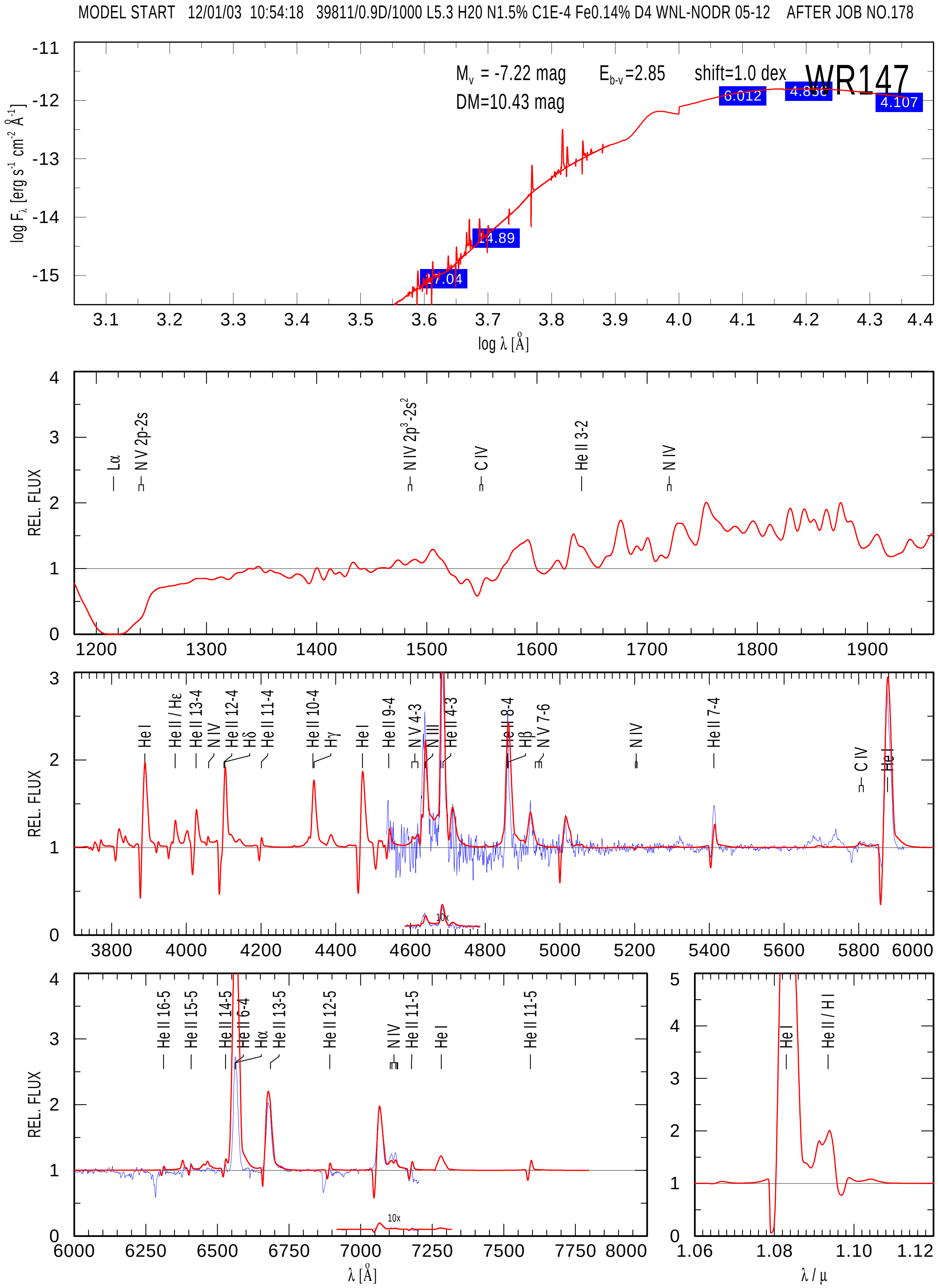

Fig. 69. Model: WNL 05-12, T_{*} = 40 kK, $\log(R_t/R_\odot)$ = 0.9

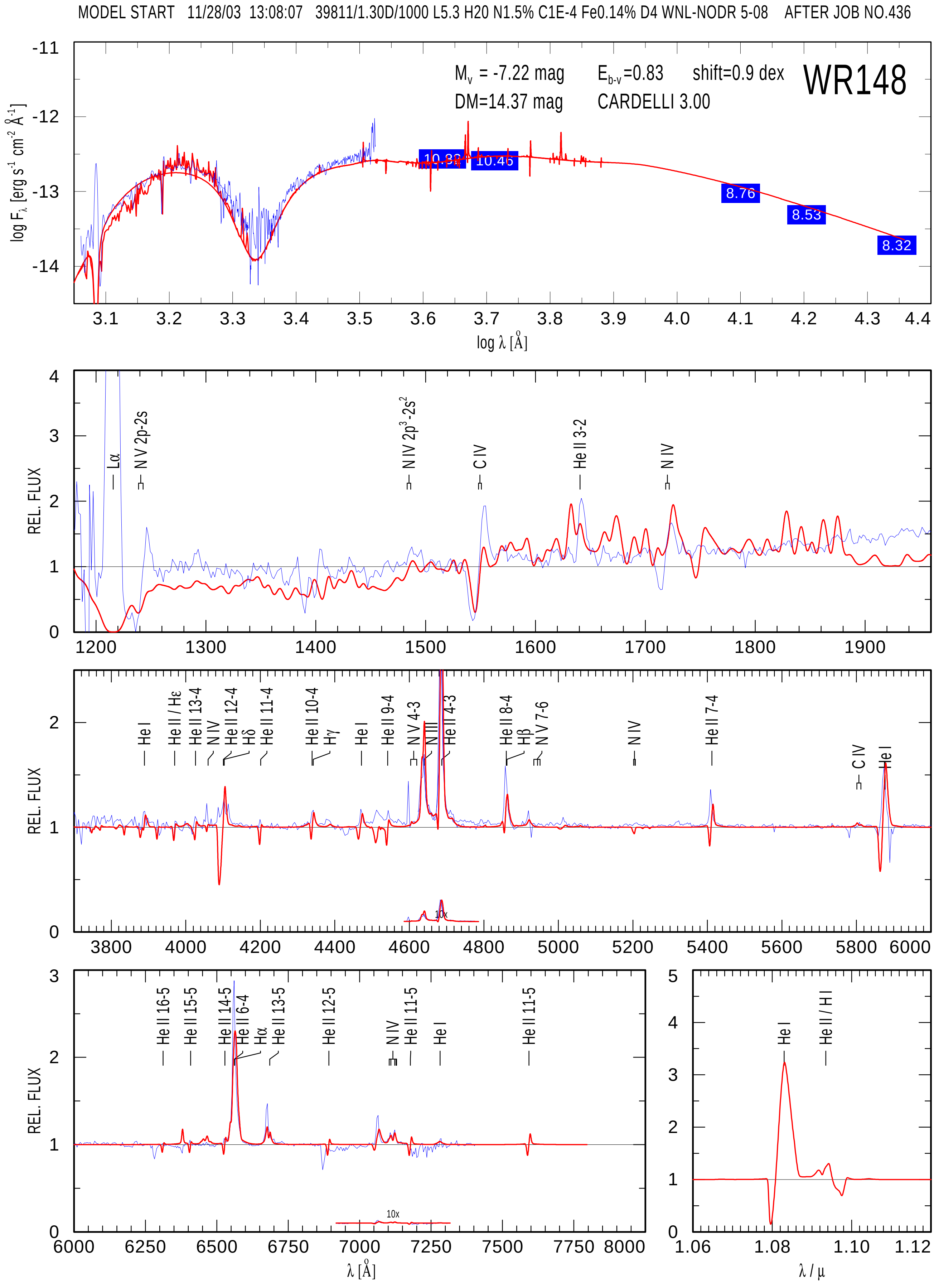

Fig. 70. Model: WNL 05-08, $T_* = 40$ kK, $\log(R_t/R_\odot) = 1.3$

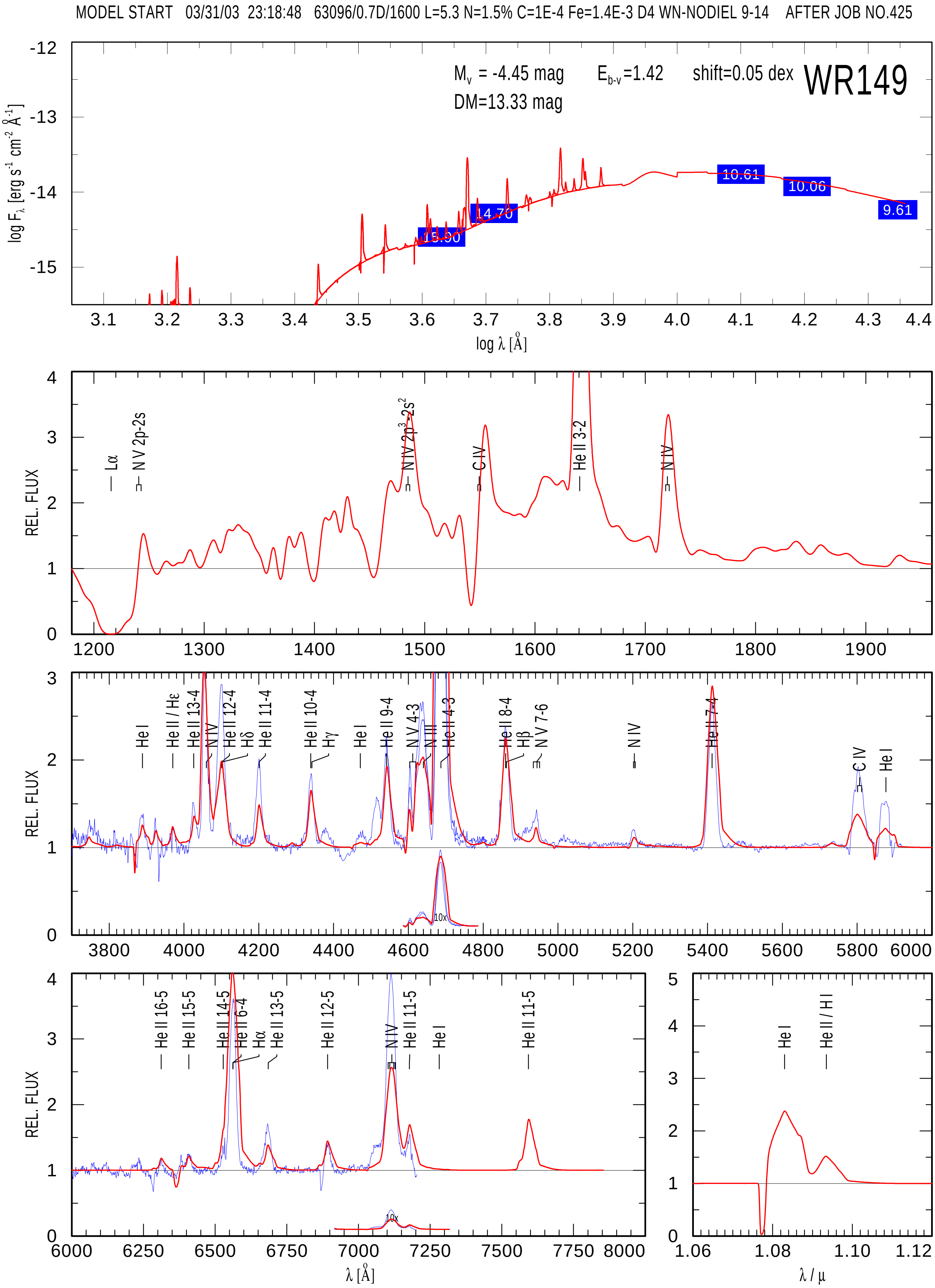

Fig. 71. Model: WNE 09-14, T_{*} = 63 kK, $\log(R_{t}/R_{\odot})$ = 0.7

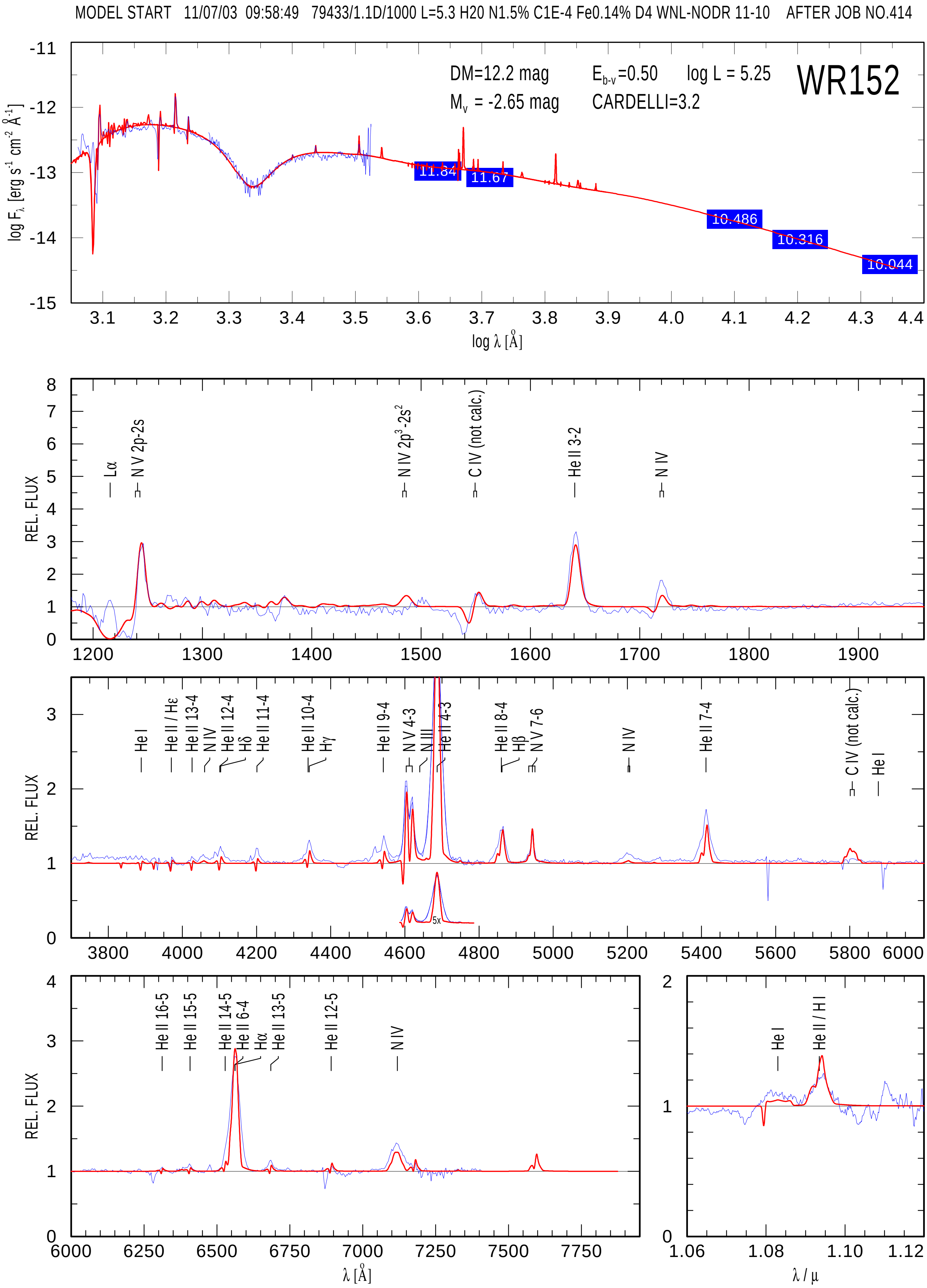

Fig. 72. Model: WNL 11-10, $T_* = 79$ kK, $\log(R_t/R_\odot) = 1.1$

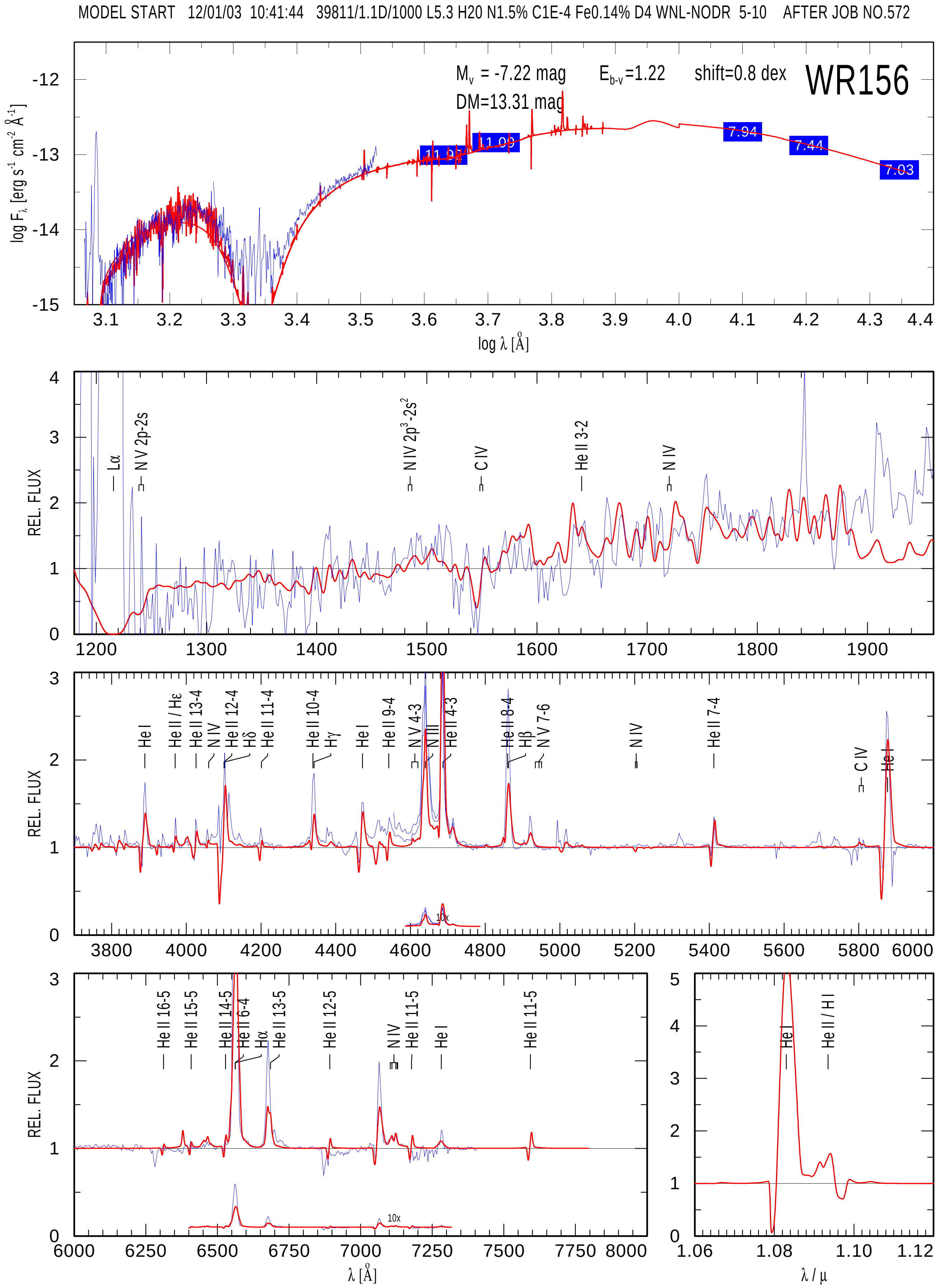

Fig. 73. Model: WNL 05-10, $T_* = 40$ kK, $\log(R_t/R_\odot) = 1.1$

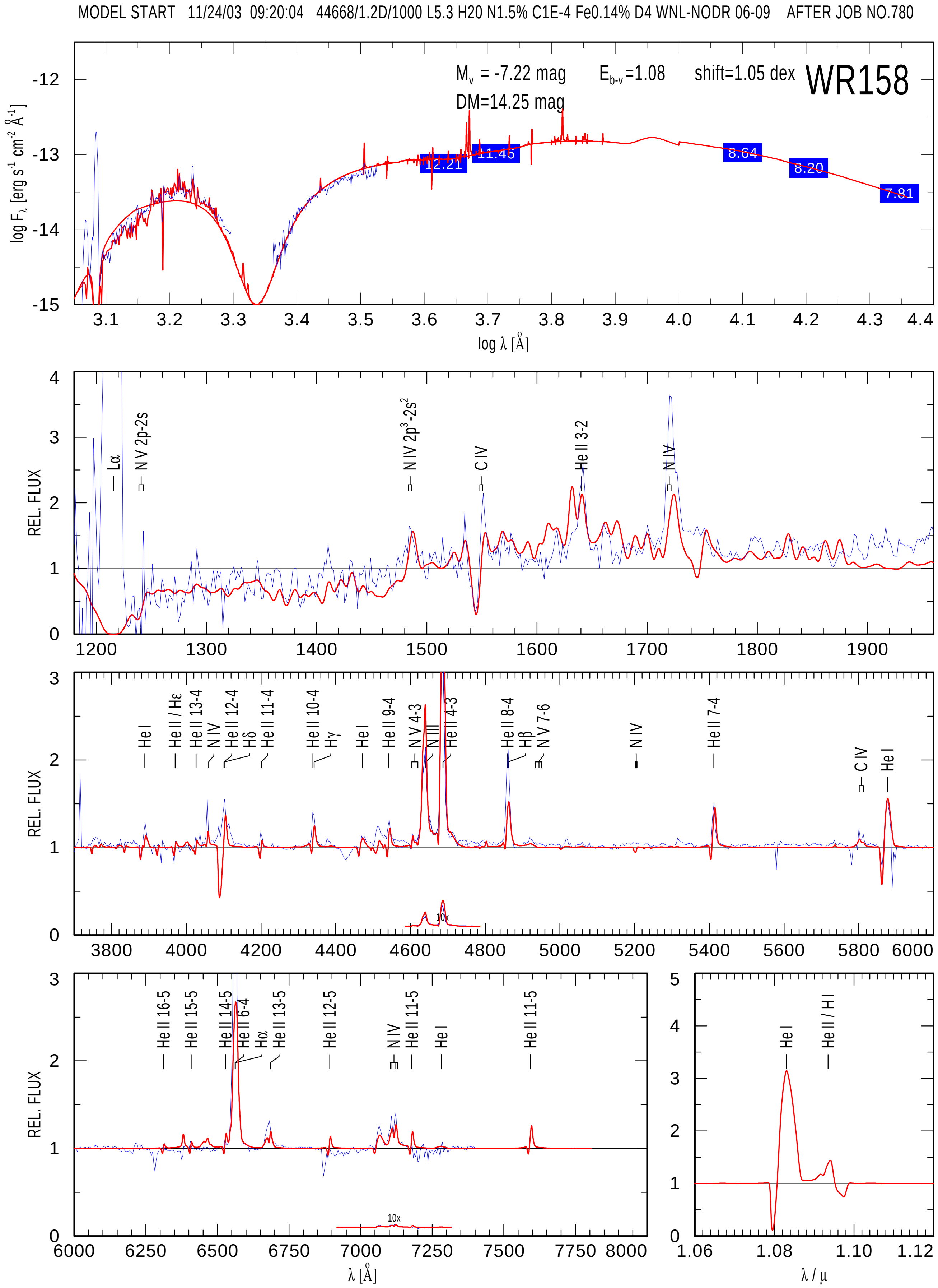

Fig. 74. Model: WNL 06-09, $T_* = 45\,\mathrm{kK}$, $\log(R_t/R_\odot) = 1.2$